Development of an iron electrowinning process using anion exchange membranes

WD van der Spoel Badenhorst

orcid.org/ 0000-0003-4854-6865

Dissertation accepted in fulfilment of the requirements for the degree Master of Science in Engineering Science with Chemical Engineering at the

North-West University

Supervisor: Prof H Krieg

Co-Supervisor: Dr DJ Branken

Graduation: May 2020

Student number: 24250643

PREFACE

I would like to thank the following people for their assistance:

Prof. H.M. Krieg, Prof. D. Bruinsma, Dr D. Branken, and Mr T. Paarlberg for their assistance with the design and construction of the various flow cells used in this study. Through continued work by all parties we were able to design flow cells for laboratory use as well as industrial application of the electrowinning of iron.

My supervisor, Prof. H.M. Krieg, who provided continual assistance in all aspects during the completion of my M.Sc.Eng, both in terms of guidance on an academic level and personal level. His assistance empowered me to not only attend my first international conference, but also publish my first academic work.

My co-supervisor, Dr D.J. Branken, who guided the project from an engineering standpoint and gave me valuable insight into various concerns that are normally are not addressed in pure research, but are required for the industrial application of the work conducted.

I would also like to thank Prof. D. Bruinsma, who assisted greatly during the entirety of the M.Sc.Eng, keeping everything on track for industrial application. He provided insight into the process development and requirements for the industrial application of the work conducted.

Dr J. Kerres, for his contributions to the work by supplying us with novel AEMs to be tested and used in the electrowinning of iron. Our co-operation led to many new discoveries as well as to the conference attendance in Sweden and the publication of work conducted together.

Mr H. Cho, for his help regarding the preparation of the novel AEMs with the inclusion of ceria (Ce_2O_3), and assistance provided in terms of their characterization. In addition to this I would like to acknowledge the valuable help of Inna Kharitonova and Galina Schumski with the ex situ characterization of the novel membranes.

Dr A. Jordaan, for her assistance during the scanning electron microscopy (SEM) imaging of the various membranes used in this study. From the SEM work conducted by Dr. Jordaan, various properties of the membranes could be discerned.

In addition, I would like to thank the following institutions:

The Chemical Resource Beneficiation unit of the North-West University (NWU) as well as the School of Chemical and Minerals Engineering at the NWU, for use of their facilities during the completion of my dissertation.

Fumatech GmbH, for supplying their R&D sample VM-FAPQ-8130-PK membrane, which was found to be the most suitable membrane for this application. They also provided information used in later capital and operating expense cost calculations of the iron electrowinning process.

Tharisa PLC, for providing funding for this research project and supplying us with information used in later capital and operating expense calculations for the iron electrowinning process. Tharisa, moreover, provided continual input into the research conducted.

ABSTRACT

Traditionally, spent leaching solutions (SLS) originating from base metal refineries are treated using (i) tailings dams, (ii) anoxic limestone drains (ALDs), or (iii) jarosite, hematite or goethite precipitation. While these methods provide adequate treatment of SLSs from various mining processes, they do not yield marketable products. As such, these treatment methods have a significant financial impact, while often having a negative impact on the environment. As an alternative to these traditional methods, anion exchange membrane-based electrowinning (EW) is proposed in this study for the treatment of SLSs. The use of specifically anion exchange membranes (AEMs) during EW (AEM-EW) enables the recovery of both electrolytic iron and the regeneration of the leaching acid for re-use with the upstream leaching process. However, as iron is a base metal with a low intrinsic value, the total cost of an AEM-EW process for the treatment of SLSs should ideally be minimized to allow for widespread application within the industry.

Therefore, the effect of various parameters, namely (i) boric acid concentration, (ii) catholyte pH, (iii) electrolyte temperature, (iv) sodium sulphate concentration, (iv) AEM type and composition, and (v) iron concentration on the AEM-EW process were investigated in this study. The addition of boric acid was found to not have any significant effect on the AEM-EW process performance and was therefore not used in any further experiments. In contrast to this, the addition of sulphuric acid to the starting catholyte, which simulated the presence of unspent acid in the SLS, led to a substantially reduced current efficiency of 9 % (12.5 g/L H_2SO_4) compared to the current efficiency of 91 % obtained when no H_2SO_4 had been added to the starting catholyte. The decrease in current efficiency after the addition of sulphuric acid to the catholyte was attributed to an increase in hydrogen evolution. Similarly, increasing both the electrolyte temperature (up to 70 °C) and sodium sulphate content (up to 100 g/L sodium sulphate) led to a significant decrease in the specific energy consumption (SEC) of the process. Preliminary results indicated that the FAB-PK-130 (Fumatech GmbH) membrane outperformed all the membranes that were initially tested. The last variable investigated was the effect of the iron concentration of the starting catholyte solution on the AEM-EW process, where it was found that low initial iron concentrations correlated with low current efficiencies and high SEC values when sodium sulphate was not added. The low current efficiency and high SEC could therefore be attributed to the low electrolyte conductivity under such conditions.

In addition to the various parameters that were tested (Chapter 3), the stability of various commercial and novel AEMs was determined using both the Fenton test and membrane

durability studies performed over a period of three weeks. Some of the novel, blended AEMs that were prepared were impregnated with Ceria (Ce_2O_3), which is known to increase the operational lifetime of membranes in an oxidative/radical environment. The Fenton test results confirmed this, as the novel 2408-2 and BM-5 membranes that were impregnated with 5 wt % Ceria showed increased Fenton stability. During AEM-EW, the novel AEMs and VM-FAPQ-8130-PK, a novel non-commercial membrane from Fumatech, confirmed the improved stability by outperforming the FAB-PK-130 membrane used in Chapter 3. The improved stability of the VM-FAPQ-8130-PK membrane compared to the FAB-PK-130 membrane was further highlighted during the membrane durability test, where the VM-FAPQ-8130-PK membrane was able to operate at an SEC of 5.83 kWh/kg iron, whereas the FAB-PK-130 membrane operated at an SEC of 8.60 kWh/kg iron after three weeks of continued operation.

Using the data obtained from this study (Chapter 3 & 4) as well as information supplied by Fumatech GmbH and Tharisa PLC, the capital expense (CAPEX) and operating expense (OPEX) of a set of scaled AEM-EW units operating in a two-stage configuration with an iron treatment capacity of 45 kg/h were estimated (Chapter 5). The CAPEX was calculated as R 1,327,360 and the levelized OPEX as R 17 per kg iron treated. It was also estimated that the power consumption of the two-stage AEM-EW process would constitute 72 % of the OPEX, while membrane replacement costs would contribute 25 % of the total OPEX, with the remainder being attributed to maintenance. This OPEX breakdown confirms the relevance of this study which aimed to reduce the power consumption of the AEM-EW process while minimising the membrane replacement cost.

Keywords: Iron electrowinning, SLS treatment, Anion Exchange Membranes (AEMs), AEM durability, AEM-EW SLS treatment process

LIST OF ABBREVIATIONS AND SYMBOLS

Abbreviations in Order of Appearance

BMR	Base metal refinery
PGM	Platinum group metal
SLS	Spent leaching solution
EW	Electrowinning
AEM	Anion exchange membrane
CEM	Cation exchange membrane
BFD	Block flow diagram
CAPEX	Capital expense
OPEX	Operating expense
MMO	Mixed metal anodes
AMD	Acid mine drainage
ALD	Anoxic limestone drain
DSA	Dimensionally stable anode
LLE	Liquid-liquid extraction
TBP	Tributyl phosphate
AEM-EW	Anion exchange membrane electrowinning
SEC	Specific energy consumption
ACD	Anode-cathode distance
IEC	Ion exchange capacity
EDTA	Ethylenediaminetetraacetic acid
ICP-OES	Inductively coupled optical emission spectroscopy
PPO	Poly(2,6-dimethyl-1,4-phenylene oxide)
PBI	Polybenzimidazole
VRFB	Vanadium redox flow battery
PEM	Proton exchange membrane
TMIm	1,2,4,5-Tetramethyl-imidazole
DMSO	Dimethyl sulfoxide
PVBCl	Poly vinylbenzyl chloride
PPOBr	Poly(p-phenylene oxide) brominated
TMIm	1,2,4,5-Tetramethyl-imidazole
F6PBI	Fluorinated polybenzimidazole
PBIOO	Polybenzimidazole
SAC	Sulfonated poly(phenylethersulfone)

SEM	Scanning electron microscopy

Symbols in Order of Appearance

m_f	Final cathode mass	(g)
m_i	Initial cathode mass	(g)
A	Current	(A)
t	Time	(s)
n	Number of electrons transferred	(-)
F	Faraday constant	(96 485.3329 s A / mol)
M	Molecular weight	(g/mol)
V	Potential	(V)
C_{HCl}	Concentration of a hydrochloric acid solution	(mol/m^3)
V_{HCl}	Volume of the hydrochloric acid solution	(L)
C_{NaOH}	Concentration of the sodium hydroxide solution	(mol/m^3)
V_{NaOH}	Volume of the sodium hydroxide solution	(L)
m_{dry}	Dry weight of the membrane	(g)
σ_{Cl^-}	Chloride conductivity	($S.m^2.mol^{-1}$)
σ	Conductivity	($S.m^{-1}$)
R_{sp}	Resistivity	($ohm.m^{-1-}$)
d	Membrane thickness	(m)
R	Ohmic resistance	($ohm.m^{-1}$)
A	Electrode surface	(m^2)
WU	Water uptake	(%)

Table of Contents

CHAPTER 1

INTRODUCTION

Table of Contents

1.1 Background

A South African mining company is in the process of developing a platinum group metal (PGM) refinery, which concentrates PGM ore via a sulphuric acid (H_2SO_4) leaching route. After leaching, a spent leaching solution (SLS) containing mainly iron sulphate, with some minor metal impurities such as cobalt (Co), nickel (Ni) and chromium (Cr), is obtained.[1] Treating this SLS will become increasingly expensive due to the enforcement of more stringent environmental regulations.[2] Traditionally, SLSs are treated using either active or passive methods such as oxidative precipitation, oxidative bacteria usage or limestone precipitation.[3-4] Such methods, however, rarely yield marketable products, and as a result, hold significant financial implications.[3] Furthermore, it has become increasingly difficult to obtain permits for the construction of active or passive treatment plants due to their large footprint and ecological impact.[5-6]

The most prevalent method for the treatment of SLSs (as with the method proposed for the concentration of PGM ore) involves the use of neutralizing (basic) chemicals (NaOH, CaO or $FeCO_3$) that raise the pH of the solution, thereby lowering the solubility of many metal species and facilitating the precipitation of metal hydroxides.[4] In the case of iron, oxidizing chemicals (H_2O_2 or active aeration) have been used to oxidize the soluble Fe(II) into the less soluble Fe(III), which eases the precipitation process.[4, 7-8] This, however, produces a large volume of sludge containing only 2-4% solids.[4] To reduce the cost of the sludge disposal, the sludge has to undergo further processing steps to produce a sludge containing at least 50 % solids.[4]

An alternative, possibly less costly treatment method for SLSs is electrowinning (EW), where electrochemical processes are used to recover specific metals. Throughout the dissertation, the term EW is used in lieu of the term membrane electrolysis, with EW referring specifically to processes involving the removal of metal ions from solutions. EW in a non-separated cell, i.e. without the use of a membrane separator (**Figure 1.1a**), has long been used successfully for the recovery of metals such as copper (Cu), Co and Ni.[9-11] While hydrogen evolution at, and dissolution of, the cathode due to acid formation in the electrolyte reduce the efficiency of the non-divided-cell EW processes, the reduced efficiency is compensated for by the relatively high value of products such as Cu and Co. For such higher-value metals, the production of an acid solution at the anode is deemed a waste reaction. However, when aiming to recover lower-value products such as iron, the above-mentioned disadvantages of the non-divided EW process significantly reduce the profitability and feasibility of this process, unless the acid can be recovered and hence reused. Also, during iron recovery, oxygen evolution at the anode causes oxidation of Fe (II) to Fe (III), which further reduces the efficiency of the electrowinning process. This kind of oxidation is, however, not a concern during the EW of Cu, Co, and Ni.[12]

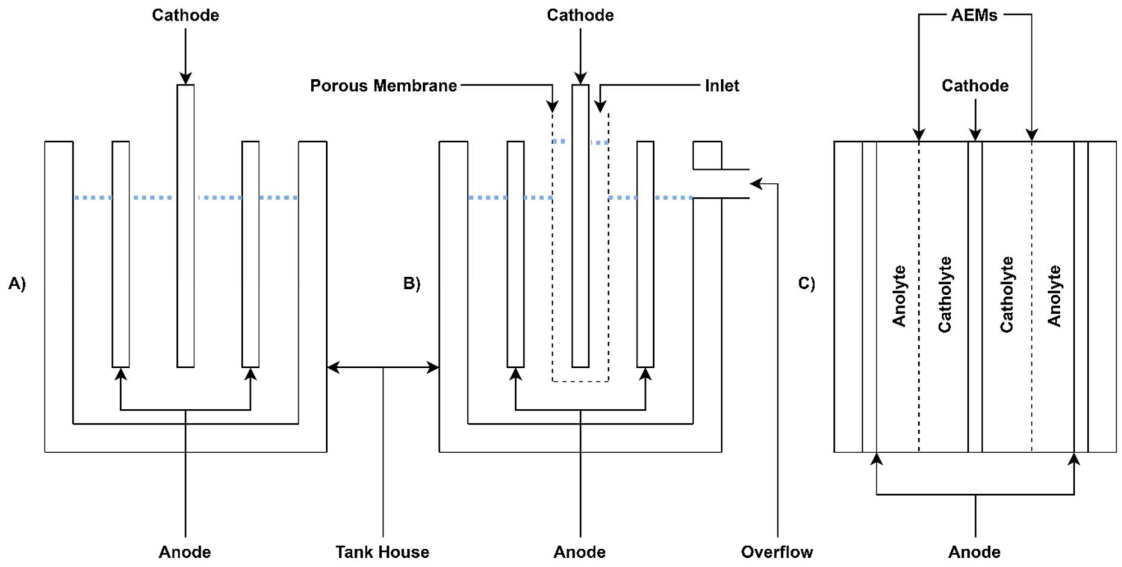

Figure 1.1: Diagrammatic representations of three basic processes used in EW of metals, i.e. a) Non-divided EW, b) Porous membrane-based EW and c) non-porous anion exchange membrane-based EW.

The above-mentioned disadvantages associated with iron EW in a non-divided cell can be overcome by placing a membrane between the anode and cathode to produce a divided cell (**Figure 1.1b, c**). Such a membrane acts as a semipermeable barrier dividing the electrolyte in a catholyte and anolyte, which reduces the transfer of oxygen from the anolyte to the catholyte, thereby reducing the amount of oxidized Fe(II) in the catholyte.[12] Additionally, the membrane slows the transfer of hydrogen from the anolyte to the catholyte, hence reducing hydrogen formation at the cathode, which should lead to an increase in the process efficiency while simultaneously affecting an increase in the acid concentration in the anolyte. An example of a membrane being used for the EW of iron is the Terylene porous membrane that was used in the Pyror process.[12] However, the use of a porous membrane necessitates pH control since the acid that is initially formed in the anolyte eventually permeates the membrane and reduces the pH of the catholyte. This effect, which is known to occur in the porous membrane-based EW of Co and Ni,[13-14] restricts the amount of acid that can be regenerated by this process.

In the Pyror process, developed (1947 - 1957) for the EW of iron from a sulphuric acid environment, [12] the cathode is inserted into a Terylene bag (**Figure 1.1b**). The iron-rich solution is then pumped over the cathode into the Terylene bag, where the iron is plated onto the cathode, while the oxidation of water on the lead anode causes the formation of sulphuric acid in the anolyte. Due to the usage of a porous membrane, the catholyte eventually permeates into the anolyte, where the oxidation of Fe(II) to Fe(III) occurs in the presence of the oxygen formed on the anode. After EW, the anolyte consists of regenerated H_2SO_4 and some Fe(III), which can be reused for leaching after reducing (hydrogen sulphide) the formed

Fe(III) to Fe(II) . The Pyror process focused mainly on the production of marketable iron. However, iron's low intrinsic value, coupled with a decline in business conditions at the end of the 1950s, ultimately led to the discontinuation of the process.[12]

The recent advent of non-porous ion-exchange membranes saw the development of membranes that are electrically conductive and allow selective transport of species, while rejecting the transfer of other species. These membranes were mainly developed for fuel cells, electrolyzers and redox flow batteries. Using such non-porous membranes in an EW process (**Figure 1.1c**) could present a significant improvement for the recovery of iron, as many of the disadvantages associated with porous membrane-based EW could be overcome.[15] For this process, anion exchange membranes (AEM) that have been developed mainly for alkaline fuel cells may be suitable,[16] as they would prohibit oxygen transfer from the anolyte to the catholyte, while significantly reducing proton and iron transfer between the anolyte and catholyte. This could lead to higher efficiencies and the regeneration of higher anolyte acid concentrations.[17] The higher efficiencies attainable with such an AEM-based EW process, in conjunction with the ability to produce higher concentrations of H_2SO_4 in the anolyte should, in turn, increase the profitability of iron EW.

While a recent study introduced the topic of AEMs in EW for iron recovery,[17] further work is required to provide a better understanding of and possibly to improve such an AEM-based EW process. As most research regarding the EW of metals has focussed on the use of commercially available proton and anion exchange membranes,[18-19] novel membranes and their influence on process performance should be further investigated. Criteria for the development of novel AEMs should entail a high selectivity towards anions such as sulphate, while rejecting both protons and the cationic metal species (Fe(II) or Fe(III)). Simultaneously, novel AEMs should have a high electrical conductance, thereby lowering the energy consumption of the process.[20-21]

1.2 Problem Statement

Due to various factors, the EW of iron is notoriously difficult. The first reason relates to the oxidation of the soluble Fe(II) to the highly insoluble Fe(III) by the oxygen produced at the anode or absorbed by the non-porous membrane.[7-8, 22] Consequently, precipitation of ferric hydroxides and oxyhydroxides that can cause fouling of equipment is possible. The second reason involves the low intrinsic value of iron as a base metal placing pressure on both the CAPEX and OPEX of such a process. It is thus imperative that an EW process for iron is optimized to minimize the operating costs. Improving the EW of iron can be achieved by optimizing process variables such as the Na_2SO_4 concentration, the temperature or the type

of membrane. When considering the low intrinsic value of the recovered electrolytic iron, regeneration of the spent acid from the SLS is additionally required. To reduce the OPEX and possible downtime during operation, the membrane durability has to be extended.

1.3 Aim and Objectives

It is accordingly the aim of this study to determine and optimize the parameters affecting an EW process to ultimately propose a possible process configuration for the treatment of iron containing SLSs.

To attain the abovementioned aim, the following objectives were identified:

- Compare the performance of an AEM-EW to a porous membrane-facilitated EW and a non-divided EW process in terms of process efficiency and amount of acid regenerated.
- Characterize the effect of the following parameters on an AEM-EW process: boric acid, catholyte pH, electrolyte temperature, sodium sulphate concentration, and AEM composition.
- Explore the behaviour of the EW system and the amount of acid recoverable at key process conditions such as reduced iron concentration and increased anolyte acid concentration.
- Explore the stability of the best-performing AEMs (commercial and novel) by subjecting them to highly acidic conditions, Fenton testing, and through extended operation in an AEM-EW unit.
- Propose a process configuration that would be capable of treating an SLS with an iron flow rate of 45 kg/h.
- Perform a preliminary capital expense (CAPEX) and operating expense (OPEX) estimation to evaluate the economic viability of the proposed AEM-EW process.

1.4 Limitations

The optimization of the electrode materials used for either the cathode or anode fell beyond the scope of this study. Accordingly, an iron sheet was used as the starter cathode due to the poor adherence of the electrolytic iron to any other metal. Similarly, a commercially available lead anode was used due to its known long service lifetime and its relatively low cost compared to mixed metal oxide (MMO) anodes.[23]

Due to export limitations from Japanese membrane manufactures, no AEMs could be obtained from Astom. This limited the study to the use of commercial membranes obtained from ResinTech Inc. (USA) and Fumatech GmbH (Germany), as well as some novel membranes manufactured by the group of Dr Kerres (University of Stuttgart, Germany). During the membrane durability study in the EW environment, only the best-performing AEMs were tested, considering cost and equipment constraints.

1.5 Dissertation Overview

In **Chapter 1**, the general treatment methods of SLS solutions obtained from various mining processes is introduced, mentioning the possible use of the EW of iron using a non-divided, porous membrane, or AEM-based process with focus on the exploration of the advantages and problems that have to be addressed for the industrial application of an EW process. Finally, the problem statement as well as the aim and objectives are discussed, followed by a review of the limitations pertaining to this study.

In **Chapter 2**, a literature overview of traditional treatment methods, both active and passive, is presented. Amongst others, methods such as tailings ponds and anoxic limestone drains are examined, followed by a discussion on the advantages and disadvantages of the various methods where iron is precipitated as either jarosite, hematite or goethite. Various EW methods and other electrochemical processes that can be used for the treatment of SLSs are then introduced. These EW methods include porous bag EW, solvent extraction methods and electro membrane processes, discussed in order of increasing complexity.

In **Chapter 3**, the focus is to determine the effect of various parameters on the performance of the EW of iron. Variables include boric acid, catholyte pH, anolyte pH, electrolyte temperature, sodium sulphate addition, and the influence of various AEMs. Additionally, the effect of iron on the EW process is determined in terms of the effect of reduced iron concentrations, iron flux and depletion of iron in the solution.

In **Chapter 4**, the stability of the membranes employed in the EW unit is investigated through Fenton tests and membrane durability tests. Moreover, novel blended AEMs that are highly stable in oxidative environments were tested in the EW unit. This chapter therefore provides insight into the lifetime of the AEM.

Finally, an overview of the results from Chapters 3 and 4 are presented in **Chapter 5**. This information is then used to propose a process design for the EW of iron, followed by preliminary CAPEX and OPEX calculations. This final chapter concludes with an evaluation of the work conducted and recommendations for further work.

1.6 Bibliography

1. Cramer, L. A.; Basson, J.; Nelson, L. R., The impact of platinum production from UG2 ore on ferrochrome production in South Africa. *J S Afr I Min Metall* **2004,** *104* (9), 517-527.
2. Goolam, N., Recent environmental legislation in South Africa. *Journal of African Law* **2000,** *44* (1), 124-128.
3. Kefeni, K. K.; Msagati, T. A. M.; Mamba, B. B., Acid mine drainage: Prevention, treatment options, and resource recovery: A review. *Journal of Cleaner Production* **2017,** *151*, 475-493.
4. Johnson, D. B.; Hallberg, K. B., Acid mine drainage remediation options: a review. *Sci Total Environ* **2005,** *338* (1-2), 3-14.
5. Rico, M.; Benito, G.; Diez-Herrero, A., Floods from tailings dam failures. *J Hazard Mater* **2008,** *154* (1-3), 79-87.
6. Ozkan, S.; Ipekoglu, B., Investigation of environmental impacts of tailings dams. *Environmental Management and Health* **2002,** *13* (3), 242-248.
7. Crowe, C. W.; Maddin, C. M. Method for preventing the precipitation of ferric compounds during the acid treatment of wells. 1986.
8. Harris, H. J. Method of preventing precipitation of iron compounds from an aqueous solution. 1964.
9. Sharma, I. G.; Alex, P.; Bidaye, A. C.; Suri, A. K., Electrowinning of cobalt from sulphate solutions. *Hydrometallurgy* **2005,** *80* (1-2), 132-138.
10. Jeffrey, M. I.; Choo, W. L.; Breuer, P. L., The effect of additives and impurities on the cobalt electrowinning process. *Minerals Engineering* **2000,** *13* (12), 1231-1241.
11. Lupi, C.; Pasquali, M., Electrolytic nickel recovery from lithium-ion batteries. *Minerals Engineering* **2003,** *16* (6), 537-542.
12. Mostad, E.; Rolseth, S.; Thonstad, J., Electrowinning of iron from sulphate solutions. *Hydrometallurgy* **2008,** *90* (2-4), 213-220.
13. Holm, M.; O'Keefe, T. J., Electrolyte parameter effects in the electrowinning of nickel from sulfate electrolytes. *Minerals Engineering* **2000,** *13* (2), 193-204.
14. Elliott, R. W.; Ambrose, J.; Ettel, V. A., Electrowinning of sulfur-containing nickel. Google Patents: 1978.
15. Tanaka, Y.; Moon, S.-H.; Nikonenko, V. V.; Xu, T., Ion-exchange membranes. *International Journal of Chemical Engineering* **2012,** *2012*.
16. Varcoe, J. R.; Slade, R. C., Prospects for alkaline anion-exchange membranes in low temperature fuel cells. *Fuel cells* **2005,** *5* (2), 187-200.
17. Rossouw, J. Die elektroherwinning van Fe en H_2SO_4 uit 'n $FeSO_4$-logingsoplossing met behulp van anioonruilmembrane. North-West University, 2018.
18. Sopian, K.; Daud, W. R. W., Challenges and future developments in proton exchange membrane fuel cells. *Renewable Energy* **2006,** *31* (5), 719-727.

19. Merle, G.; Wessling, M.; Nijmeijer, K., Anion exchange membranes for alkaline fuel cells: A review. *Journal of Membrane Science* **2011,** *377* (1-2), 1-35.

20. Carrillo-Abad, J.; Garcia-Gabaldon, M.; Ortiz-Gandara, I.; Bringas, E.; Urtiaga, A. M.; Ortiz, I.; Perez-Herranz, V., Selective recovery of zinc from spent pickling, baths by the combination of membrane-based solvent extraction and electrowinning technologies. *Separation and Purification Technology* **2015,** *151*, 232-242.

21. Carrillo-Abad, J.; Garcia-Gabaldon, M.; Perez-Herranz, V., Study of the zinc recovery from spent pickling baths by means of an electrochemical membrane reactor using a cation-exchange membrane under galvanostatic control. *Separation and Purification Technology* **2014,** *132*, 479-486.

22. Crowe, C. W. Method of preventing precipitation of ferrous sulfide and sulfur during acidizing. 1987.

23. Mirza, A.; Burr, M.; Ellis, T.; Evans, D.; Kakengela, D.; Webb, L.; Gagnon, J.; Leclercq, F.; Johnston, A., Corrosion of lead anodes in base metals electrowinning. *Journal of the Southern African Institute of Mining and Metallurgy* **2016,** *116* (6), 533-538.

CHAPTER 2

LITERATURE SURVEY

Table of Contents

2.1 Introduction

Due to the increasing demand for PGMs, a South African-based mining company is in the process of constructing a base metal refinery (BMR) for the recovery of PGMs from a low-grade iron-rich ore.[1-2] During BMR processes for PGM recovery, waste streams are produced,[3-4] typically containing varying amounts of nickel (Ni), cobalt (Co), copper (Cu) and iron (Fe), depending on the source of the ore.[5] The depletion of high-grade PGM ores has, however, led to the use of lower-grade ores, altering the effluent compositions that have to be treated in view of their negative environmental impact.[5]

A simplified flow sheet of the proposed BMR process is presented in **Figure 2.1**. Prior to the BMR process, the majority of metallic (Cr, Ni, Co, Cu) and non-metallic impurities, mostly sulphur, are removed through various methods, including selective leaching for metallic impurities and roasting for non-metallic impurities.[6-7] The feedstock for this specific BMR process will contain large amounts of Fe and trace amounts of Ni, Co and Cu in addition to the PGMs.[8] Initially, the feed enters a roaster to remove sulphur as sulphur dioxide (SO_2). After roasting, the resulting PGM ore is transferred to a smelter to produce a PGM-iron alloy, which is atomized prior to the leaching circuit. After atomization, the PGM-iron alloy is leached using sulphuric acid (H_2SO_4) at elevated temperatures and atmospheric pressure to produce a PGM concentrate that can be recovered as a solid. The spent leaching solution (SLS) resulting from the leaching contains primarily Fe(II) sulphate ($FeSO_4$) and unspent sulphuric acid (H_2SO_4). For the purpose of this dissertation, the treatment possibilities for SLSs before disposal are divided into traditional methods, discussed in Section 2.2, and electromembrane processes, discussed in Section 2.3.

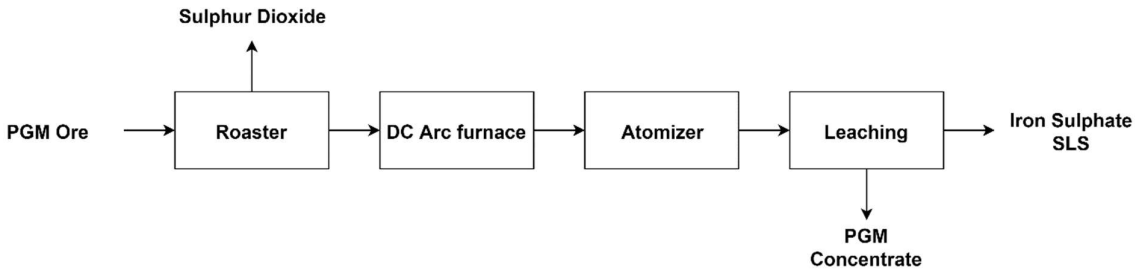

Figure 2.1: Flowsheet of the proposed BMR process for PGM recovery from low-grade ores.

2.2 Traditional Methods

Traditionally, the methods that are used to treat the acidic $FeSO_4$-rich SLS are often divided into active and passive treatment methods.[9] In SLS treatment methods, the Fe(II) present in

the SLS is generally oxidized to the less soluble Fe(III), which then is precipitated from the SLS in various forms of Fe.[10] For most of these methods, the unspent acid present in the SLS has to be neutralized using caustic media before the removal of Fe, thereby reducing the risk of acid mine drainage (AMD) formation.[9, 11-12] However, these traditional treatment methods still have a significant negative environmental impact despite acid neutralisation by still posing a risk of groundwater contamination and AMD formation.[13] Accordingly, obtaining permits for the construction of these effluent treatment methods have become increasingly difficult, resulting in the need for improved treatment methods. As mentioned above, traditional treatment methods are commonly grouped into passive methods such as tailings dams and anoxic limestone drains (Section 2.2.1), and active methods such as jarosite, goethite, and hematite precipitation (Section 2.2.2).[9]

2.2.1 Passive Treatment Methods

Passive treatment methods are most commonly used for the treatment of SLSs due to both their ease of operation and the small input required once operation of the treatment has commenced.[9] However, these methods require large areas for construction while having potentially long-lasting environmental effects after the discontinuation of the operation, which require remedial actions to be taken.[9] For the purpose of this discussion, tailings dams and limestone drains will be briefly discussed.

2.2.1.1 Tailings Dams

The use of tailings dams is the most prevalent waste treatment method for streams originating from BMR processes and other mining activities.[14-15] Tailings dams require the construction of artificial dams or the use of naturally occurring dams in which tailings (process effluents that are generated from various industrial processes) can be dumped. Before the SLS is pumped into a tailings dam, the remaining acid in the SLS is neutralized using, for example, caustic media, which additionally facilitates the precipitation of the Fe. This is achieved by passively oxidizing the Fe(II) through dissolved oxygen. The subsequent precipitation of the Fe(III) is further aided by the evaporation of the water during storage in the dam. Fe precipitation can occur as either Fe(II)/Fe(III) hydroxide or Fe(III) oxyhydroxides, depending on the prevailing conditions and treatment method.[12, 16] Typical problems associated with the use of tailings dams include the cost of construction, maintenance and rehabilitation, as well as the risk for the surrounding environment due to the possibility of AMD.[14, 17-18] Additionally, if poorly maintained, tailings dams can fail and cause flooding and contamination of the surrounding

region.[15] Despite these disadvantages, tailings dams are still widely used due to the ease of operation, relatively low cost and high SLS capacity.[14]

2.2.1.2 Anoxic Limestone Drains

Anoxic limestone drains (ALDs) are another common treatment method for SLSs generated by BMR processes and other mining activities. In a typical ALD, a channel is dug, filled with a limestone bed and covered in an impermeable plastic liner to prevent the intrusion of oxygen, as illustrated in the basic design shown in **Figure 2.2**.[19-20] The use of ALDs have a large initial construction cost. However, their lifespan, depending on the SLS feedstock composition, is several years if properly maintained.[19-20]

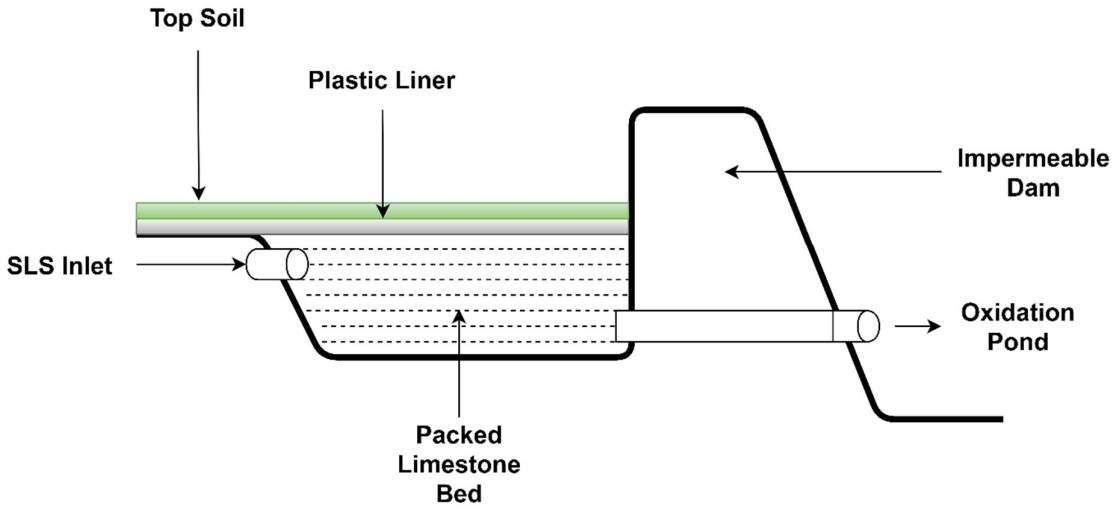

Figure 2.2: Typical layout of an anoxic limestone drain used in the treatment of SLSs and AMD, before sending the streams to oxidation and settling ponds.

During operation, the SLS is fed through the bed of limestone, where the unspent acid present in the SLS reacts with the limestone, thereby increasing the pH (see **Eq. 2.1** and **2.2**).[21] The retention time of the SLS in the ALD is adjusted to sufficiently neutralize all the unspent acid before leaving the limestone bed. After neutralization, the now alkaline SLS is fed into oxidation and settling ponds.[19] During oxidation, Fe(II) is passively oxidized to Fe(III) through dissolved oxygen, and precipitated for example as Fe(III) hydroxides, depending on the process conditions.

$$CaCO_3 + H_3O^+(aq) \rightarrow Ca^{2+}(aq) + HCO_3^-(aq) + H_2O \quad (2.1)$$

$$CaCO_3 + SO_4^{2-}(aq) + H_3O^+ \rightarrow CaSO_4 + H_2O + HCO_3^- \quad (2.2)$$

Despite the low cost of ALD systems, they are limited in their use and only suitable for treating SLS containing Fe(II), i.e. requiring that any Fe(III) present has to be reduced to Fe(II) before being fed to the ALD.[20] The reason therefore is that the presence of even small amounts of Fe(III) in the ALD will result in the precipitation of Fe(III) hydroxides in the high pH environment,[21] resulting in fouling of the surface of the limestone used within the ALD, preventing further contact of the SLS with the limestone bedding.[20] Watzlaf *et al,* for example, showed that ALDs used to treat SLS containing as little as 21 ppm Fe(III) had a lifetime of only 8 months.[20]

2.2.2 Active Treatment Methods

In contrast to the previously discussed passive treatment methods, active treatment methods require continuous input for operation.[9] In addition, processing conditions for such operations are more intense, for example requiring increased temperatures, higher than atmospheric pressures and specialty chemicals.[9] A further drawback associated with active treatments is the low total solid content of the produced sludge, ranging from 2-4 % depending on the SLS treated,[9] often necessitating additional steps to increase the total solid content of the sludge. For example, evaporation has been used to concentrate the solid content to 50 %, which significantly lowers the cost of disposal.[9] Generally, active methods require the neutralization of the unspent acid using neutralisation agents before the precipitation of the Fe from the SLS. These neutralisation agents can include lime, calcium hydroxide and sodium hydroxide, depending on the effectiveness and cost of the process as well as the desired form of the iron precipitate.[9]

As a benefit, these methods often require a smaller physical footprint and are more easily dismantled after discontinuation of the process compared to the passive treatment methods. Another benefit is that active methods can yield marketable products, which compensates for the required continuous and often more expensive input. The best-known examples of active precipitation are jarosite, goethite and haematite precipitation.

2.2.2.1 Jarosite Precipitation

During Jarosite precipitation, the unspent acid of the Fe-containing SLS is neutralized using caustic media, followed by precipitation of the Fe(III) as jarosite ($NaFe_3(SO_4)(OH)_6$). Jarosite has the advantage that it is more easily filtered compared to Fe(III) hydroxides, which are

known to form fine hydrolytic polymers that are difficult to filter.[22] The formation of jarosite occurs according to **Eq. 2.3** in solutions with a pH of 2-4. During the jarosite formation, sulphuric acid is formed, which requires continual pH adjustment of the SLS being treated.[23]

$$3Fe_2(SO_4)_3 + Na_2SO_4 + 12H_2O \rightarrow 2NaFe_3(SO_4)(OH)_6 + H_2SO_4 \quad (2.3)$$

The rate of jarosite precipitation depends on various process variables such as the sodium sulphate concentration, the agitation rate, the pH, and the temperature.[23-24] Recently, bacterial cultures were used to accelerate the slow formation of jarosite.[25] However, while the use of bacterial cultures can accelerate the rate of jarosite formation, their use is restricted to specific temperature and pH ranges.[25]

Jarosite precipitation is mostly used for the selective precipitation of Fe from spent picking solutions containing Fe and zinc to increase the zinc purity before it is sent to electrowinning for recovery.[23, 26-27] Despite the ease of operation of the jarosite process, both the zinc industry and SLS treatment have moved away from jarosite precipitation as jarosite is not a marketable product.[24] The zinc industry currently uses mostly solvent extraction, while SLS treatment is done using other methods including those discussed in this section.[24, 27]

2.2.2.2 Goethite Precipitation

Fe can also be removed from SLSs through precipitation as goethite ($\alpha - FeOOH$) with a process varying slightly from the jarosite process.[28] Similar to the jarosite process, the goethite process requires the neutralization of the unspent acid using caustic media.[28] In contrast to the jarosite process, however, the goethite process is performed at elevated temperatures of 80 - 90 °C and can only be used to treat Fe levels of up to 1 g/L Fe.[24] During goethite precipitation, Fe(II) is oxidized to Fe(III) by dissolved oxygen in the presence of water, forming goethite and free protons as shown in **Eq. 2.4**.[28-29]

$$2Fe^{2+} + 0.5O_2 + 3H_2O \rightarrow 2FeOOH + 4H^+ \quad (2.4)$$

Compared to the jarosite precipitation, the formation of goethite occurs significantly faster due to the increased temperature of the process. The goethite process can be further accelerated through active aeration of the solution which does not require significant additional costs. Similar to jarosite, goethite is readily filterable, but suffers from the same low marketability as

jarosite, while also requiring continual pH adjustments. The largest drawback however, is that goethite only forms selectively in Fe solutions containing less than 1g/L Fe, above which Fe hydroxides are being formed.[30] These fine hydroxides quickly reduce the efficiency of the filters while causing damage to the equipment used.[10]

2.2.2.3 Hematite Precipitation

Hematite (Fe_2O_3) is the most marketable of the discussed Fe precipitates and, similarly to jarosite and goethite, is more readily filterable than Fe hydroxides.[31] The marketability of hematite is, however, offset by the extreme conditions required for its formation.[31] In contrast to both jarosite and goethite, the formation of hematite (**Eq. 2.5**) requires high temperatures, seed crystals and a pure oxygen environment at non-ambient pressures.[31-32] These intensive process conditions hinders the widespread adoption of the technology.[31-32]

$$2FeCl_3 + 3H_2O \rightarrow 2Fe_2O_3 + 6HCl \quad (2.5)$$

Despite the intensive process conditions, the Iijima Zinc Refiner in Akita Japan uses hematite precipitation to treat their SLSs,[31, 33] operating at 180 – 200 °C under 18 atm pressure of pure oxygen.[31, 33] Under these conditions, the hematite process removes nearly all Fe from the SLSs, allowing for the discharge of the SLS after treatment.[31] Regardless of the benefits of the hematite precipitation, the technology is not widely adopted for the treatment of SLSs or for the production of hematite, with most hematite being produced from jarosite feedstock.[34]

2.3 Electromembrane Processes

Alternatively to the passive and active traditional methods discussed above where the SLS is merely treated as waste management, the electromembrane processes could add value to the SLS, reducing treatment cost.[35-36] Value can be added both in the form of metallic Fe (purity depends on the type of SLS) being produced and the possible regeneration of the spent acid. Basically, the electromembrane processes have two commonalities: they entail electrowinning (EW) and they use membranes, which can be either porous or non-porous as will be discussed in Sections 2.3.1 and 2.3.2, respectively. When using non-porous membranes, three processes can be distinguished: (i) anion exchange membrane EW, (ii) anion/cation exchange membranes and (iii) liquid-liquid extraction with diffusion dialysis.

These will be discussed in order off increasing complexity of the processes. Before discussing the porous and non-porous processes in more detail, an overview of the relevant electrochemical reactions and side reactions are summarized in **Table 2.1**.[37]

Table 2.1: List of possible electrochemical reactions occurring both on the anode and cathode during electromembrane processes.[37]

Cathode		
Desired reaction	**E^0 (V)**	**Equation**
$Fe^{2+} + 2e^- \rightarrow Fe$	-0.44	2.6
Side reaction		
$Fe^{3+} + e^- \rightarrow Fe^{2+}$	+0.77	2.7
$2H^+ + 2e^- \rightarrow H_2$	0.00	2.8

Anode		
Desired reaction		
$2H_2O \rightarrow O_2 + 4H^+ + 4e^-$	+1.23	2.9
Side reaction		
$Fe^{2+} \rightarrow Fe^{3+} + e^-$	-0.77	2.10

All of the discussed processes attempt in specific ways to overcome some of the inherent challenges found when electrochemically treating Fe SLSs. One such challenge, as discussed previously, is the oxidation of the soluble Fe(II) to the less soluble Fe(III), which forms hydroxides that can foul both the membranes and the equipment used.[10, 38] Oxidation can occur on the anode directly (**Eq. 2.10**) or indirectly by oxidizing the Fe(II) using the oxygen formed at the anode (**Eq. 2.9**), according to **Eq 2.11**.

$$2Fe^{2+} + \frac{1}{2}O_2 + 3H_2O \rightarrow 2Fe(III)O(OH) + 4H^+ \qquad (2.11)$$

These parasitic side reactions not only cause fouling, but also reduce the current efficiency of the process by reducing the number of electrons available for the desired reaction vs the parasitic side reactions. To reduce the undesired production of Fe(III), electromembrane processes use either porous/non-porous anion exchange membranes (AEM), or non-porous cation exchange membranes (CEM), which prevent migration of the Fe from the catholyte to the anolyte and thus prevent **Eq 2.9** and **Eq 2.10**. Additionally, membranes prevent the

transfer of the produced acid from the anolyte to the catholyte, thereby allowing for more effective acid regeneration, which can then be re-used for leaching and reducing hydrogen evolution (**Eq 2.8**). This hydrogen evolution would severely reduce the current efficiency of the EW process.

2.3.1 Porous Membrane Electrowinning

The first patent filed relating to porous membrane electrowinning of Fe was granted in 1911 to Alexander S. Ramage.[39] In the patent, a process is described where the anodes and cathodes are separated by a porous membrane, with the membrane acting as a semi-permeable barrier.[39] During the process, the reduction of Fe(II) (see **Eq. 2.6**) results in the plating of metallic Fe onto the cathode, while oxidation of water on the anode (**Eq. 2.9**) produces free protons.[39] These free protons, in turn, form sulphuric acid with the free sulphates in the solution,[39-40] showing the possible removal of Fe from the solution, coupled with the regeneration of the spend sulphuric acid.[39-40]

While showing the feasibility of Fe EW, the process was plagued with numerous challenges that reduced the efficiency of the process. According to the patent, both the anode and cathode chambers are fed using the same Fe sulphate solution. This, however, led to the oxidation of the Fe(II) at the anode according to both **Eq. 2.10** and **Eq. 2.11** as discussed above. To overcome this, the electrolytes were continuously fed with hydrogen sulphide to reduce the produced Fe(III) back to Fe(II), thereby preventing precipitation and losses in energy efficiencies by preventing **Eq. 2.7**.[11, 39] Furthermore, since no overpressure was applied on the catholyte (solution in contact with the cathode), the anolyte (solution in contact with the anode) would permeate to the cathode chambers. This resulted in the formation of hydrogen gas according to **Eq. 2.8**, reducing the effectiveness further.

Improvement upon the original 1911 patent by Alexander S. Ramage came in the form of the Pyror process that was developed between 1947 and 1957.[39-41] The Pyror process focussed on the extraction of Fe from copper-bearing pyrite ore produced at the Løkken mine in Norway. A simplified flowsheet of the process is given in **Figure 2.3**.[41] Please note that the term electrolysis was used in this flowsheet, which is interchangeable with the term electrowinning.[41]

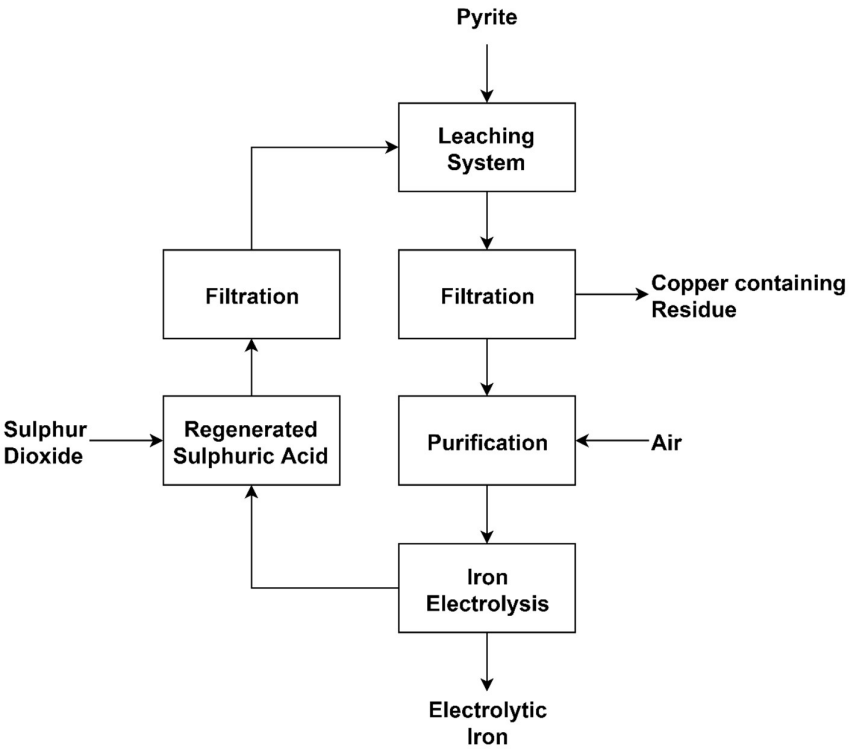

Figure 2.3: Schematic representation of the Pyror process.[41]

Although the Pyror process was largely based on the original patent, it was able to reduce various of the parasitic side reactions that occurred during the EW of Fe in the original patent, providing a process that was able to operate at a current efficiency of approximately 85 %.[41] Whereas the original patent used $FeSO_4$ as both the catholyte and anolyte, the Pyror process replaced the anolyte with a solution of Glauber Salt (Na_2SO_4) instead of the $FeSO_4$.[41] Furthermore, a porous membrane (Terylene bag) was placed around the cathode. Applying an overpressure to the catholyte prevented the migration of the anolyte into the catholyte. This resulted in two significant advantages:

Firstly, the applied overpressure in conjunction with the porous membrane significantly reduced the amount of dissolved oxygen migrating into the catholyte, reducing the oxidation of Fe(II) to Fe(III) via the dissolved oxygen side reaction (**Eq. 2.11**). Consequently, less Fe(III) had to be electrolytically reduced back to Fe(II) (**Eq. 2.7**) before forming metallic Fe (**Eq. 2.6**), thereby increasing the current efficiency. Secondly, the overpressure prevented the migration of the protons produced at the anode (**Eq. 2.9**) to the catholyte, reducing the amount of hydrogen formation (**Eq. 2.8**).[41] This served to both increase the current efficiency and improve the plating quality of the Fe by reducing hydrogen adsorption onto the plated Fe and reducing metal brittleness.[42]

A schematic illustration of the Pyror-based EW process is shown in **Figure 2.4**. Unlike the original 1911 patent regarding the EW of iron, the membrane is not used as a typical separator to divide the catholyte and anolyte cells, but rather acts as a bag enclosing the cathode, commonly referred to as a cathode bag, which is similar to that used in the EW process of Ni.[39-41, 43] During operation, the SLS (catholyte) is fed into the Terylene membrane bag surrounding the cathode, where the reduction of Fe(II) and subsequent plating of the metalling Fe occur (**Eq. 2.6**). Due to the slight overpressure applied on the cathode bag, the catholyte slowly permeates through the Terylene membrane, entering the anolyte solution. Any non-plated Fe(II) in solution is then oxidized to Fe(III), either via the dissolved oxygen produced at the anode, or through the direct contact with the anode (**Eq. 2.10** and **Eq. 2.11**). Simultaneously, the water in the anolyte containing the Na_2SO_4 added for conductivity is oxidized (**Eq. 2.9**), forming oxygen and protons that subsequently form sulfuric acid with the free sulphates present in the anolyte. The anolyte overflow, consisting of Fe(II)/Fe(III) and regenerated sulphuric acid, is subsequently aerated with hydrogen sulphide, reducing the formed Fe(III) back to Fe(II), as was described in the original 1911 patent.[41] After aeration, the catholyte solution is re-used as the leaching solution for the leaching of the pyrite ore.[41]

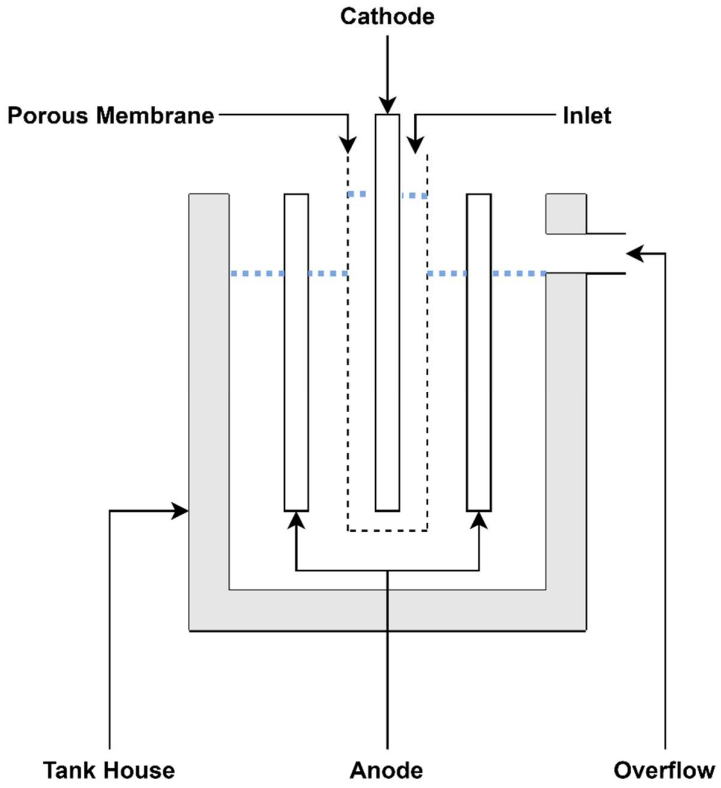

Figure 2.4: Schematic illustration of the Terylene membrane-based Pyror process.[41]

Even though the Pyror process was later discontinued due to a decline in economic conditions, it gives insight into various factors that influence the efficiency of an Fe EW process.[41] It showed, for example, that $FeSO_4$ solutions typically have a low conductivity leading to an increased energy consumption.[41] This was addressed in the Pyror process through the aforementioned addition of Na_2SO_4, which, additionally to decreasing the energy consumption, also increased the current efficiency from 65 % to 85 %. This increase in efficiency is attributed to Na^+ instead of H^+ ions being used for conductivity, reducing the amount of hydrogen reaching the cathode and thus reducing hydrogen evolution (**Eq. 2.8**).[41] Additionally, electrolyte temperature was shown to influence the EW of Fe, where an increased electrolyte temperature led to both an improvement in the plating quality and a reduced energy consumption. It is, however, clear that an economic trade-off has to be sought between electrolyte temperature and energy consumption.[37, 44]

2.3.2 Non-Porous Membrane Electrowinning

While non-porous ion exchange membranes (AEMs and CEMs) are typically used in alkaline membrane electrolysis, electrodialysis and fuel cell applications,[45] their application in Fe EW is relatively new.[46] Most AEMs offer high alkaline stability but do not necessarily exhibit the high acid- and oxidative environment stability required for the EW of Fe and the regeneration of the spent acid.[47-49] However, novel AEMs have been developed that are stable in acidic environments and, for example, have been used for the recovery of the remaining acid from SLS by means of diffusion dialysis.[36, 50-51] This electrodialysis or diffusion dialysis does, however, not treat the residual Fe in the SLS after removal of the acid and as such is not discussed further.[50, 52-54]

2.3.2.1 Anion Exchange Membrane Electrowinning

In recent years, a variety of stable AEMs suitable for the EW of Fe have been developed that are mostly prepared by blending polymers to provide both anion conductivity and stability.[30] Typically, these blends contain an anion exchange polymer (or its halo-methylated precursor) and a chemically and mechanically stabilising matrix polymer. By combining polymers such as a stable polybenzimidazole and a sulphonated anion-exchange polymer, ionic cross-links are formed which further chemically stabilize the blended AEMs.[30] In a recent study, a 3-component blended membrane consisting of i) poly(2,6-dimethyl-1,4-phenylene oxide) (PPO) quaternized with tetra-methylimidazole, ii) a polybenzimidazole as the matrix polymer, and iii) a sulphonated polymer as ionic cross-linker, showed excellent stability and performance in

both acidic and oxidative environments.[30] The first method employing the use of an AEM for the EW of Fe was patented in 1957 by Bodamer and Collins.[55] It is, amongst others, the aim of this study to evaluate the suitability of such novel membranes for the EW of Fe using an electromembrane process.

While the Pyror process resulted in a significant improvement on the original 1911 patent, it still had the challenge that eventually Fe(II) migrated from the catholyte to the anolyte, resulting in the oxidation to Fe(III) with all the related disadvantages discussed previously.[35, 39, 41] Additionally, the movement of protons from the anolyte through the porous bag to the catholyte was not completely prevented by the slight overpressure, resulting in hydrogen evolution at the anode.[35, 39, 41] The use of a non-porous AEM would prevent, or significantly reduce, both the transfer of Fe from the catholyte to the anolyte and the transfer of protons from the anolyte to the catholyte, thereby preventing the two parasitic side reactions (**Eq. 2.7** and **Eq. 2.8**) that reduce the efficiency of the Fe EW process.[47, 56] In addition, the separation of the catholyte and anolyte by a non-porous membrane should increase the concentration of the acid in the anolyte, as it is not diluted by the catholyte diffusing into the anolyte, as is the case in the Pyror process.

The compartmentalized cell design commonly used when employing an AEM is illustrated in **Figure 2.5**.[54-55] During the process, the catholyte, consisting of $FeSO_4$ (unspent acid can be neutralized beforehand using $FeCO_3$), is circulated over the cathode where Fe(II) is electrochemically reduced to metallic Fe (**Eq. 2.6**), depleting the Fe(II) in solution. Simultaneously, the water in the anolyte, with added Na_2SO_4 for conductivity, is oxidized on the anode (**Eq. 2.9**), producing protons that form sulphuric acid with the sulphate ions in solution. During operation, the AEM prevents the migration of both Fe species (preventing the oxidation of Fe(II) to Fe(III)) and sulphuric acid into the anolyte. Such an AEM-EW process was patented by Cardarelli in 2011.[56] With a certain embodiment of the patent, he was able to obtain a current efficiency of 98 % and a SEC of 3.42 kWh/kg Fe, which is a significant improvement on the Pyror process, which operated at a current efficiency of 85 % and an SEC of 4.25 kWh/kg Fe. The increase in the current efficiency attained with the AEM process is attributed to the elimination of parasitic reactions (**Eq. 2.7**, **2.8**, **2.10** and **2.11**),[56] and clearly illustrates the advantages offered by an AEM-based EW process compared to the porous membrane-based process.

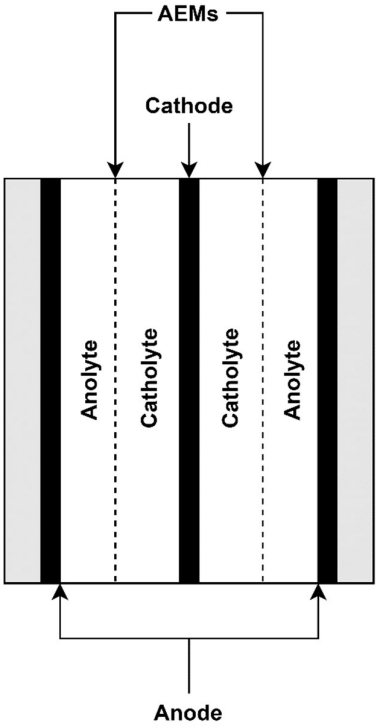

Figure 2.5: Schematic illustration of an iron electrowinning process using an AEM to separate the anolyte and catholyte.[56]

It is interesting to note that the patent filed by Cardarelli in 2011 also used dimensionally stable type oxygen-evolving anodes (DSA-O2), instead of the typically used lead alloys.[35, 39, 55-57] These alternative anode materials allowed higher current densities to be maintained during the process due to the catalytic water oxidation properties of DSA-O2 anodes, yielding lower water oxidation overpotentials.[56, 58] Additionally, DSA-02 anodes have longer lifetimes compared to their lead alloy-based counterparts due to their higher corrosion resistance.[58-59] However, despite the advantages of using DSA-02 anodes, the technology has not been widely adopted due to the cost and the difficulties encountered during the large scale manufacturing of the anodes.[60] The increased costs can be attributed to i) the cost of the material, ii) temperatures exceeding 750 °C required for the coating of the base titanium anode with IrO_2 and iii) the common occurrence of defects in the crystalline coating.[60]

Both patents from 2011 and 1954 used elevated temperatures during EW to decrease the voltage required while improving the ductility of the plated Fe, which is in accordance with the observations made from the Pyror process.[55-56] These findings corroborated what has been reported in a patent published in 1909, in which the ductility of the plated iron was improved by increasing the electrolyte temperature to 70 °C.[40]

2.3.2.2 *Anion/Cation Exchange Membrane Electrowinning*

As discussed earlier, traditional diffusion dialysis methods have been successfully used to recover the spent acid from SLSs. However, additional treatment steps are required for the removal of the metal species from the SLSs.[49, 51, 53-54, 61] These additional steps could include, amongst others, jarosite, goethite or hematite precipitation.[51, 62] However, simultaneous acid recovery and metal removal can be achieved using both an AEM and a CEM.[51, 63-64] In such an AEM/CEM configuration (**Figure 2.6**), the prior neutralization of the unspent acid in the catholyte is not required.[56, 64]

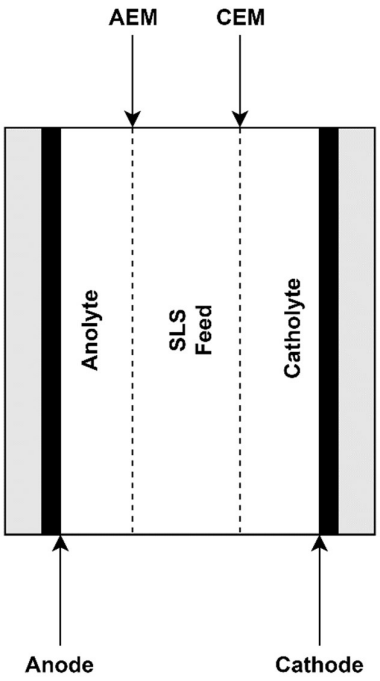

Figure 2.6: Simplified illustration of an EW process for simultaneous acid recovery and Fe EW.

In this configuration, the SLS (containing unspent acid and metal) is fed into a central chamber with a CEM between the feed and the cathode, and an AEM between the feed and the anode.[56] During operation, the Fe(II) species from the feed cross the CEM where it is electrolytically plated onto the cathode (**Eq. 2.6**), while the sulphate ions cross the AEM to form sulphuric acid by combining with the free protons generated by the oxidation of water on the anode (**Eq. 2.9**).[56] This simultaneous EW and acid recovery of SLSs is mostly used for the recovery of zinc from spent pickling solutions. However, despite the benefits offered by the simultaneous

recovery of the metal and acid using an AEM and CEM, operational challenges were observed.

One such problem was a high overpotential that was required for operation, caused by the electrical resistance of the membranes that was obtained irrespective of the potential conductivity of the membranes. Additionally, the CEM, which here acts as a separator between the feed and the catholyte, has a significantly higher proton flux compared to the proton flux of an AEM. This results in an increased hydrogen production at the cathode (**Eq. 2.8**) reducing the current efficiency of the process,[30] paired with an increased hydrogen adsorption leading to brittleness of the plated metallic Fe. It was mentioned previously that many of the more novel AEMs are highly stable in oxidative environments. CEMs, however, do not offer the high stability in such environments and undergo degradation significantly faster.[30] One of the reasons for the higher stability of AEMs comes from the Donnan exclusion of the oxidative Fe(II) species from the internal structure of the membrane. When using a CEM, the Fe(II) must be present in the internal structure of the CEM to facilitate the transport to the catholyte.[30] This presence of Fe(II) contributes to the faster degradation of the internal structure of the CEM.[30]

2.3.3.3 Liquid-Liquid Extraction and Diffusion Dialysis

The final and perhaps most complicated electromembrane process was patented by Watanabe *et al* in 1978. A simplified flowsheet thereof is presented in **Figure 2.7**.[65] By combining liquid-liquid extraction (LLE) and electrodialysis, the unspent acid is recovered and the Fe(II) is removed from the solution as metallic Fe.[65] According to the patent, the Fe(II) present in the SLS is oxidized to Fe(III) through electrolysis in a preliminary unit, after which the Fe(III) ions are selectively extracted using a suitable solvent.[65] During the extraction phase, 75 % of the Fe(III) is removed from the SLS into an organic phase containing 30 % D2EHPA (extractant), 5 % octanol (modifier), and kerosene as the diluent.[65-66] Subsequently, the aqueous SLS with a reduced Fe content and unspent acid can be re-used for leaching.[65]

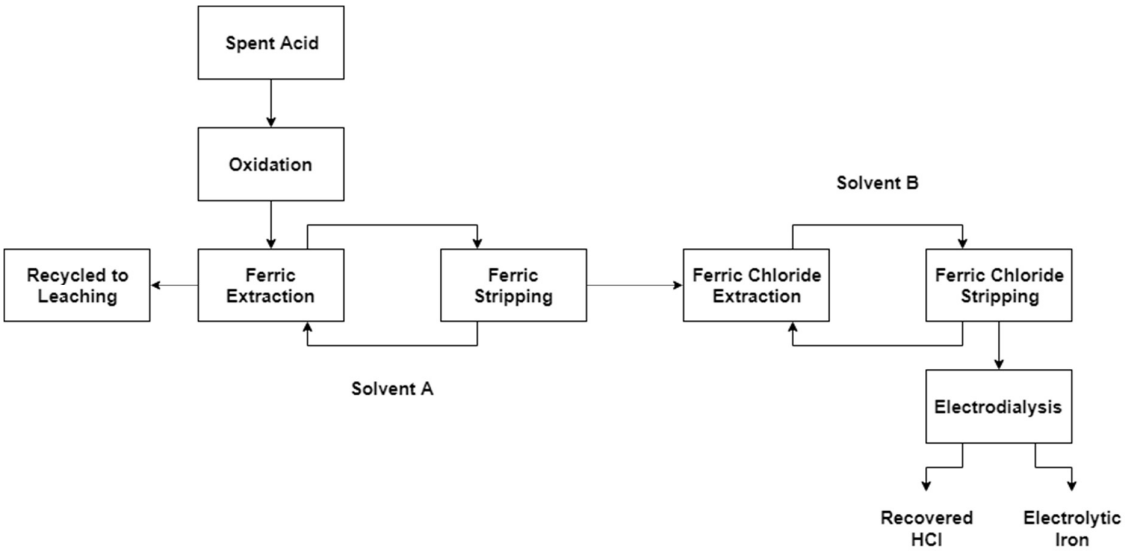

Figure 2.7: Flowsheet of a liquid-liquid extraction method for iron-rich sulphate solutions as patented by Watanabe et al. in 1978.[65]

After extraction, the Fe(III) in the organic phase is stripped from the solvent using hydrochloric acid.[65-66] The Fe(III) is subsequently removed from the hydrochloric acid strippant through contacting with a second solvent containing 50 % tributyl phosphate (TBP). During the second stripping, the Fe(III) is stripped from the TBP using water, resulting in a Fe(III) chloride solution.[65] After the two extractions, the Fe(III) chloride solution is sent to an electrodialysis unit as the catholyte, where the Fe(III) is plated as metallic Fe by first reducing it to Fe(II) according to **Eq. 2.7**, followed by reduction to Fe_s (**Eq. 2.6**). The now depleted hydrochloric acid is subsequently fed as the anolyte to the electrodialysis unit where it is regenerated using the protons produced during the oxidation of water at the anode (**Eq. 2.9**). The regenerated acid can then be re-used for the first stripping of the Fe(III) from the D2EHPA solvent.[65]

Although the process avoids the use of CEMs and has the capability to recover the unspent acid in the SLS, it is not widely used. This can be attributed to the complexity of the process, cost of operation and various health concerns regarding the numerous chemicals used. The complexity of the process is significant, requiring multiple steps for the removal of the Fe from the SLS, compared to the previous methods discussed only requiring a single operation.[65] Furthermore, the organic solvents used during this process are expensive, with significant losses during the process due to the degradation of the extractants in the presence of hydrochloric acid.[67] Finally, the regeneration of hydrochloric acid in an electrodialysis cell carries extensive safety concerns due to the parasitic reactions resulting in the formation of chlorine gas.[37] All of these factors combined have prohibited the successful implementation of

this patent in spite of its simultaneous recovery of the unspent acid and removal of the Fe as metallic Fe from the SLS.

2.4 Conclusion

It is evident that, in spite of various treatment methods, Fe SLS streams still present a significant challenge to the scientific and engineering community. The majority of the traditional treatment methods (Section 2.2) do not yield marketable end products, while often having a negative impact on the environment. This has led to more research into the suitability of electromembrane processes (Section 2.3) for the treatment of the SLSs. It was shown that electromembrane processes can both remove the Fe as metallic Fe and regenerate the spent sulphuric acid from an Fe SLS, thereby alleviating the operational costs related to SLS disposal.

Electromembrane processes can use either porous or non-porous membranes. While the Pyror process (Section 2.3.1), using a porous membrane, is easy to operate, it has the disadvantage of using hydrogen sulphide, contains operations inefficiencies and cannot concentrate high acidic values. For non-porous membranes, an AEM, an AEM/CEM and an LLE/diffusion dialysis process was discussed. While being interesting, both the AEM/CEM and LLE/diffusion dialysis processes are fairly complicated with specific disadvantages, including cost, safety concerns and operational risks.

Although various patents showcase the viability and advantages of anion exchange membrane electrowinning (AEM-EW), they did not optimize the operational conditions, nor rigorously evaluate the economic viability of the process. Although the AEM-EW process yields marketable and valuable products, the low value of the metallic Fe and regenerated acid will have to be balanced against sufficiently low operating costs. To address this, research on the effect of various operating and process parameters such as Na_2SO_4 concentration, electrolyte temperature, AEM type and stability, amount of acid recovered, and scalability of an AEM-EW process needs to be conducted.

2.5 Bibliography

1. Sinisalo, P.; Lundström, M., Refining Approaches in the Platinum Group Metal Processing Value Chain—A Review. *Metals* **2018,** *8* (4), 203.
2. Kramer, J.; Driessen, W. L.; Koch, K. R.; Reedijk, J., Highly selective extraction of platinum group metals with silica-based (poly) amine ion exchangers applied to industrial metal refinery effluents. *Hydrometallurgy* **2002,** *64* (1), 59-68.
3. Forbes, P.; van Blottnitz, H.; Gaylard, P.; Petrie, J. G., Environmental assessment of base metal processing: a nickel refining case study. *Journal of the Southern African Institute of Mining and Metallurgy* **2000,** *100* (6), 347-353.
4. Rule, C. M., Energy considerations in the current PGM processing flowsheet utilizing new technologies. *J S Afr I Min Metall* **2009,** *109* (1), 39-46.
5. Mwase, J. M.; Petersen, J.; Eksteen, J. J., A conceptual flowsheet for heap leaching of platinum group metals (PGMs) from a low-grade ore concentrate. *Hydrometallurgy* **2012,** *111*, 129-135.
6. Liddell, K. S.; Adams, M. D., Kell hydrometallurgical process for extraction of platinum group metals and base metals from flotation concentrates. *Journal of the Southern African Institute of Mining and Metallurgy* **2012,** *112* (1), 31-36.
7. Hu, X. L.; Chen, W. M.; Xie, Q. L., Sulfur phase and sulfur removal in high sulfur-containing bauxite. *Transactions of Nonferrous Metals Society of China* **2011,** *21* (7), 1641-1647.
8. Cramer, L. A.; Basson, J.; Nelson, L. R., The impact of platinum production from UG2 ore on ferrochrome production in South Africa. *J S Afr I Min Metall* **2004,** *104* (9), 517-527.
9. Johnson, D. B.; Hallberg, K. B., Acid mine drainage remediation options: a review. *Sci Total Environ* **2005,** *338* (1-2), 3-14.
10. Harris, H. J. Method of preventing precipitation of iron compounds from an aqueous solution. 1964.
11. Morgan, B.; Lahav, O., The effect of pH on the kinetics of spontaneous Fe (II) oxidation by O2 in aqueous solution–basic principles and a simple heuristic description. *Chemosphere* **2007,** *68* (11), 2080-2084.
12. Song, Y. W.; Wang, M.; Liang, J. R.; Zhou, L. X., High-rate precipitation of iron as jarosite by using a combination process of electrolytic reduction and biological oxidation. *Hydrometallurgy* **2014,** *143*, 23-27.
13. Ozkan, S.; Ipekoglu, B., Investigation of environmental impacts of tailings dams. *Environmental Management and Health* **2002,** *13* (3), 242-248.
14. Franks, D. M.; Boger, D. V.; Cote, C. M.; Mulligan, D. R., Sustainable development principles for the disposal of mining and mineral processing wastes. *Resources Policy* **2011,** *36* (2), 114-122.
15. Rico, M.; Benito, G.; Diez-Herrero, A., Floods from tailings dam failures. *J Hazard Mater* **2008,** *154* (1-3), 79-87.
16. Cudennec, Y.; Lecerf, A., The transformation of ferrihydrite into goethite or hematite, revisited. *Journal of Solid State Chemistry* **2006,** *179* (3), 716-722.

17. Kefeni, K. K.; Msagati, T. A. M.; Mamba, B. B., Acid mine drainage: Prevention, treatment options, and resource recovery: A review. *Journal of Cleaner Production* **2017,** *151*, 475-493.

18. Akcil, A.; Koldas, S., Acid Mine Drainage (AMD): causes, treatment and case studies. *Journal of Cleaner Production* **2006,** *14* (12-13), 1139-1145.

19. Cravotta, C. A., 3rd, Size and performance of anoxic limestone drains to neutralize acidic mine drainage. *J Environ Qual* **2003,** *32* (4), 1277-89.

20. Watzlaf, G. R.; Schroeder, K. T.; Kairies, C. L., Long-term performance of anoxic limestone drains. *Mine Water and the Environment* **2000,** *19* (2), 98-110.

21. Hedin, R. S.; Watzlaf, G. R., The effects of anoxic limestone drains on mine water chemistry. *USBM SP A* **1994,** *6*, 185-194.

22. Spiro, T. G.; Allerton, S. E.; Renner, J.; Terzis, A.; Bils, R.; Saltman, P., The hydrolytic polymerization of iron (III). *Journal of the American Chemical Society* **1966,** *88* (12), 2721-2726.

23. Dutrizac, J. E., The effect of seeding on the rate of precipitation of ammonium jarosite and sodium jarosite. *Hydrometallurgy* **1996,** *42* (3), 293-312.

24. Langová, Š.; Riplová, J.; Vallová, S., Atmospheric leaching of steel-making wastes and the precipitation of goethite from the ferric sulphate solution. *Hydrometallurgy* **2007,** *87* (3-4), 157-162.

25. Daoud, J.; Karamanev, D., Formation of jarosite during Fe2+ oxidation by Acidithiobacillus ferrooxidans. *Minerals Engineering* **2006,** *19* (9), 960-967.

26. Ren, X.; Wei, Q.; Hu, S.; Wei, S., The recovery of zinc from hot galvanizing slag in an anion-exchange membrane electrolysis reactor. *J Hazard Mater* **2010,** *181* (1-3), 908-15.

27. Carrillo-Abad, J.; Garcia-Gabaldon, M.; Ortiz-Gandara, I.; Bringas, E.; Urtiaga, A. M.; Ortiz, I.; Perez-Herranz, V., Selective recovery of zinc from spent pickling, baths by the combination of membrane-based solvent extraction and electrowinning technologies. *Separation and Purification Technology* **2015,** *151*, 232-242.

28. Chang, Y. F.; Zhai, X. J.; Li, B. C.; Fu, Y., Removal of iron from acidic leach liquor of lateritic nickel ore by goethite precipitate. *Hydrometallurgy* **2010,** *101* (1-2), 84-87.

29. Acero, P.; Ayora, C.; Torrento, C.; Nieto, J. M., The behavior of trace elements during schwertmannite precipitation and subsequent transformation into goethite and jarosite. *Geochimica Et Cosmochimica Acta* **2006,** *70* (16), 4130-4139.

30. Badenhorst, W. D.; Rossouw, C.; Cho, H.; Kerres, J.; Bruinsma, D.; Krieg, H., Electrowinning of Iron from Spent Leaching Solutions Using Novel Anion Exchange Membranes. *Membranes (Basel)* **2019,** *9* (11), 137.

31. Dutrizac, J. E.; Riveros, P. A., The precipitation of hematite from ferric chloride media at atmospheric pressure. *Metall Mater Trans B* **1999,** *30* (6), 993-1001.

32. Yamaguchi, T.; Kimura, T., Kinetic Studies on the Precipitation of Hematite from Iron-Rich Spinel Solid Solutions. *Journal of the American Ceramic Society* **1976,** *59* (7-8), 333-335.

33. Onozaki, A.; Sato, K.; Kuramochi, S., Effect of some impurities on iron precipitation at the Iijima Zinc Refinery. *Iron Control in Hydrometallurgy* **1986**, 742-752.

34. Kunda, W.; Veltman, H., Decomposition of jarosite. *Metallurgical Transactions B* **1979,** *10* (3), 439-446.

35. Cain, J. R., Electrolytic process for the regeneration of pickle liquor. Google Patents: 1934.

36. Regel-Rosocka, M., A review on methods of regeneration of spent pickling solutions from steel processing. *J Hazard Mater* **2010,** *177* (1-3), 57-69.

37. Atkins, P.; De Paula, J.; Keeler, J., *Atkins' physical chemistry*. Oxford university press: 2018.

38. Crowe, C. W. Method of preventing precipitation of ferrous sulfide and sulfur during acidizing. 1987.

39. Ramage, A. S., Process of making sulfuric acid and electrolytic iron. Google Patents: 1911.

40. Fischer, F., Process for the manufacture of ductile electrolytic iron. Google Patents: 1911.

41. Mostad, E.; Rolseth, S.; Thonstad, J., Electrowinning of iron from sulphate solutions. *Hydrometallurgy* **2008,** *90* (2-4), 213-220.

42. Lupi, C.; Pilone, D., Electrodeposition of nickel□ cobalt alloys: the effect of process parameters on energy consumption. *Minerals Engineering* **2001,** *14* (11), 1403-1410.

43. Elliott, R. W.; Ambrose, J.; Ettel, V. A., Electrowinning of sulfur-containing nickel. Google Patents: 1978.

44. Reipa, V.; Holden, M. J.; Mayhew, M. P.; Vilker, V. L., Temperature dependence of the formal reduction potential of putidaredoxin. *Biochim Biophys Acta* **2000,** *1459* (1), 1-9.

45. Merle, G.; Wessling, M.; Nijmeijer, K., Anion exchange membranes for alkaline fuel cells: A review. *Journal of Membrane Science* **2011,** *377* (1-2), 1-35.

46. Kerres, J. A.; Krieg, H. M., Poly(vinylbenzylchloride) Based Anion-Exchange Blend Membranes (AEBMs): Influence of PEG Additive on Conductivity and Stability. *Membranes (Basel)* **2017,** *7* (2), 32.

47. Varcoe, J. R.; Atanassov, P.; Dekel, D. R.; Herring, A. M.; Hickner, M. A.; Kohl, P. A.; Kucernak, A. R.; Mustain, W. E.; Nijmeijer, K.; Scott, K.; Xu, T. W.; Zhuang, L., Anion-exchange membranes in electrochemical energy systems. *Energy & Environmental Science* **2014,** *7* (10), 3135-3191.

48. Arges, C. G.; Ramani, V., Investigation of Cation Degradation in Anion Exchange Membranes Using Multi-Dimensional NMR Spectroscopy. *Journal of the Electrochemical Society* **2013,** *160* (9), F1006-F1021.

49. Tongwen, X.; Weihua, Y., Tuning the diffusion dialysis performance by surface cross-linking of PPO anion exchange membranes—simultaneous recovery of sulfuric acid and nickel from electrolysis spent liquor of relatively low acid concentration. *Journal of hazardous materials* **2004,** *109* (1-3), 157-164.

50. Agrawal, A.; Sahu, K. K., An overview of the recovery of acid from spent acidic solutions from steel and electroplating industries. *J Hazard Mater* **2009,** *171* (1-3), 61-75.

51. Luo, J. Y.; Wu, C. M.; Xu, T. W.; Wu, Y. H., Diffusion dialysis-concept, principle and applications. *Journal of Membrane Science* **2011,** *366* (1-2), 1-16.

52. Stachera, D. M.; Childs, R. F.; Mika, A. M.; Dickson, J. M., Acid recovery using diffusion dialysis with poly(4-vinylpyridine)-filled microporous membranes. *Journal of Membrane Science* **1998,** *148* (1), 119-127.

53. Tongwen, X.; Weihua, Y., Industrial recovery of mixed acid (HF+ HNO3) from the titanium spent leaching solutions by diffusion dialysis with a new series of anion exchange membranes. *Journal of membrane science* **2003,** *220* (1-2), 89-95.

54. Tongwen, X.; Weihua, Y., Sulfuric acid recovery from titanium white (pigment) waste liquor using diffusion dialysis with a new series of anion exchange membranes—static runs. *Journal of Membrane Science* **2001,** *183* (2), 193-200.

55. Bodamer, G. W.; Collins, H., Electrolytic treatment of waste sulfate pickle liquor. Google Patents: 1957.

56. Cardarelli, F., Electrochemical process for the recovery of metallic iron and sulfuric acid values from iron-rich sulfate wastes, mining residues and pickling liquors. Google Patents: 2011.

57. Fahlstrom, P. A. H. H.; Mioen, T. K.; Bjorling, G. E., Method for extracting and recovering iron and nickel in metallic form. Google Patents: 1977.

58. Msindo, Z.; Sibanda, V.; Potgieter, J. H., Electrochemical and physical characterisation of lead-based anodes in comparison to Ti–(70%) IrO 2/(30%) Ta 2 O 5 dimensionally stable anodes for use in copper electrowinning. *Journal of applied electrochemistry* **2010,** *40* (3), 691-699.

59. Mirza, A.; Burr, M.; Ellis, T.; Evans, D.; Kakengela, D.; Webb, L.; Gagnon, J.; Leclercq, F.; Johnston, A., Corrosion of lead anodes in base metals electrowinning. *Journal of the Southern African Institute of Mining and Metallurgy* **2016,** *116* (6), 533-538.

60. Comninellis, C.; Plattner, E. In *Characterization of DSA type oxygen (DSA-O2) evolving electrodes*, Proceedings of the Symposium on Performance of Electrodes for Industrial Electrochemical Processes, Electrochemical Society: 1989; p 229.

61. Rogener, F.; Sartor, M.; Ban, A.; Buchloh, D.; Reichardt, T., Metal recovery from spent stainless steel pickling solutions. *Resour Conserv Recy* **2012,** *60*, 72-77.

62. Simate, G. S.; Ndlovu, S., Acid mine drainage: Challenges and opportunities. *Journal of Environmental Chemical Engineering* **2014,** *2* (3), 1785-1803.

63. Negro, C.; Blanco, M. A.; Lopez-Mateos, F.; DeJong, A. M. C. P.; LaCalle, G.; Van Erkel, J.; Schmal, D., Free acids and chemicals recovery from stainless steel pickling baths. *Separation Science and Technology* **2001,** *36* (7), 1543-1556.

64. Marti-Calatayud, M. C.; Buzzi, D. C.; Garcia-Gabaldon, M.; Ortega, E.; Bernardes, A. M.; Tenorio, J. A. S.; Perez-Herranz, V., Sulfuric acid recovery from acid mine drainage by means of electrodialysis. *Desalination* **2014,** *343*, 120-127.

65. Watanabe, M.; Nishimura, S., Process for recovery of waste H2 SO4 and HCl. Google Patents: 1978.

66. Meerholz, K.; van der Westhuizen, D. J.; Krieg, H. M., Automation of membrane based solvent extraction unit for Zr and Hf separation. *Separation and Purification Technology* **2017,** *179*, 204-214.

67. Azam, M.; Alam, S.; Khan, F., The solubility/degradation study of organophosphoric acid extractants in sulphuric acid media. *Journal of Chemical Engineering* **2010**, 18-21.

CHAPTER 3

Characterization and Optimization of Process Variables

Table of Contents

3.1 Introduction

As discussed in Chapter 2, electrowinning (EW) is an alternative treatment method for spent leaching solutions (SLS), which can produce electrolytic iron (Fe) while allowing for the regeneration of sulphuric acid (H_2SO_4). Since SLSs containing iron are traditionally not treated using EW, the effect of various process parameters on the EW process performance has not yet been well documented in literature. While the influence of various parameters such as boric acid (H_3BO_3), temperature, catholyte/anolyte pH and the effect of sodium sulphate (Na_2SO_4) are well known for metals such as nickel (Ni), information regarding the EW of iron is mostly limited to patent applications.[1-3] Hence, to determine the suitability of EW for the recovery of iron from SLSs, the influence of the above-mentioned parameters on the EW of iron from the SLSs should be investigated. Considering the low intrinsic value of iron compared to metals such as Ni, it is also desirable to optimize the cost-effectiveness of iron EW (by optimizing efficiency and specific energy consumption) to ultimately yield a commercially competitive alternative processing technology.

There are various important parameters when optimizing the EW of an SLS. It was shown in the previous chapter that the configuration, i.e. a cell without and with a porous or non-porous membrane, influences the effectiveness of EW and should be investigated. When considering the process itself, one parameter where opposing views are currently held involves the use of H_3BO_3 for EW. While H_3BO_3 acts as a pH buffer, its effectiveness in preventing excessive H_2 gas formation during EW has been disputed.[3-5] For this reason, characterizing the effect of H_3BO_3 on the EW of iron is important, since its addition may lead to extra operating costs, while possibly causing further process complications.[6] An additional parameter that can have a substantial effect on the EW process is temperature, where an increase in temperature to a certain point is known to lead to a reduction in the required applied potential, which reduces the specific energy consumption (SEC) of the EW process.[7] The reason for this seems to be that the energy required for the reduction of iron at elevated temperatures is obtained from both the electrical potential and the thermal energy applied to the system.[7]

Another variable to be considered is the influence of unspent acid in the catholyte on the efficiency, as high concentrations of H_2SO_4 can lower the current efficiency both through excessive H_2 production (**Table 2.1**) and leaching of the starter iron sheet. Similarly, high acid concentrations in the anolyte can reduce the effectiveness of the EW process by means of proton tunnelling through the membrane to the catholyte, where it can again lead to the aforementioned parasitic reactions.

During EW, sodium sulphate (Na_2SO_4) is commonly added to increase the conductivity of the solution, thereby reducing the required electrical potential and thus the SEC. Concurrently, the charge carrying capability of Na_2SO_4, where the Na^+ ions replace the H^+ ions for charge transport, reduces the H_2 gas evolution on the cathode.[8-9] Similarly, the iron concentration can affect the conductivity of the solution while an absence of iron on the cathode can lead to water reduction, which can further lead to hydrogen gas and hydroxide formation. Therefore, the effect of low iron concentrations, as well as iron depletion during operation, should also be tested at both low and high Na_2SO_4 concentrations. Finally, the advances made in the field of anion exchange membranes (AEMs) relating to their selectivity, conductivity and stability have led to their use in an increasing number of processes.[10-12] It would therefore be interesting to evaluate the influence of such AEMs during the EW of iron from SLSs on the performance (current efficiency, acid retention, applied voltage and iron flux) as well as the design and cost of such a process.

It is therefore the aim of this chapter to evaluate the influence of the parameters described above on the performance of the EW of Fe from a simulated SLS. This will be done by firstly comparing three configurations of EW cells before investigating the effect of boric acid, temperature, catholyte/anolyte pH, Na_2SO_4, varying AEMs and iron on the performance of an EW based process for the recovery of Fe from a simulated SLS.

3.2 Materials and Methods

In this section, the cells developed for this study are presented (Section 3.2.1), before discussing the conditions used to determine the influence of the variables discussed above (Section 3.2.2).

3.2.1 EW Cells

For all EW experiments presented in the chapter, two in-house manufactured custom-made EW cells (**Figure 3.**) were used, one without a membrane and one with a membrane. Both cells were constructed from 10 mm thick polycarbonate sheets with an anode-cathode distance (ACD) of 20 mm. All experiments were batch experiments with either an electrolyte reservoir (non-separated cell) or a catholyte and anolyte reservoir (membrane-separated cell). Where no membrane was used in the non-separated cell (**Figure 3.1a**), either a porous Terylene membrane (to replicate the Pyror EW process),[9] or an AEM was used in the divided cell (**Figure 3.1b**). In both cases, the anode (half-reaction: $H_2O \rightarrow ½O_2 + H^+ + 2e^-$) was constructed of 2 mm thick lead doped with 0.06% Cu (Castle Lead Works). The lead plate was

passivated (PbO_2 coating on its surface) through AEM-EW of a solution containing 40 g/L Fe (using $FeSO_4.7H_2O$, ACE Chemicals, 99 %) and 60 g/L Na_2SO_4 (ACE Chemicals, 99 %) as catholyte with a 60 g/L Na_2SO_4 anolyte for 5 hours at 70 °C using the FAB-PK-130 membrane in the membrane-separated flow cell.[13] The cathode starter plate (half-reaction: $Fe^{2+} + 2e^- \rightarrow Fe_{(s)}$) consisted of 316 stainless steel, with the plated deposits being removed after each 5-hour run in order to keep the ACD constant throughout testing. A superficial flow velocity of 1 cm/s of both the catholyte and anolyte (or electrolyte in the case of the non-separated cell) was maintained between the electrodes and the membrane surface. This relatively high flow rate was chosen to minimize the concentration gradients over the electrode and membrane surfaces. Moreover, the cell was fitted with inlet and outlet flow dividers to prevent the formation of dead zones over the cathode, anode, and membrane.

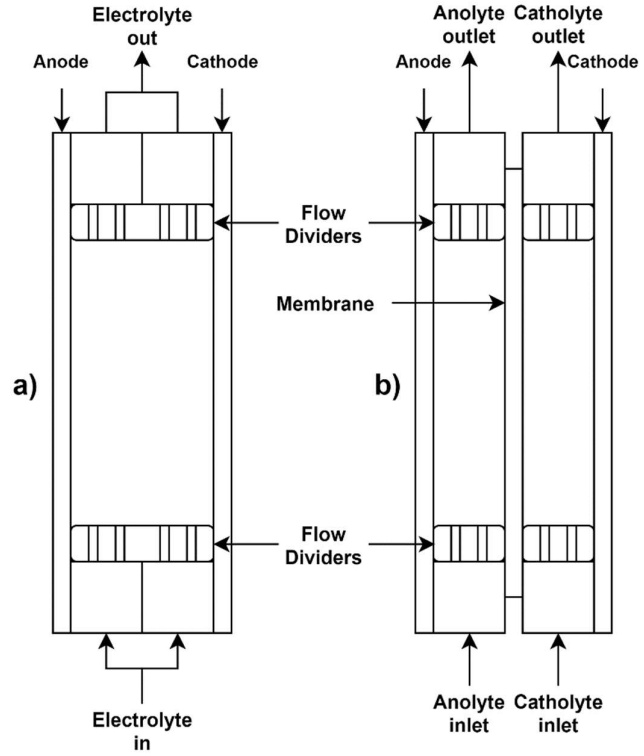

Figure 3.1: Diagram of the non-separated (a) and the membrane-separated flow cells (b) used in this study.

The temperature of the electrolytes was controlled using an externally circulating water bath (Julabo FP50-HL) with the electrolyte solutions in jacketed flasks. All the experiments were conducted at a constant current density of 300 A/m^2, which requires a constant current of 0.48 A being applied to the 0.0016 m^2 electrode area (4 cm x 4 cm plates). The constant current was applied using a galvanostatic power source (BioLogic HCP-803 or the BioLogic SP 204)

and regulating the applied voltage. The voltages were recorded at hourly intervals to determine the SEC of the process.

Samples of 10 ml each were taken from the electrolytes hourly for 5 hours, where the first sample was taken before the potential was applied. The iron content in the samples was analysed using ICP-OES (Agilent 5110). Furthermore, the pH of the samples was measured using a Metrohm 774 pH meter with a Unitrode 6.0258.010 electrode. To determine the amount of iron plated after 5 hours, the cathode was weighed before and after each experiment (Gibertini, Europe 500). The change in mass, in conjunction with the applied voltage, was then used to determine both the current efficiency (**Eq 3.1**) and the SEC (**Eq. 3.2**) of the process.

$$Current\ efficiency\ (\%)\ =\ \frac{(m_f - m_i)}{(\frac{It}{nF})M}\ x\ 100\ \% \tag{3.1}$$

where m_f and m_i refer to the final and initial cathode mass (g), respectively, I is the applied current (A), t is the time (s), n is the number of electrons transferred, F is Faraday's constant (96.485 sA/mol) and M is the molecular weight of Fe (g/mol). Similarly, the SEC expressed in kilowatt-hours per kilogram of iron plated was determined using **Eq. 3.2** where V is the applied potential (V) and m the total mass plated on the cathode (g) over time (t).

$$SEC\ (kWh/kg)\ =\ \frac{IV}{m/t} * 3600 \tag{3.2}$$

3.2.2 Variables

The investigation of the first variable (Section 3.2.2.1) entailed the evaluation of the three configurations (the non-separated cell as well as the Terylene- and AEM-separated cells). All other variables (Section 3.2.2.2 – 3.2.2.7) were investigated using only the AEM-divided cell. In this section, only three variables were kept constant, namely the electrode area of 4x4 cm, the current density of 300 A/m^2 and the superficial velocity of 1 cm/s. Unless noted otherwise, experiments were run for 5 h at an electrolyte temperature of 70 °C.

3.2.2.1 EW Configuration

Non-Divided Cell

For the EW without a membrane, using the setup shown in **Figure 3.a**, 500 ml of electrolyte was prepared by dissolving 398 g $FeSO_4.7H_2O$ (ACE Chemicals, 99%) in deionised water to obtain an 80 g/L Fe solution. Additionally, 60 g/L Na_2SO_4 (ACE Chemicals, 99%) was added as supporting electrolyte.[9]

Divided Cell Using a Porous (Terylene) Membrane

For the porous membrane-divided cell configuration, a DP580 Terylene membrane, supplied by Clear Edge Filtration SA (Pty) Ltd, was used to separate the cathode and anode (**Figure 3.b**). While the flowrates of the catholyte and anolyte were kept constant at a superficial velocity of 1 cm/s, the catholyte tank was raised by approximately 10 cm compared to the anolyte vessel to provide a slight head on the catholyte compartment. This resulted in the slow permeation of the catholyte into the anolyte solution through the porous membrane. The catholyte was prepared in the same manner as the electrolyte used in the non-separated cell study, i.e. consisting of a 500 ml solution containing 80 g/L Fe (as $FeSO_4.7H_2O$), 60 g/L Na_2SO_4 and in this case also 10 g/L H_3BO_3 (ACE Chemicals, 99.9 %). The 500 ml anolyte solution contained only 60 g/L Na_2SO_4 as supporting electrolyte.[9]

Divided Cell Using An AEM

A non-porous AEM was tested using the separated cell (**Figure 3.1b**). The same volume and composition of catholyte and anolyte as discussed in the Terylene experiments were used. For benchmarking, a commercial AEM (FAB-PK-130) obtained from Fumatech GmbH was used. The AEM was pre-treated in a 0.5 M NaCl solution (ACE Chemicals 99.9 %) at 25 °C for 24 hours before being used in the EW cell. Again, a superficial flow rate of 1 cm/s was used.

3.2.2.2 Boric Acid

To determine the effect of boric acid on the EW of iron, the AEM-EW cell was used. The catholyte contained 80 g/L Fe, 60 g/L Na_2SO_4, and 10 g/L EDTA (ACE Chemicals, 99 %) with either 0 or 10 g/L boric acid being added, while the anolyte contained 60 g/L Na_2SO_4. During testing with and without boric acid, the EW cell was operated with the FAB-PK-130 membrane.

3.2.2.3 Catholyte/Anolyte pH

Catholyte pH

As the SLS finds its origin from the leaching process, it could contain unspent acid when sent to the EW unit. Therefore, varying amounts of H_2SO_4 (0, 12.5 or 25 g/L, LabChem 98 %) was added to the catholyte to simulate unspent acid being sent to the EW unit and to determine the effect of such unspent acid. During testing of the AEM (FAB-PK-130), the EW cell was used with a catholyte containing 80 g/L Fe, 60 g/L Na_2SO_4 and 10 g/L EDTA, while the anolyte contained 60 g/L Na_2SO_4. Again, the electrolytes were kept at 70 °C.

Anolyte pH

To determine the upper limit of the acid concentration that can be produced before impairing the EW process efficiency, anolyte solutions with varying starting H_2SO_4 concentrations (0, 50, 100 or 200 g/L) containing 60 g/L Na_2SO_4 were prepared. The catholyte contained 80 g/L Fe as $FeSO_4$, 10 g/L EDTA, and 60 g/L Na_2SO_4. In this section, the FAB-PK-130-separated EW cell was used.

3.2.2.4 Temperature

In **Chapter 2** it was shown that various patents focussing on the EW of iron from SLS solutions operate at temperatures of up to 70 °C. Therefore, to determine the effect of temperature on the EW process, FAB-PK-130-separated EW experiments were repeated at three temperatures (30, 50 and 70 °C). The anolyte contained 60 g/L Na_2SO_4 and the catholyte 80 g/L Fe as $FeSO_4$, 10 g/L EDTA, and 60 g/L Na_2SO_4.

3.2.2.5 Sodium Sulphate

While Na_2SO_4 is commonly added to EW solutions to increase the conductivity of the electrolytes and to reduce the number of parasitic reactions that occur, the amounts recommended in literature varied significantly. To determine the effect of Na_2SO_4 addition, 0, 60 or 100 g/L Na_2SO_4 was added to both the catholyte and anolyte. In addition, 80 g/L Fe as $FeSO_4$ and 10 g/L EDTA were added to the catholyte. Both electrolytes were kept at 70 °C, while all other parameters remained constant when operating the FAB-PK-130-separated EW cell.

3.2.2.6 Membrane Screening

Various parameters regarding specifically the AEM for the non-porous membrane-separated EW process were investigated in this section: firstly, the type of AEM, then the influence of the anolyte pH and the thickness of the membrane, and finally an initial stability screening of the membranes.

Membrane Type

The recent increase of differing AEMs has both eased and complicated the process of deciding which membrane is most suitable for the EW of iron. Therefore, to determine which membrane provides the best performance in the EW cell, 6 commercial membranes were selected for this study (**Table 3.1**), where Membranes 1-5 were acquired from Fumatech GmbH and Membrane 6 from ResinTech Inc. All membranes were pre-treated through immersion in 60 g/L Na_2SO_4 overnight in order to saturate the transfer sites for optimal performance before use in the divided EW cell. During testing of the various AEMs, the catholyte contained 80 g/L Fe as $FeSO_4$, 10 g/L EDTA, and 60 g/L Na_2SO_4, while the anolyte contained 60 g/L Na_2SO_4. Both electrolytes were kept at 70 °C while all other variables remained constant as described earlier.

Table 3.1: List of membranes tested during this study with key specifications.*

No.	Membrane	Reinforcement	Thickness (µm)	Stability (pH)	IEC (meq/g)
1	FAB-PK-130	PEEK	130	0 - 14	1.0 – 1.1
2	FAS-PK-130	Polyester	130	0 - 9	1.0 – 1.4
3	FAD-PET-75	Polyester	75	0 - 9	1.5 – 1.7
4	FAP-330-PE	PEEK/PTFE	330	0 - 11	1.1 – 1.3
5	FAPQ-375-PE	PEEK/PTFE	375	0 - 11	1.1 – 1.3
6	AMB-SS	Not stated	2.1	0 - 10	1.0 – 1.1

* Data provided by suppliers

Anolyte pH

All of the membranes (**Table 3.1)** were additionally tested with the addition of 0, 50 or 100 g/L H_2SO_4 to the anolyte, while the FAB-PK-130 membrane was also tested at 200 g/L H_2SO_4. Furthermore, the catholyte contained 80 g/L Fe as $FeSO_4$, 10 g/L EDTA, and 60 g/L Na_2SO_4, while the anolyte contained 60 g/L Na_2SO_4. Both electrolytes were kept at 70 °C while all other variables remained constant as described earlier.

Membrane Thickness

The effect of putting two membranes on top of each other was tested to determine the influence of membrane thickness on the transfer of H^+ from the anolyte to the catholyte. Standard EW conditions were used, namely 80 g/L Fe as $FeSO_4$, 10 g/L EDTA, and 60 g/L Na_2SO_4 for the catholyte and 60 g/L Na_2SO_4 for the anolyte. Additionally, 100 g/L H_2SO_4 was added to the anolyte to provide a sufficient concentration gradient as driving force for the H^+ transfer from the anolyte to the catholyte. For this experiment, only the AMB-SS membrane was tested, as the membranes from Fumatech formed oxygen pockets between the membranes, leading to significantly increased applied voltages.

Membrane Stability

From the membrane screening done in the section on the type of membrane, the three best-performing membranes (FAB-PK-130, AMB-SS and FAS-PK-130) were subjected to acid degradation tests by placing them in a solution containing 100 g/L H_2SO_4 for periods of one week. After each week, the membranes were tested in the EW unit with the standard electrolyte compositions of 80 g/L Fe as $FeSO_4$, 10 g/L EDTA, and 60 g/L Na_2SO_4 for the catholyte and 60 g/L Na_2SO_4 for the anolyte. A total of four 1-week experiments were completed for each membrane.

3.2.2.7 Influence of Iron

Since this study aimed at developing an iron-based EW process, three variables relating to the influence of iron on the process were investigated.

Iron Flux

To characterize the iron flux through the AEM, the standard EW conditions were used, namely 80 g/L Fe as $FeSO_4$, 10 g/L EDTA, and 60 g/L Na_2SO_4 for the catholyte, and 60 g/L Na_2SO_4 for the anolyte. The Fe content in the anolyte was analysed after 5 hours using ICP-OES (Agilent, 5110). Additionally, the effect of H^+ tunnelling on the transport of Fe through the membrane was investigated using anolyte solutions consisting of 0 and 100 g/L H_2SO_4, respectively.

Iron Concentration

To investigate the effect of Fe concentration in the catholyte on the EW performance, catholyte solutions containing either 80 or 10 g/L Fe were used in the EW unit. In addition to this, the Na_2SO_4 concentration of the catholyte and anolyte was also varied between 0 and 100 g/L for both the 80 and 10 g/L Fe catholyte solutions, while all other variables remained constant.

Iron Depletion

To study the EW performance as a function of depleting Fe concentrations in the catholyte, a 2.5 L solution with 40 g/L Fe as $FeSO_4$, 10 g/L EDTA, and 60 g/L Na_2SO_4 for the catholyte and a 2.5 L anolyte solution consisting of 60 g/L Na_2SO_4 were prepared; with the FAB-PK-130 used as the membrane. These electrolyte solutions were used in a modified EW unit with an anode-cathode spacing of 5 cm, compared to 2 cm used in the smaller version. In this unit the active electrode area was 20x30 cm and a constant current density of 300 A/m^2 was used during operation, which equated to a constant current of 18 A. The power supply used in this case was a 400 W TDK-Lambda Z+ series programmable DC power supply and was operated through the USB interface. The software used to control the power supply and to log its output signal is described in the **Appendix B**. The performance of the cell was analysed over a period of 5 hours as a function of the depleting Fe content, with the catholyte/anolyte pH and voltage being measured. All other experimental conditions were identical to those used in the smaller EW (4x4 cm) unit.

3.3 Results and Discussion

The following results and discussion section will discuss the effects of the parameters described above on the performance of iron EW, thereby providing insight into the process optimization required for the EW of iron.

3.3.1 EW Configuration

The first step of identifying a suitable EW method was to test the three most commonly proposed methods, namely non-separated-, porous Terylene-based, and non-porous AEM-based EW of iron. Results of the different methods of EW are summarized in **Table 3.2**. For the pH measurements, the error obtained from triplicate runs was 5.54 %, while the error on the current efficiency and SEC were 2.05 % and 1.01 %, respectively (**Appendix A**). The non-separated process was operated using an electrolyte containing 80 g/L Fe as $FeSO_4$, 60 g/L Na_2SO_4, 10 g/L EDTA and 10 g/L H_3BO_3. The porous and AEM processes used a catholyte containing 80 g/L Fe as $FeSO_4$, 60 g/L Na_2SO_4, 10 g/L EDTA and 10 g/L H_3BO_3 and an anolyte containing 60 g/L Na_2SO_4. A significant improvement in all parameters is noted when moving from the non-separated EW set-up, via the porous membrane-based system, to the system using the non-porous AEM. When compared to the non-separated EW, the current efficiency, for instance, increased by 56 % and 78 % when using the porous and non-porous membranes, respectively. The increase in the current efficiency coincided with a decrease in the SEC of the system, with the AEM-EW unit yielding a nearly 5 times reduction in energy consumption per kg of Fe plated compared to the non-separated system.

Table 3.2: Performance parameters obtained from testing the three Fe-EW configurations.

Parameter	Non-separated	Porous	AEM
Current Efficiency (%)	21	77	99
SEC (kWh/kg Fe)	17.70	9.50	3.80
Catholyte pH (End)	2.05	2.90	2.51
Anolyte pH (End)	2.05	1.56	1.34

This increase in current efficiency can be ascribed to the separation of the cathodic and anodic reactions preventing the side reactions listed in **Table 2.1**. The separation of the anodic and cathodic reactions led to a decrease in the number of side reactions (see Section 2.3) that occur. As discussed in the previous chapter, the most important side reactions include the

evolution of H_2 gas through reduction of free protons at the cathode, as well as the prevention of oxidation of Fe(II) to Fe(III) by the oxygen produced at the anode. In the electrolyte of the non-separated cell, a light brown suspension formed during operation, which can be attributed to the formation of ferric oxyhydroxides.[14] This precipitation increased when the pH of the electrolyte increased to above 2. However, when using the divided cells (Terylene or AEM), no precipitate was observed, confirming the lower oxidation rate of the Fe(II) in the absence of dissolved oxygen. This contributed to the higher current efficiency and reduced SEC when compared to the non-separated EW option. When comparing the porous Terylene and non-porous AEM results, it is further clear that the AEM-based process yielded the lowest anolyte pH, highest current efficiency and lowest SEC. This can again be ascribed to an even more complete prevention of side reactions due to the limitation of species transport between the anolyte and catholyte. Hence, in view of the results obtained, all further optimizations were done using only the AEM-EW configuration.

3.3.2 Boric Acid

Since boric acid (H_3BO_3) is traditionally used in porous membrane EW,[4] the effect thereof on the AEM-EW system was the first variable investigated. According to literature, H_3BO_3 acts as a pH buffer in EW systems to reduce the amount of H_2 evolution at the cathode, while improving the surface morphology of the plated metal.[2-3] The effect of boric acid was investigated using a catholyte solution consisting of 80 g/L Fe as $FeSO_4$, 60 g/L Na_2SO_4, 10 g/L EDTA with (10 g/L) or without H_3BO_3. The effect of H_3BO_3 on the voltage during the EW process is shown in **Figure 3.8**, from which it is evident that H_3BO_3 addition had no significant effect on the applied voltage for the duration of the experiments. As the process operated at a fixed current density, the voltage output of the power supply is adjusted to supply the required current. During operation, the average voltage with 0 g/L H_3BO_3 was 4.60 V, while the average voltage after the addition of 10 g/L H_3BO_3 was 4.63 V, which falls within the error margin (0.23 V) of these experiments.

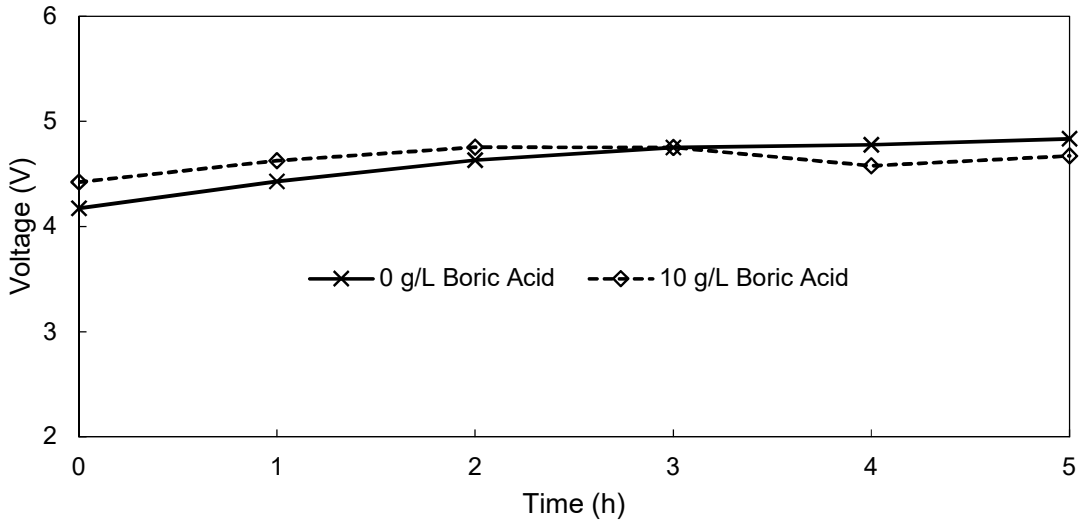

Figure 3.8: Influence of H_3BO_3 on the applied voltage during AEM-EW of iron as a function of time.

The effect of H_3BO_3 addition on the catholyte and anolyte pH was subsequently measured. From **Figure 3.2**, the buffering capability of the H_3BO_3 in the anolyte and catholyte is evident, as higher pH values were recorded where H_3BO_3 was present. When using H_3BO_3, the end anolyte pH was 1.37, compared to the anolyte end pH of 1.29 without H_3BO_3, which is a difference of 0.08. This difference, while small, was significant in view of the error margin for the anolyte pH that was 0.07 (**Appendix A**). In addition, the buffering nature of the H_3BO_3 resulted in an increase in the current efficiency from 88 to 94 % when 10 g/L H_3BO_3 was added to the catholyte and anolyte. As previously mentioned, the increased efficiency was most likely due to reduced H_2 formation on the cathode as a result of the increased pH in the catholyte. It is shown in Section 3.3.7.3, however, that this effect becomes insignificant when the AEM-EW unit is operated for periods longer than 5 hours. In view of the limited effect on efficiency and Fe plating in relation to the additional cost and processing that would be required, it was decided to not continue adding H_3BO_3.

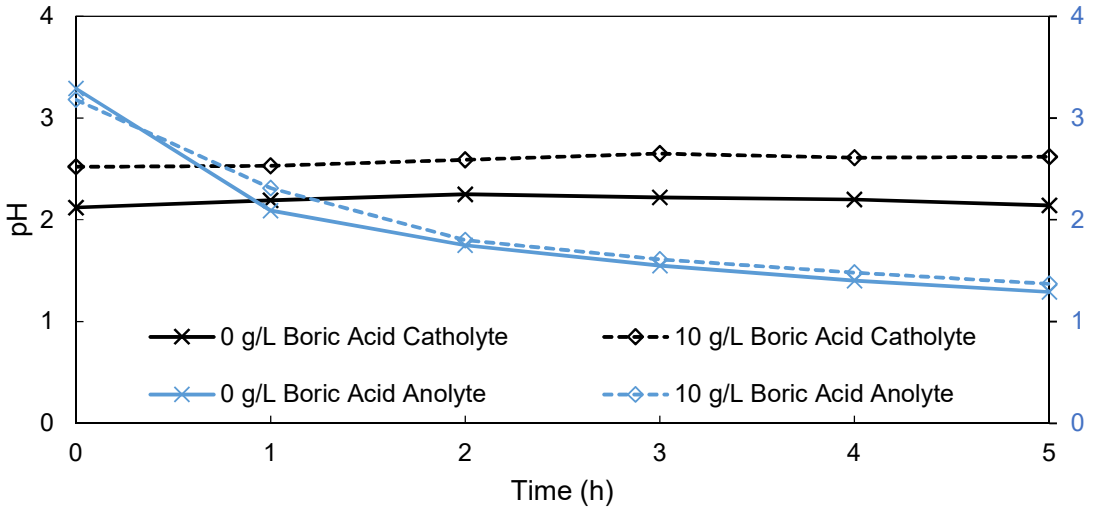

Figure 3.2: Influence of H_3BO_3 on the catholyte (primary y-axis) and anolyte pH (secondary y-axis) during the AEM-EW of iron as a function of time.

3.3.3 Temperature

EW is traditionally operated at elevated (electrolyte) temperatures which result in a reduced energy consumption and improved plating quality while allowing for higher concentrations of dissolved metal species in the electrolyte.[2] For this reason, the influence of temperature (30 to 70 °C) on the performance of the AEM-EW was investigated using standard catholyte (80 g/L Fe as $FeSO_4$, 60 g/L Na_2SO_4 and 10 g/L EDTA) and anolyte (60 g/L Na_2SO_4) solutions. From **Figure 3.3** it is evident that temperature has a significant effect on the applied voltage as it decreased from 4.94 V to 3.87 V as the temperature increased from 30 °C to 70 °C. This effect can be ascribed to the increased thermal energy in the system, which reduces the amount of electrical potential energy required both for the reduction of the Fe and the oxidation of the water.[2, 7]

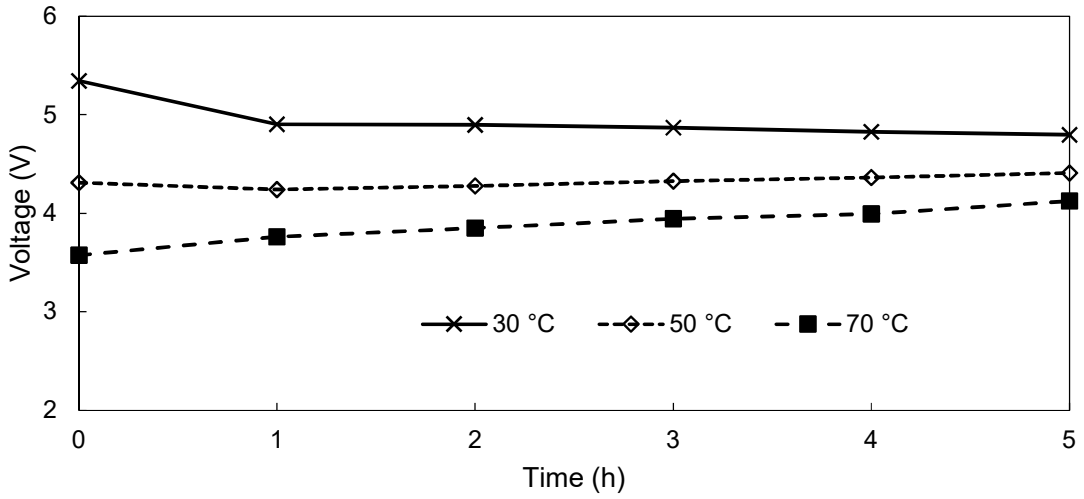

Figure 3.3: Influence of the electrolyte temperature on the voltage as a function of time.

The increase in temperature also affected the catholyte pH, as can be seen in **Figure 3.4**. The increase in pH with increasing temperature correlates with an increase in H_2 production at the cathode due to the effect described earlier, where increased temperature leads to a lower required voltage for the electrochemical reaction to occur. Consequently, the end pH increased from 2.30 at 30 °C to 3.17 at 70 °C. The increased H_2 formation, however, did not have a significant impact on the current efficiency of the EW unit that dropped only slightly from 94 % at 30 °C to 91 % at 70 °C, which is due to the logarithmic nature of the pH scale. Despite the lower current efficiency, the SEC of the system significantly improved from 5.3 kWh/kg Fe at 30 °C to 4.7 kWh/kg Fe at 70 °C, which represents a 10.6% decrease.

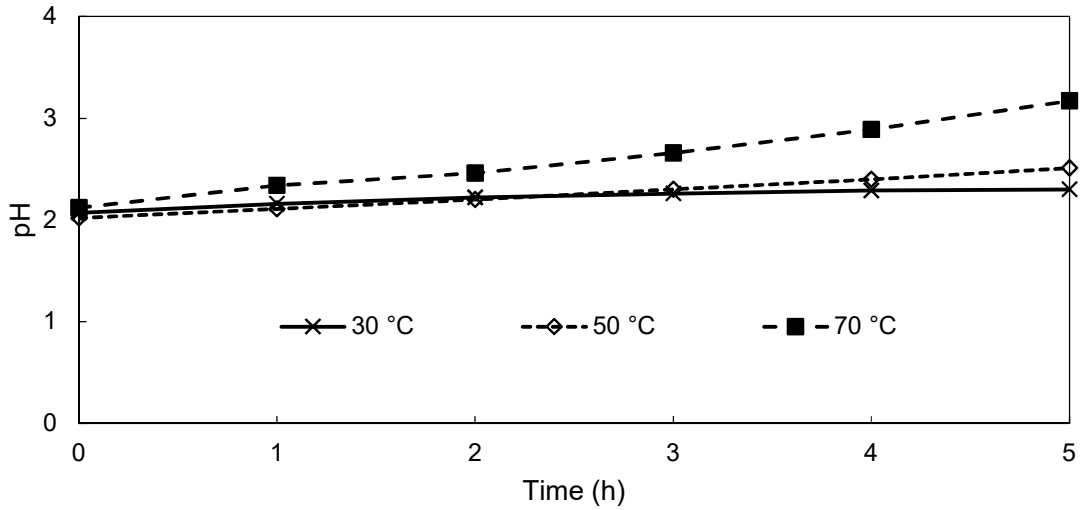

Figure 3.4: Influence of the electrolyte temperature on the catholyte pH as a function of time

The benefits of the EW unit operating at higher temperatures are further showcased in **Figure 3.5**, from which it is clear that the pH of the anolyte decreased with increasing temperature. This decrease in the anolyte pH correlated with a higher rate of acid production, where a pH of 1.51 was reached after 5 hours at 30 °C, compared to a pH of 1.35 at 70°C. Despite the small change, it is considered relevant due to the small error margin as shown in **Appendix A**. This increase in the rate of acid production can be attributed to the oxidation of water occurring more easily at the anode at elevated temperatures.[7]

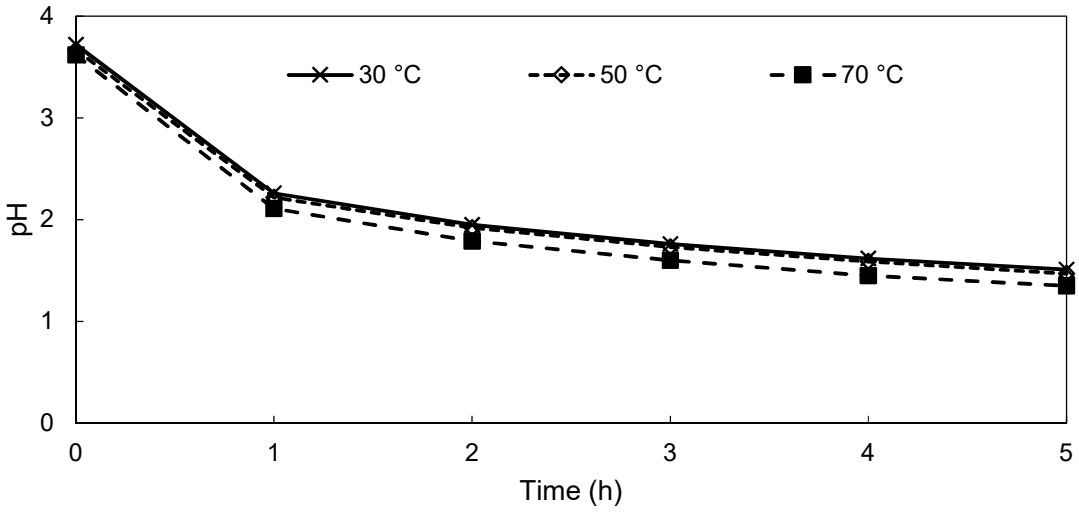

Figure 3.5: Influence of the electrolyte temperature on the anolyte pH as a function of time.

The results of the key parameters of the AEM-EW unit when varying the temperature between 30 and 70 °C are summarised in **Table 3.3**. It is evident that the EW unit performance increased with increasing temperature, while the current efficiency decreased slightly from 94% at 30 °C to 91% at 70 °C. In addition, this slight drop in the current efficiency was accompanied by a decrease in the applied voltage, which resulted in a decreased specific energy consumption. Similarly, the rate of acid production in the anolyte also increased with increasing temperature, clearly confirming the advantages of operating the EW of iron at elevated temperatures. Therefore, further optimisation of variables effecting the AEM-EW were operated at a constant temperature of 70 °C

Table 3.3: Summary of results obtained from the AEM-EW unit with increasing temperature.

Parameter	30 °C	50 °C	70 °C
Current Efficiency (%)	94	91	91
SEC (kWh/kg Fe)	5.30	4.90	4.70
Average Voltage (V)	4.94	4.32	3.87
Catholyte pH (End)	2.30	2.51	3.17
Anolyte pH (End)	1.51	1.47	1.35

3.3.4 Catholyte/Anolyte pH

3.3.4.1 Catholyte pH

As the focus of this study was on the treatment of SLSs that could contain unspent acid, the effect of acid in the initial catholyte feed on the AEM-EW was investigated by using a feed catholyte containing 0, 12.5 or 25 g/L H_2SO_4 (containing 80 g/L Fe as $FeSO_4$, 60 g/L Na_2SO_4 and 10 g/L EDTA). As is clear from the results presented in **Figure 3.6**, the applied voltages decreased slightly (from 3.87 to 3.54 and 3.36 V) with increasing acid content (0, 12.5 and 25 g/L, respectively). This decrease in the voltage is likely due to the increased conductivity of the catholyte solution with the addition of H_2SO_4.[8, 15]

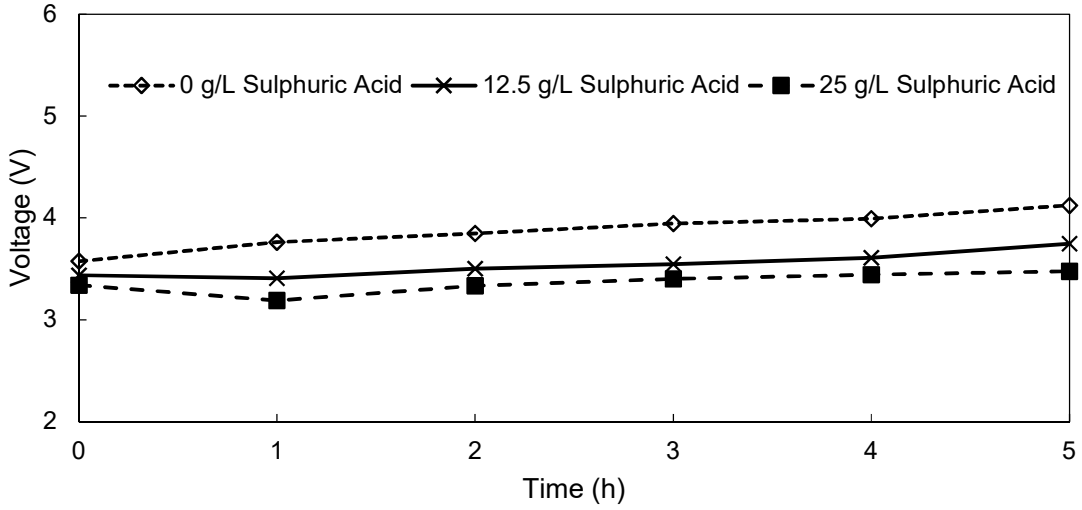

Figure 3.6: Influence of the addition of H_2SO_4 to the catholyte on the voltage behaviour of the AEM-EW of iron as a function of time.

While the catholyte pH, as expected, decreased with increasing H_2SO_4 concentration, the increasing slopes of the pH values over time were independent of the H_2SO_4 concentration (**Figure 3.7**). This increase in the pH values over time indicate H_2 gas formation, as would be expected at pH values below 7.[7] With the increased H_2 gas evolution observed at higher H_2SO_4 concentrations, the current efficiency of the EW unit decreased significantly from 88 to 9 and – 83 % for 0, 12.5 and 25 g/L H_2SO_4, respectively. Accordingly, the SEC increased from 4.87 to 430 kWh/kg Fe when adding 12.5 g/L H_2SO_4. The current efficiency of – 83 % at 25 g/L H_2SO_4 implies that the mass of the plate after 5 hours was lower than its initial weight, i.e. iron was dissolved during the experiment, clearly showing the detrimental effect of higher acid content in the catholyte feed. With a negative current efficiency, it was also not possible to calculate the SEC at 25 g/l H_2SO_4.

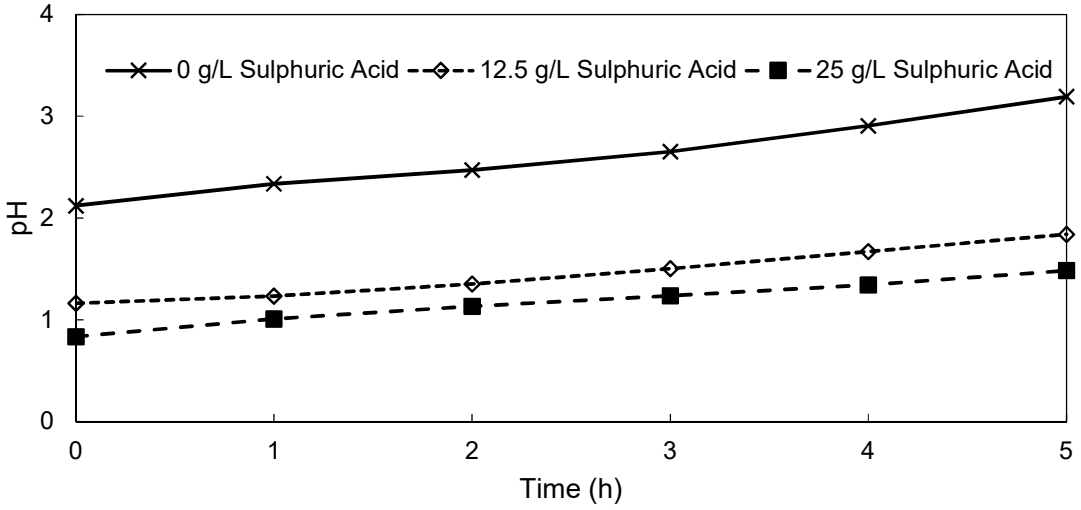

Figure 3.7: Influence of the addition of H_2SO_4 to the catholyte on the catholyte pH as a function of time.

It is clear from **Figure 3.8** that the addition of H_2SO_4 to the initial catholyte solution had no significant effect on the anolyte pH. In Section 3.3.1, the superior performance of the AEM-EW was ascribed to the reduced crossover of ions resulting in fewer side reactions. The results presented in **Figure 3.8** confirm the rejection of even high concentrations of H^+ by these AEMs. If the AEMs had not been capable of selectively transporting anionic species and rejecting cationic species, an increase in the H^+ concentration in the anolyte would have occurred and a decrease in the anolyte pH would have been observed.[12, 16]

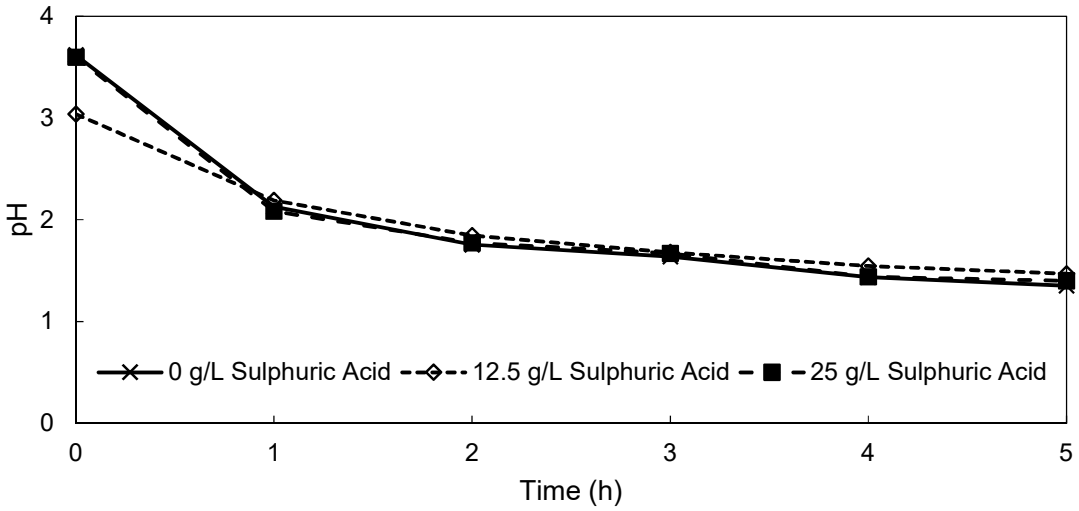

Figure 3.8: Influence of the addition of H_2SO_4 to the catholyte on the anolyte pH as a function of time.

A summary of the key results obtained when adding H_2SO_4 to the catholyte is shown in **Table 3.4**. It is clear that adding H_2SO_4 to the catholyte was detrimental for the performance of the AEM-EW, implying that the reduction in current efficiency overshadowed the possible benefit of the increased conductivity in the catholyte. This implies that any unspent acid present in the SLS feed solution should be neutralised (for example using NaOH or $Fe(CO_3)$) before the AEM-EW process is applied to the SLS. Alternatively, the EW unit itself could be used to consume the unspent acid through the reduction of free H^+ into H_2 gas, which would, however, result in the EW unit running at lower current efficiencies until the acid had been removed.

Table 3.4: Summary of key results obtained from the AEM-EW when adding various amounts of H_2SO_4 to the feed catholyte.

Parameter	0 g/L	12.5 g/L	25 g/L
Current Efficiency (%)	88	9	-83
SEC (kWh/kg Fe)	4.78	430	N/A*
Average Voltage (V)	3.87	3.54	3.36
Catholyte pH (End)	3.19	1.84	1.48
Anolyte pH (End)	1.35	1.47	1.40

* Final mass of cathode was less than initial mass.

3.3.4.2 Anolyte pH

As the regeneration of spent acid in the anolyte was one of the objectives for this study, it was essential to determine the influence of increasing acid concentrations in the anolyte on the performance of the iron EW. The effect of varying the H_2SO_4 concentrations from 0 to 200 g/L in the anolyte on the applied voltage with the FAB-PK-130 membrane is depicted in **Figure 3.9**. In line with the observations discussed in Section 3.3.4.1 (adding H_2SO_4 to the catholyte), the addition of H_2SO_4 to the anolyte resulted in a decrease of 0.61 V when increasing the H_2SO_4 concentration from 0 to 200 g/L H_2SO_4. This decrease can again be ascribed to the resulting increase in the electrolyte conductivity.[15] It is further noteworthy that, when the initial H_2SO_4 concentrations were 100 and 200 g/L H_2SO_4, the voltages reached a plateau after 1 hour instead of continually increasing as was observed for 0 and 50 g/L H_2SO_4. This plateau of the applied voltage is possibly due to the saturation of the AEM transport sites and inclusion of H^+-ions into the polymer matrix, which further increased conductivity.[17-18] This would result in a reduction of the overall resistance of the membrane, thereby lowering the voltage applied to the EW unit.[19]

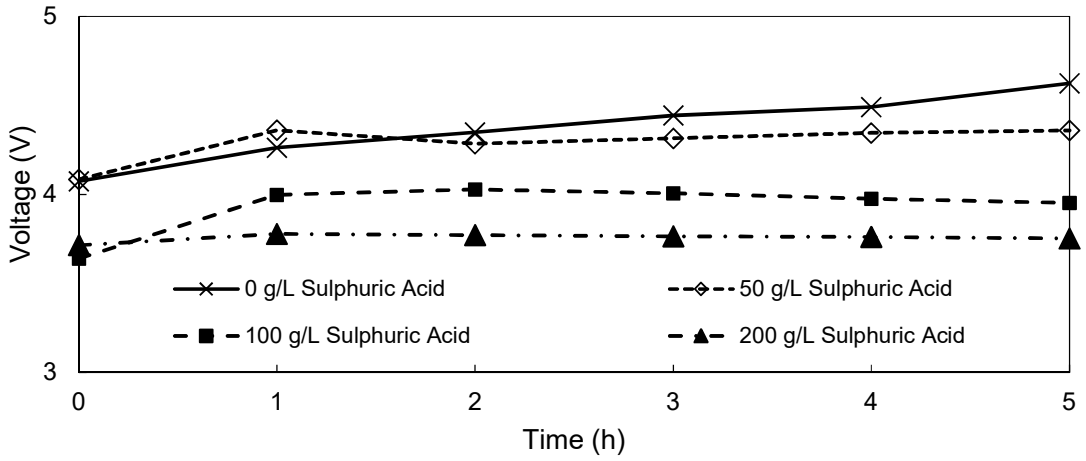

Figure 3.9: Influence of H_2SO_4 on the applied voltage during EW with varying amounts of H_2SO_4 added to the anolyte.

In contrast to the positive effect observed regarding the voltage , increased concentrations of H_2SO_4 had a negative effect on the catholyte pH, which increased over time, as shown in **Figure 3.10**. Such a decrease in catholyte pH during the operation of the EW strongly indicates the transfer of H^+ from the anolyte to the catholyte due to proton tunneling.[20-21] It can be noted that, at H_2SO_4 concentrations above 50 g/L, the catholyte pH either stabilized or even started to decrease. Coupled with the decrease in catholyte pH, the current efficiency also decreased from 88 % at 0 g/L H_2SO_4 to 61% at 200 g/L H_2SO_4. Nonetheless, this decrease in

current efficiency was relatively small between 0 g/L H_2SO_4 (88%) and 100 g/L H_2SO_4 (78%), indicating that the FAB-PK-130 membrane offered good H^+ rejection at H_2SO_4 concentrations below 100 g/L. The sharp decrease in the current efficiency between 100 and 200 g/L H_2SO_4 also yielded a significant increase in the SEC from 4.78 kWh/kg Fe at 0 g/L H_2SO_4 to 5.42 kWh/kg at 100 g/L H_2SO_4, while an SEC of 8.41 kWh/kg Fe was determined at 200 g/L H_2SO_4. This suggests that the operational limit of the AEM-EW process for acid reduction should be 100 g/L H_2SO_4 to optimize the current efficiency of the process.

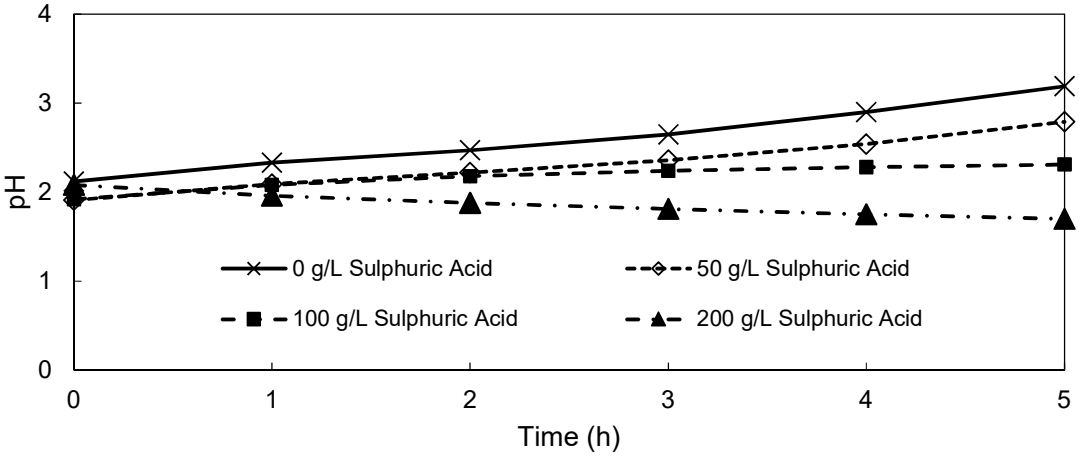

Figure 3.10: Influence of H_2SO_4 on the catholyte pH during EW with varying amounts of H_2SO_4 added to the anolyte.

3.3.5 Sodium Sulphate

As previously noted, sodium sulphate (Na_2SO_4) is frequently added to increase the conductivity of EW solutions by taking over the charge transfer while not partaking in the redox reactions, thereby effectively reducing H_2 production.[8-9] The effect of the Na_2SO_4 concentration in the anolyte and catholyte was investigated using the standard catholyte of 80 g/L Fe as $FeSO_4$ and 10 g/L EDTA, while adding 0, 60 or 100 g/L Na_2SO_4 to both the catholyte and anolyte. The effect of the Na_2SO_4 concentration on the applied voltage is shown in **Figure 3.11**, from which it is evident that the average applied voltage decreased from 4.07 V at 0 g/L Na_2SO_4 to 3.57 V at 60 g/L Na_2SO_4. Increasing the Na_2SO_4 concentration of the electrolytes to 100 g/L led to a further reduction in the average applied voltage of 0.28 V relative to that at 60 g/L Na_2SO_4. The increased Na_2SO_4 concentration also resulted in smaller fluctuation in the voltage profile for the 5 hours of each experiment. Accordingly, the applied voltage reached a plateau after one hour at a Na_2SO_4 concentration of 100 g/L Na_2SO_4, while the applied voltage continued to increase steadily when the Na_2SO_4 concentrations were 0 and 60 g/L. This

increase was attributed to the increase of the electrolyte conductivity with time due to the formed H_2SO_4.

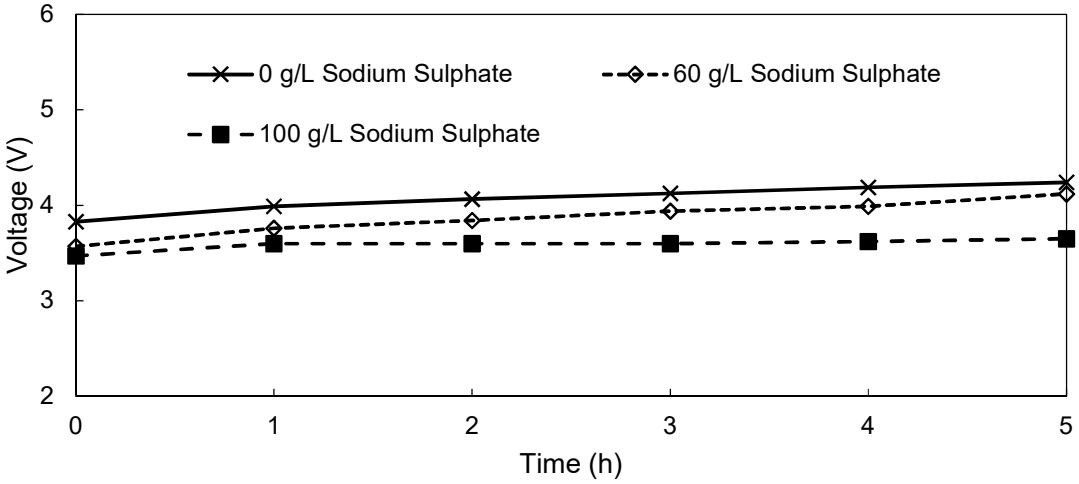

Figure 3.11: Influence of the addition of Na_2SO_4 on the voltage as a function of time.

It was stated above that the Na_2SO_4 would replace the H^+ as the charge carrier in the EW unit. This was confirmed when observing the change in pH of the catholyte. According to **Figure 3.12**, an increase in the Na_2SO_4 concentration yielded a slightly slower increase of the pH, suggesting that the addition of Na_2SO_4 reduced the formation of H_2 gas at the cathode, which increased the current efficiency. Correspondingly, the current efficiency increased with Na_2SO_4 addition and attained current efficiencies of 90 %, 91 %, and 97 % for 0, 60 and 100 g/L Na_2SO_4, respectively. Subsequently, an increase in the current efficiency and a lowering of the voltage (**Figure 3.11**) led to a decrease in the SEC of the EW unit. Increasing the Na_2SO_4 concentration from 0 to 100 g/L reduced the SEC by 1.2 kWh/kg Fe, which is nearly a 25 % reduction. In the absence of Na_2SO_4 in the electrolyte, a sharp increase in the catholyte pH was observed after 4 hours. This indicates the onset of water reduction resulting in the formation of hydroxide ions.[7] It confirms that, in the absence of Na_2SO_4, there were insufficient charge-carrying species present in the catholyte.

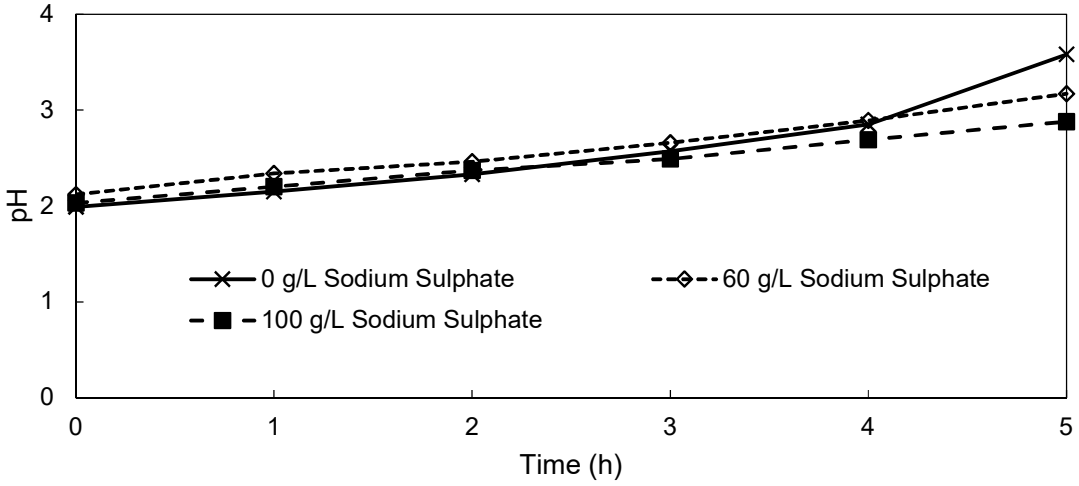

Figure 3.12: Influence of the addition of Na_2SO_4 to the catholyte on the catholyte pH as a function of time

In contrast to the catholyte pH, the anolyte pH shown in **Figure 3.13** displayed no significant dependence on the Na_2SO_4 concentration, where a catholyte end pH of 1.43 and 1.40 was obtained with 0 g/L and 100 g/L Na_2SO_4, respectively. The negligible effect of the Na_2SO_4 on acid production can be attributed to the fact that a higher voltage (2.71 V, compared to 2.07 V for water oxidation) would be required before sodium would undergo any electrochemical redox reactions.[7]

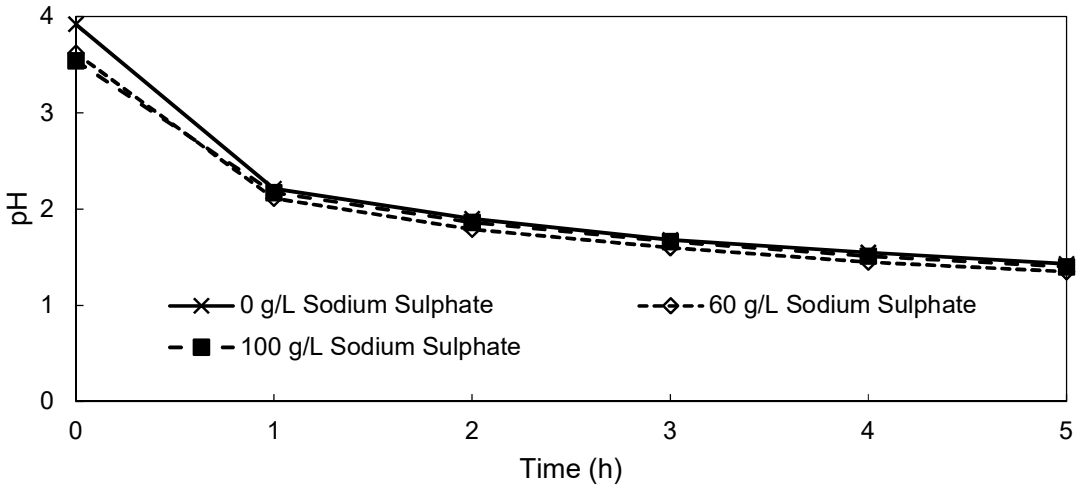

Figure 3.13: Influence of the addition of Na_2SO_4 to the anolyte pH as a function of time.

A summary of the effect of Na_2SO_4 is given in **Table 3.5**. The most pronounced effect is the substantial increase in the current efficiency of the EW unit with increasing Na_2SO_4, increasing from 90 % to 97 % when adding 100 g/L Na_2SO_4. As was expected, the increased current efficiency yielded a significantly lower SEC, which was reduced by 1.2 kWh/kg Fe when adding 100 g/L Na_2SO_4. Higher Na_2SO_4 concentrations (150 and 200 g/L) were also tested (data not shown), however, above 100 g/L precipitation occurred both due to temperature fluctuation and possible volume losses due to evaporation. To avoid any possibility of precipitation, further experiments were done using 60 g/L Na_2SO_4 .

Table 3.5: Summary of key variables obtained from the EW unit during the addition of 0, 60 and 100 g/L Na_2SO_4 to both the catholyte and anolyte.

Parameter	0 g/L	60 g/L	100 g/L
Current Efficiency (%)	90	91	97
SEC (kWh/kg Fe)	4.9	4.6	3.7
Average Voltage (V)	4.07	3.87	3.59
Catholyte pH (End)	3.58	2.89	2.69
Anolyte pH (End)	1.43	1.34	1.40

3.3.6 Membrane Screening

3.3.6.1 Type

The voltages obtained with the different AEMs presented in Section 3.2.2.6 are shown in **Figure 3.14**. The different voltage profiles obtained from each AEM can be ascribed to either the varying thickness or conductivity of the membranes. Notably, FAB-PK-130 had the most resistance and required the highest applied voltage during operation. Apart from the difference in average voltage, all the membranes obtained from Fumatech exhibited a constant applied voltage over the duration of the experiments, while the applied voltage decreased over time for the AMB-SS membrane from Resintech, which could be attributed to apparent decay or swelling of the membrane. The FAP-330-PE membrane required the lowest applied voltage with an average of 3.26 V compared to the average voltage of 3.79 V required for the FAB-PK-130 membrane.

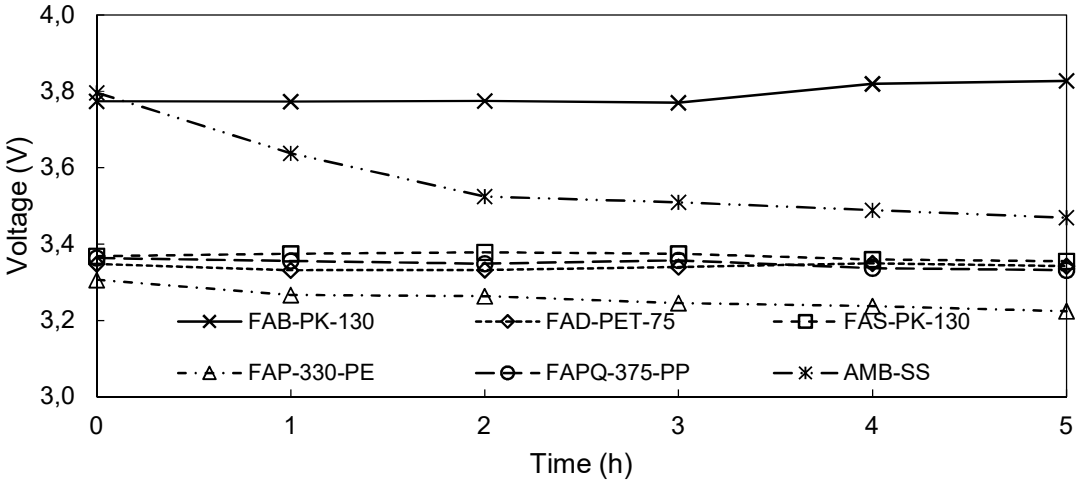

Figure 3.14: Influence of the AEM type on the voltage as a function of time.

The effect of the membrane type on the catholyte pH is shown in **Figure 3.15**. After 5 hours, the FAB-PK-130 yielded the highest catholyte pH while the FAP-330-PE membrane yielded the lowest catholyte pH. A higher catholyte pH at the end of the experiment indicates that the membrane was more selective for the transfer of anion species, effectively rejecting H^+ ion transfer, which is in agreement with the higher resistance described above. Similarly, the FAP-330-PE membrane that showed the lowest applied voltage (**Figure 3.14)** had the highest H^+ transfer rate and thus the lowest selectivity. Additionally, the high final catholyte pH values correlate with high current efficiencies due to the reduced H^+ reduction on the cathode. Accordingly, the FAB-PK-130 membrane displayed a current efficiency of 94 %, compared to the current efficiency of 85 % achieved with the FAP-330-PE membrane. Despite the low selectivity and current efficiency displayed by the FAP-330-PE membrane, the low applied voltage required with this membrane yielded an SEC of 3.55 kWh/kg Fe, which was 0.29 kWh/kg Fe lower than that of the FAB-PK-130 membrane reported on thus far.

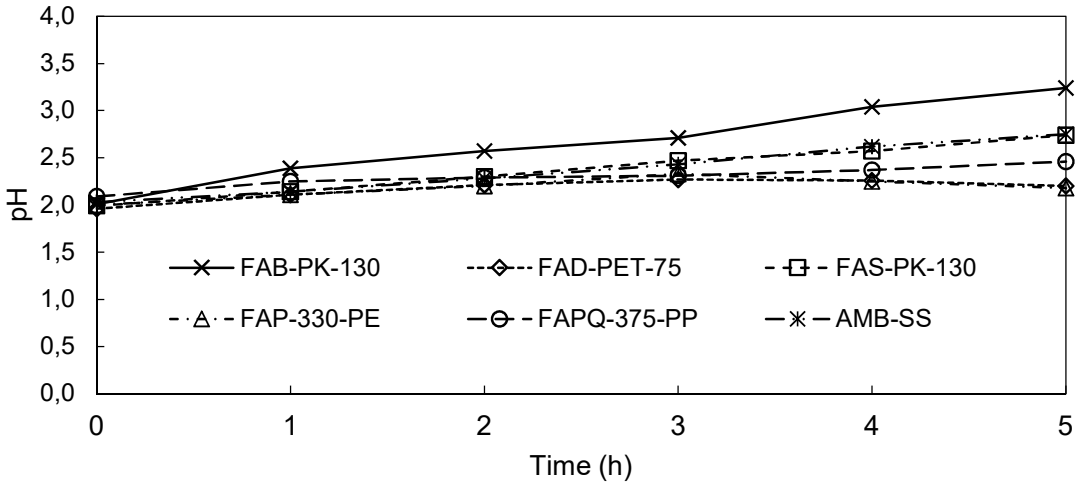

Figure 3.15: Influence of the AEM type on the catholyte pH as a function of time.

Not much information could be obtained from the anolyte pH values shown in **Figure 3.16**, yet the FAB-330-PE membrane yielded slightly higher anolyte pH values, which indicate that it might not be the optimal membrane for acid production. The lowest pH value was obtained using the FAB-PK-130 membrane, seeing that it yielded an anolyte pH of 1.35, which was 0.29 lower compared to the pH obtained with the FAP-330-PE membrane.

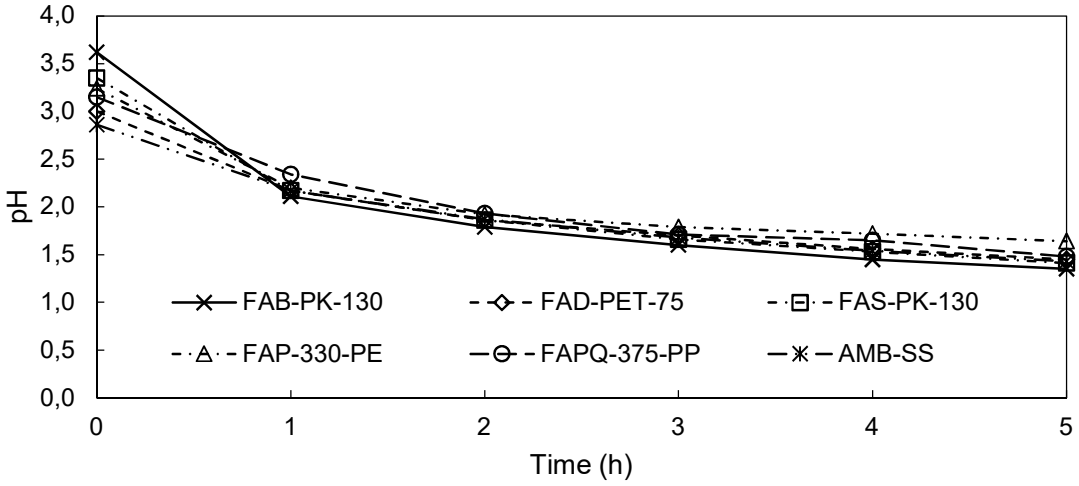

Figure 3.16: Influence of the AEM type on the anolyte pH as a function of time.

The performance of the various AEM membranes tested in this section is summarized in **Table 3.6**. The FAB-PK-130 membrane stands out since it presents the best performance in the EW unit in terms of its high current efficiency (94 %), highest final catholyte pH (3.24) and lowest final anolyte pH (1.35). However, the FAB-PK-130 displayed the highest SEC compared to

some of the other membranes such as the FAP-330-PE and the FAS-PK-130. As noted previously, the high SEC is attributed to the high resistance and hence H^+ selectivity of the FAB-PK-130 membrane. However, in view of its superior performance in terms of current efficiency and pH values, the FAB-PK-130 membrane was used in all work presented in this study unless otherwise noted.

Table 3.6: Summary of key variables obtained from the AEM-EW unit using various AEMs as separators between the catholyte and anolyte.

Membrane	Current Efficiency (%)	SEC (kWh/kg)	Catholyte pH (End)	Anolyte pH (End)
FAB-PK-130	94	3.84	3.24	1.35
FAD-PET-75	83	3.86	2.20	1.45
FAS-PK-130	87	3.71	2.74	1.41
FAP-330-PE	85	3.55	2.80	1.64
FAPQ-375-PP	83	4.12	2.46	1.48
AMB-SS	88	3.88	2.75	1.43

3.3.6.2 Anolyte pH

As the regeneration of spent acid was one of the objectives of this study (Section 3.3.2.4), the effect of adding 100 g/L H_2SO_4 to the anolyte solution on the performance of the various membranes was determined and is presented in **Table 3.7**. Under these elevated acidic conditions, the majority of membranes yielded current efficiencies below 50 % with only the FAB-PK-130 managing to achieve an acceptable current efficiency of 78 %. Similarly, all the membranes except for the FAB-PK-130 operated at an SEC above 9 kWh/kg Fe. Both the high current efficiency and low SEC obtained by the FAB-PK-130 can be attributed to the high H^+ rejection discussed previously, confirming what was noted earlier that the FAB-PK-130 is the optimal membrane for acid production in the AEM-EW unit.

Table 3.7: Summary of key variables of varying membranes during EW with 100 g/L H_2SO_4 present in the anolyte solution.

Name	pH Catholyte (End)	pH Anolyte (End)	Efficiency (%)	SEC (kWh/Kg)
FAB-PK-130	1.45	0.05	78	4.51
FAD-PET-75	0.66	0.33	6.0	49.8
FAS-PK-130	1.16	0.40	13	23.0
FAP-330-PP	0.62	0.17	6.0	45.1
FAPQ-375-PE	1.10	0.05	1.0	276
AMB-SS	1.40	0.40	32	9.66

3.3.6.3 Membrane Thickness

While studying the influence of increasing acid concentrations in the anolyte on the EW performance, a loss of protons to the catholyte was observed above an H_2SO_4 concentration of 100 g/L, as depicted in **Figure 3.10**.[20-21] Therefore, the effect of multiple, stacked membranes, i.e. increased membrane thickness, on the rate of H^+ transport from the anolyte to the catholyte was investigated in this section using an anolyte H_2SO_4 concentration of 100 g/L.[20, 22] In the experimental section, it was mentioned that, for this study, only the AMB-SS membrane was suitable and hence tested. A summary of the key results obtained from the EW unit when using two stacked AMB-SS membranes are given in **Table 3.8**. It is evident that the current efficiency increased when using two membranes (80%) instead of a single membrane (32%). Additionally, the anolyte end pH value was significantly lower when using two membranes. The increased current efficiency coupled with the lower anolyte end-pH indicates that the amount of H^+ transport across the AEM was significantly reduced when a second membrane was used as had been expected. However, the addition of a second membrane significantly increased the voltage applied to the EW unit from 3.21 V to 5.35 V, negating much of the two aforementioned benefits.

Table 3.8: Summary of key variables obtained from the EW unit during the testing of a single AMB-SS membrane and two AMB-SS membranes together.

Parameter	1 x AMB-SS	2 x AMB-SS
Average Voltage (V)	3.21	5.35
Current Efficiency (%)	32	80
SEC (kWh/kg Fe)	9.63	6.42
Catholyte pH (End)	1.40	1.80
Anolyte pH (End)	0.40	0.15

3.3.6.4 Membrane Stability

As shown in the previous sections, the FAB-PK-130 membrane-separated EW unit can be operated with a reasonable performance even in the presence of 100 g/L H_2SO_4 in the anolyte. However, the durability of the membrane in such a highly acidic environment is unknown since the corresponding pH is below the manufacturer's specifications. In order to study the acid stability, the FAB-PK-130 membrane was submersed in a 100 g/L H_2SO_4 solution for 4 weeks, with a weekly 5-hour EW test, as described in Section 3.2.2.6. The resulting voltages applied to the EW unit for each subsequent week is shown in **Figure 3.17**. A slight increase of the average voltage was noted after the first week, where the average increased from 3.68 V for the first week to 3.74 V after week 2. However, after week 2, the average voltage stabilised at around 3.75 V. The observed small increase in voltage is perhaps due to a slight degradation of the membrane during the first week, which increased its resistance. However, no degradation was observed in weeks 2-4.

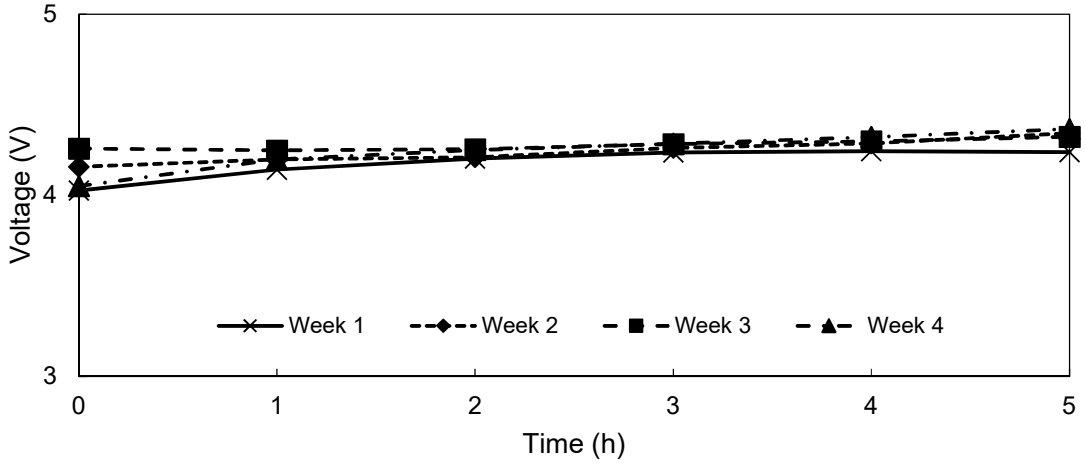

Figure 3.17: Influence of the membrane being subjected to acidic conditions on the average applied voltage obtained from the EW unit after screening of the FAB-PK-130.

A slightly larger effect was noted for the catholyte pH over time, as shown in **Figure 3.18**. After prolonged immersion in the highly acidic solution, the catholyte pH started to increase. Accordingly, the end catholyte pH of 2.61 before immersion increased to 3.08 after 4 weeks of immersion. Notwithstanding, despite the increase in the catholyte pH after immersion, the current efficiency decreased from 92 % before immersion to 78 % after 4 weeks. This decrease in the current efficiency is in contrast to the previously observed trend where an increase in the end catholyte pH correlated with an increased current efficiency (Section 3.3.4.2). With the decreasing current efficiency, the SEC increased from 3.84 kWh/kg Fe before acid immersion to 4.61 kWh/kg Fe after 4 weeks of immersion.

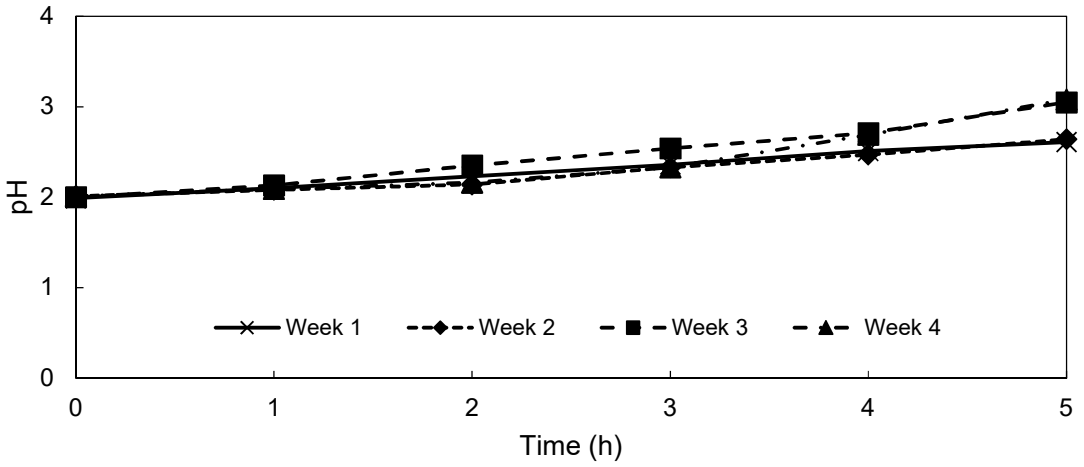

Figure 3.18: Influence of the membrane being subjected to acidic conditions on the catholyte pH obtained from the EW unit after screening of the FAP-PK-130.

The effect of acid degradation on the anolyte pH was minimal according to **Figure 3.19**, where a difference of less than 5 % was noted between the anolyte end values between Week 1 and Week 4, a value that is within the standard deviation determined earlier (**Appendix A**). Therefore, the effect of acid degradation on the H^+ rejection properties of the AEM was found to be negligible, which is in agreement with literature where most AEMs used are stable against acid attack.[23]

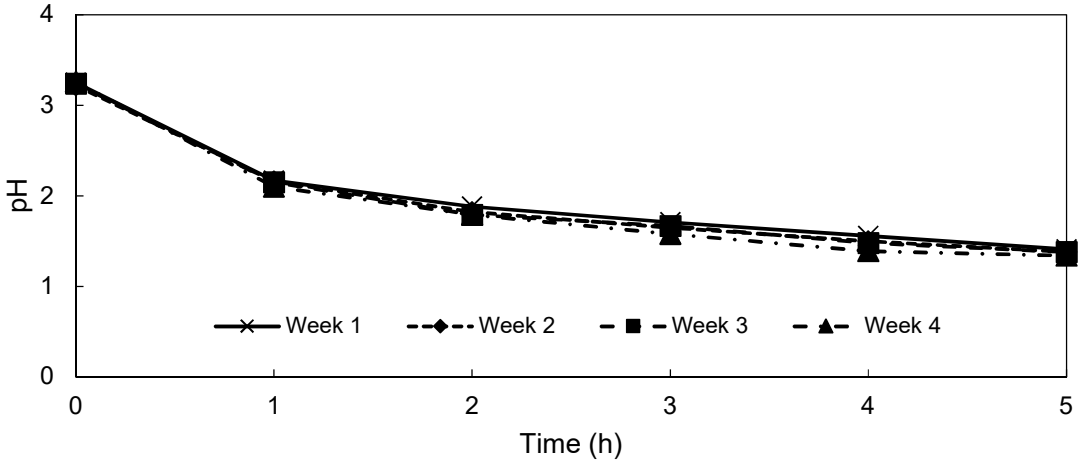

Figure 3.19: Influence of the membrane being subjected to acidic conditions on the anolyte pH obtained from the EW unit after screening of the FAB-PK-130 membrane.

A summary of the variables obtained during the acid degradation experiments with the FAB-PK-130 membrane is given in **Table 3.9**. After immersion, a slight increase in the average voltage was observed, coupled with a decrease in the current efficiency of the EW unit. These

two changes caused a significant change in the SEC (performance) during operation of the EW unit, increasing from 3.84 kWh/kg Fe to 4.61 kWh/kg after 4 weeks.[24]

Table 3.9: Summary of key variables obtained from the EW unit when determining the acid stability of the Fumatech FAB-PK-130 membrane.

Parameters	Week 1	Week 2	Week 3	Week 4
Average Voltage (V)	3.68	3.74	3.78	3.75
Current Efficiency (%)	92	84	82	78
SEC (kWh/kg Fe)	3.84	4.28	4.42	4.61
Catholyte pH (End)	2.61	2.64	3.05	3.08
Anolyte pH (End)	1.41	1.38	1.38	1.34

For comparison, the same stability experiments were repeated using the AMB-SS and FAS-PK-130 membranes. Summaries of the results are presented in **Table 3.10** and **Table 3.11**, respectively. In terms of performance, the AMB-SS membrane (**Table 3.10)** showed significantly less signs of deterioration over time compared to the FAB-PK-130 membrane. In fact, the AMB-SS performance slightly improved over time displaying a decrease in the average voltage, while the catholyte and anolyte end pH values remained near constant over time. This consistency may be attributed to the AMB-SS being more fluorinated than the FAB-PK-130. The manufacturer, however, does not supply this information and it can thus not be confirmed. However, in literature, fluorinated AEMs show higher stability compared to non-fluorinated AEMs.[25]

Table 3.10: Summary of key variables obtained from the EW unit during the testing of the Resintech AMB-SS after being subjected to acidic conditions.

Parameters	Week 1	Week 2	Week 3	Week 4
Average Voltage (V)	3.67	3.49	3.41	3.41
Current Efficiency (%)	83	85	86	80
SEC (kWh/kg Fe)	4.28	3.94	3.41	3.41
Catholyte pH (End)	2.6	2.58	2.57	2.55
Anolyte pH (End)	1.41	1.39	1.38	1.36

As with the AMB-SS membrane, the FAS-PK-130 (**Table 3.11**) showed more consistent performance when subjected to acidic immersion. Although the catholyte and anolyte end-pH values were similar, the current efficiencies varied over the 4 weeks of testing.

Table 3.11: Summary of key variables obtained from the EW unit during the testing of the Fumatech FAS-PK-130 after being subjected to acidic conditions.

Parameters	Week 1	Week 2	Week 3	Week 4
Average Voltage (V)	3.38	3.30	3.27	3.25
Current Efficiency (%)	89	77	90	80
SEC (kWh/kg Fe)	3.65	4.12	3.49	3.9
Catholyte pH (End)	2.46	2.57	2.35	2.9
Anolyte pH (End)	1.41	1.41	1.46	1.37

3.3.7 Iron Concentration

In this final section, three parameters in terms of the Fe concentration will be investigated: i) the Fe flux or transport across the various membranes in the absence and presence of H_2SO_4 in the anolyte (Section 3.3.7.1), ii) the EW performance as a function of both the Fe and Na_2SO_4 concentrations (Section 3.3.7.2) and iii) the performance change with depleting Fe content (Section 3.3.7.3).

3.3.7.1 Iron Flux

To establish an accurate mass balance for the EW process, the transport of Fe through the AEM needs to be accurately quantified.[26] For this reason, the Fe flux of the membranes listed in Section 3.2.2.6 was determined with 0 and 100 g/L H_2SO_4 present in the anolyte. The measured flux for each membrane is listed in **Table 3.12**. Accordingly, all membranes had fluxes ranging between 1.37 – 9.39 g/h/m^2 Fe and 0.23 – 1.58 g/h/m^2 Fe without and with the addition of H_2SO_4, respectively. The variation in the flux of the membranes can be attributed to the different polymers used in each membrane (unfortunately not provided by the suppliers) and their varying thicknesses. At a current density of 300 A/m^2, the plating rate of the Fe at the cathode is 312.5 g/h/m^2, therefore less than 3 % of the iron plated in the EW unit is lost. For the FAB-PK-130 membrane, the flux was significantly lower with less than 1 % of the iron plated in the EW unit being transported to the anolyte in the absence of H_2SO_4. The Fe flux was significantly reduced after the addition of 100 g/L H_2SO_4 to the anolyte,[26] where all membranes exhibited Fe fluxes below 5.85 g/h/m^2. Consequently, the Fe lost to the anolyte was reduced to less than 2 % of the plated Fe. The reduced iron flux with increasing anolyte acid content is attributed to the competing transfer of protons and the iron being transferred.

During testing, the FAB-PK-130 membrane used thus far exhibited an even lower Fe transport rate of 1.05 g/h/m^2, which makes it a suitable membrane for the EW of iron.

Table 3.12: The flux of Fe (g/h/m^2) from the catholyte to anolyte for varying membranes at both 0 g/L and 100 g/L H_2SO_4 in the anolyte.

0 g/L H_2SO_4						
AEM	FAB-PK-130	FAD-PET-75	FAS-PK-130	FAP-330-PE	FAPQ-375-PP	AMB-SS
Flux [a]	2.52	6.34	1.37	3.30	9.39	4.04
100 g/L H_2SO_4						
AEM	FAB-PK-130	FAD-PET-75	FAS-PK-130	FAP-330-PE	FAPQ-375-PP	AMB-SS
Flux [a]	1.05	1.58	0.96	0.23	5.85	0.60

[a] Fe flux (g/h/m^2) from catholyte to anolyte

3.3.7.2 Fe Concentration

As the aim of the EW unit is to significantly reduce the amount of Fe present in the SLS, establishing the lower operational limit with regard to the Fe concentration in the catholyte is of interest. Therefore, the relationship between the Na_2SO_4 (0, 60 & 100 g/L) and the Fe concentration (10 & 80 g/L Fe) on the performance of the EW cell was investigated in this section. **Figure 3.90** depicts the voltage values obtained from the EW unit for both 10 and 80 g/L Fe at the three Na_2SO_4 concentrations used.[8, 27] As was the case with the results on the effect of Na_2SO_4 on its own (Section 3.3.5), a significant reduction in the applied voltage was noted throughout when increasing the Na_2SO_4 content in the electrolytes, irrespective of the amount of Fe present. Accordingly, when Na_2SO_4 was added to the electrolytes, the average applied voltage dropped by 0.75 V in the 10 g/L Fe case, and by 0.48 V in the 80 g/L Fe case. It is interesting to note that, in the absence of Na_2SO_4, the voltage in 10 and 80 g/L Fe increased over time, while reaching a plateau already after 1 hour when Na_2SO_4 was added.

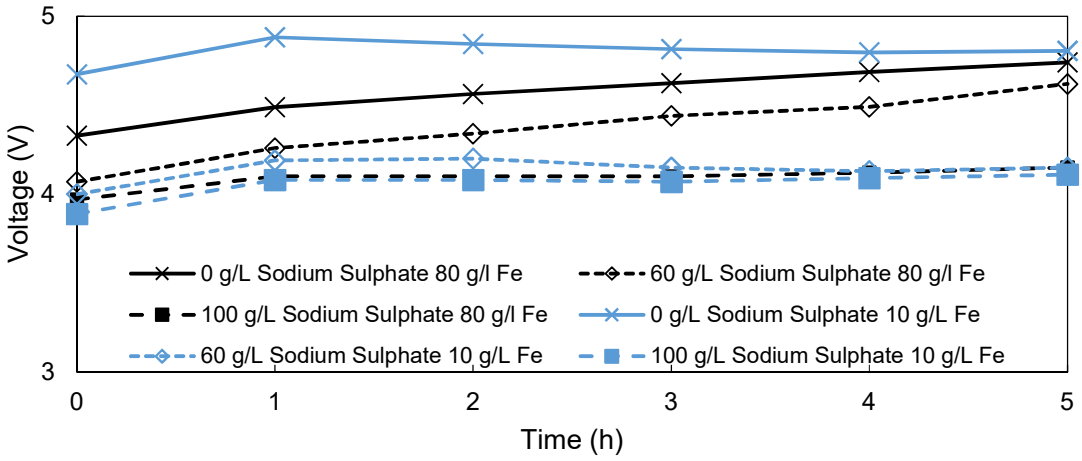

Figure 3.90: Influence of the addition of varying amounts of Na_2SO_4 during the EW of both 80 g/L Fe and 10 g/L Fe on the voltage applied to the EW unit.

In contrast to the seemingly small effect of the Fe concentration on the applied voltage of the EW unit, the effect of reduced Fe content was more pronounced on the catholyte pH (**Figure 3.21)**. It is evident that the catholyte pH in the presence of 80g/L Fe was significantly lower compared to that of catholytes containing 10 g/L Fe. However, the Na_2SO_4 electrolyte concentration did not significantly influence the catholyte pH, irrespective of the Fe content. This implies that the significant pH difference observed was not primarily caused by a difference in conductivity of the catholyte solutions.[8] The difference is more probably due to an increased hydrogen evolution at the cathode in the absence of Fe through the reduction of water, which forms H_2 gas and OH^-,[7] leading to an increasing pH of the catholyte.[7, 17] This increased hydrogen evolution at low Fe concentrations seems plausible when considering the current efficiencies obtained. In the case of 10 g/L Fe with 100 g/L Na_2SO_4, the current efficiency was 87 %, compared to a current efficiency of 97 % obtained with 80 g/L Fe and 100 g/L Na_2SO_4. The primary reason for this is a reduced rate of diffusion of Fe ions from the bulk solution to the cathode surface before reduction can take place at the low Fe-ion concentration in the catholyte.[28] Subsequently, an SEC of 4.6 kWh/kg Fe was obtained at 10 g/L Fe, compared to an SEC of 3.7 kWh/kg Fe when using a catholyte solution containing 80 g/L Fe.

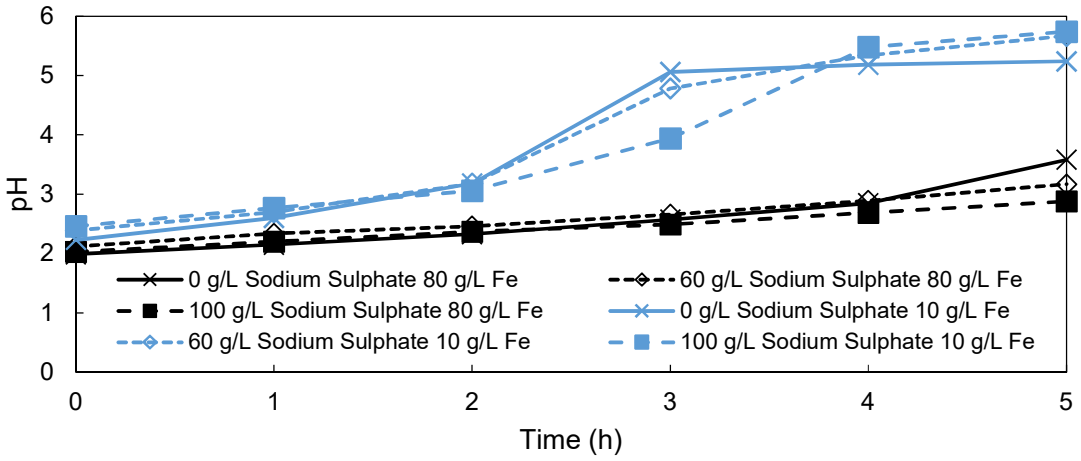

Figure 3.21: Influence of the addition of varying amounts of Na_2SO_4 on the catholyte pH during the EW of 80 g/L Fe and 10 g/L Fe in the EW unit.

As was the case in **Figure 3.90**, the concentration of the Fe in the catholyte solution had little effect on the anolyte pH, as shown in **Figure 3.22**. As such, the average anolyte end pH when using 10 g/L and 80 g/L Fe was 1.41 and 1.39, respectively, which was not statistically significant. This implies that the Fe concentration in the catholyte did not affect the H^+ production in the anolyte through the oxidation of water.

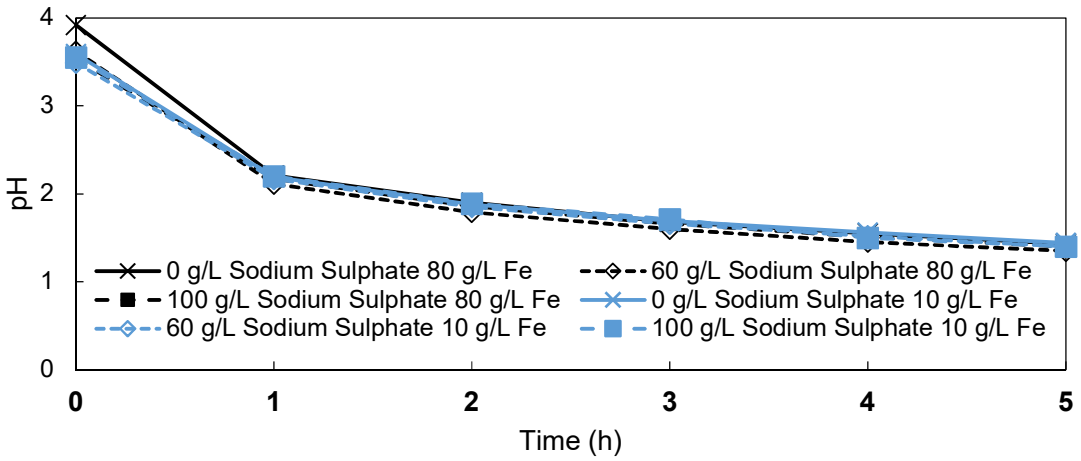

Figure 3.22: Influence of the addition of varying amounts of Na_2SO_4 on the anolyte pH during the EW of 80 g/L Fe and 10 g/L Fe in the EW unit.

A summary of the key variables when comparing the 10 g/L to the 80 g/L Fe catholyte solutions using 0, 60 or 100 g/L Na_2SO_4 is presented in **Table 3.13**. At 10 g/L Fe, the EW unit runs at significantly reduced current efficiencies, leading to an increase in the SEC of the EW unit. Therefore, to curtail operating costs, the EW should ideally be run at iron concentrations above

10 g/L Fe. The EW operating parameters should therefore be adjusted. For example, lowering the applied current density typically increases the current efficiency with low metal concentration electrolytes.[7, 29] This occurs because of the layer of participating Fe ions that does not deplete as quickly near the cathode, thereby decreasing the amount of water reduced.[28]

Table 3.13: Summary of key variables during the EW of 80 g/L Fe and 10 g/L Fe using varying amounts of Na_2SO_4 in the EW unit.

Parameters	**0 g/L Na_2SO_4**	**60 g/L Na_2SO_4**	**100 g/L Na_2SO_4**
	80 g/L Fe		
Average Voltage (V)	4.07	3.87	3.59
Current Efficiency (%)	90	91	97
SEC (kW/h/kg Fe)	4.9	4.6	3.7
Catholyte pH (End)	3.58	3.17	2.88
Anolyte pH (End)	1.43	1.35	1.4

Parameters	**0 g/L Na_2SO_4**	**60 g/L Na_2SO_4**	**100 g/L Na_2SO_4**
	10 g/L Fe		
Average Voltage (V)	4.30	3.64	3.55
Current Efficiency (%)	85	86	87
SEC (kW/h/kg Fe)	5.7	4.7	4.6
Catholyte pH (End)	5.24	5.67	5.74
Anolyte pH (End)	1.44	1.4	1.4

3.3.7.3 Depletion of Fe from Solution

To determine the influence of the desired depletion of Fe on performance, it was decided to operate a larger EW unit with the FAB-PK-130 membrane to the point where Fe depletion of the catholyte occurs. The reason for using the larger unit was to attain faster depletion of Fe using the same experimental duration as before (5 hours). Both variations in voltage and Fe transport from the catholyte to the anolyte over the duration of the experiment are depicted in **Figure 3.23**. Higher voltages were observed during operation of the larger EW unit (image of the unit is shown in **Appendix C**). This increased voltage is due to the increased anode-to-cathode distance (ACD = 5 cm compared to 2 cm in the smaller unit). The increased ACD resulted in a higher overall resistance from both the catholyte and anolyte solutions.[30] The voltage declined steadily from 6.68 V to 5.41 V after 5 hours. The decline in the voltage implies that the conductivity of the membrane increased over time, probably due to H^+/H_2SO_4 absorption.[12] Additionally, a total of 0.21 g of Fe was transported to the anolyte over 5 hours,

corresponding to an Fe flux through the FAB-PK-130 membrane of 0.68 g/h/m^2. During the experiment, a total of 92.8 g of Fe was plated onto the cathode. Therefore, 93 % of the Fe fed to the EW was removed within 5 hours, leaving a depleted catholyte solution with a residual Fe content of 2.8 g/L, which is significantly lower than the 10 g/L recommended in the previous section.

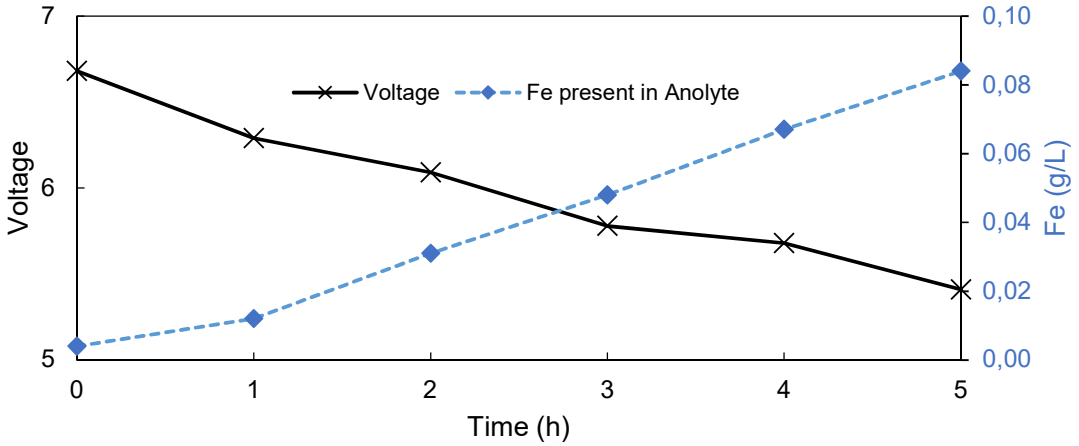

Figure 3.23: Influence of the depletion of iron in the catholyte on both the voltage obtained (primary y-axis) and the Fe content in the anolyte (secondary y-axis) during the operation of the enlarged EW unit for 5 hours.

In addition to the voltage and Fe transfer, the catholyte and anolyte pH were measured (**Figure 3.24**). It is clear that the catholyte pH increased continually, which indicated that no significant proton transfer occurred through the AEM,[20] which is supported by the high current efficiency of 99% that was observed. Together with the high current efficiency and average voltage of 5.98 V, the SEC equated to 5.6 kWh/kg Fe. Furthermore, the anolyte pH showed the inverse trend of the catholyte pH, reaching a final pH of 0.44 after the 5 hours. Accordingly, an anolyte solution with an H_2SO_4 concentration of approximately 35 g/L was produced, while 93% of the iron in the initial catholyte solution (40 g Fe/L) was recovered from the catholyte as electrolytic iron, confirming that this process is able to recover both the iron and the H_2SO_4.

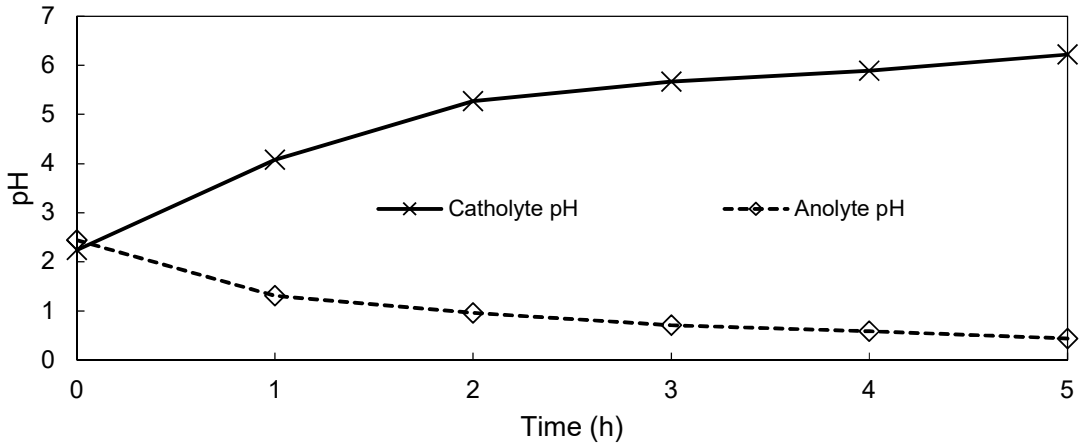

Figure 3.24: Influence of iron depletion in the catholyte on both the anolyte and catholyte pH obtained during operation of the enlarged AEM-EW unit for 5 hours.

3.4 Conclusion

Various EW methods for the treatment of $FeSO_4$ SLS solutions were tested and it was found that the AEM-based EW process far outperformed the other methods tested, even operating at significantly lower SEC values. Subsequently, the following AEM-EW process variables were investigated: (i) boric acid addition, (ii) electrolyte temperature, (iii) catholyte/anolyte pH, (iv) sodium sulphate addition, v) AEM (type, thickness and duration) and vi) Fe (amount, transport and depletion). Boric acid had no effect on the AEM-EW process and was not further used. Increasing the electrolyte temperature to 70 °C led to a significant decrease in the SEC of the AEM-EW process. To simulate the effect of unspent acid in the SLS, H_2SO_4 was added to the catholyte. However, even small additions (12.5 g/L) led to a low current efficiency and high SEC. The anolyte pH had a relatively small effect up to 100 g/L H_2SO_4, which is therefore the recommended maximum recoverable acid value. Finally, Na_2SO_4 addition significantly decreased the SEC while increasing the current efficiency of the AEM-EW process, yielding an optimum of 100 g/L Na_2SO_4.

When screening the various commercial membranes, both with and without H_2SO_4 addition to the anolyte, the FAB-PK-130 notably outperformed all other membranes in terms of current efficiency, SEC, and acid regeneration. The FAB-PK-130 membrane did, however, show increased degradation during stability testing, which will be elaborated on in Chapter 4. When studying the influence of Fe, it was found that the performance decreased when the Fe concentrations reached below 10 g/L Fe, which could be slightly compensated for by adding Na_2SO_4(100 g/L). Finally, during the depletion of the iron from the catholyte, a current efficiency of 99 % at an SEC of 5.6 kWh/kg Fe was attained. During the reduction of the iron

concentration from 40 g/L Fe to 2.7 g/L Fe, approximately 35 g/L H_2SO_4 was produced before side reactions occurred. All these factors considered, the optimal AEM-EW process (highest current efficiency and lowest SEC) should entail an iron concentration above 10 g/L, a catholyte pH above 2, an anolyte sulphuric acid content below 100 g/L, and an electrolyte temperature of 70 °C, while being operated with 100 g/L sodium sulphate.

3.5 Bibliography

1. Lupi, C.; Pilone, D., Electrodeposition of nickel□ cobalt alloys: the effect of process parameters on energy consumption. *Minerals Engineering* **2001,** *14* (11), 1403-1410.
2. Holm, M.; O'Keefe, T. J., Electrolyte parameter effects in the electrowinning of nickel from sulfate electrolytes. *Minerals Engineering* **2000,** *13* (2), 193-204.
3. Jing, L.; Yang, Q.-H.; Zhang, Z., Effects of additives on nickel electrowinning from sulfate system. *Transactions of Nonferrous Metals Society of China* **2010,** *20*, s97-s101.
4. Tripathy, B. C.; Singh, P.; Muir, D. M., Effect of manganese(II) and boric acid on the electrowinning of cobalt from acidic sulfate solutions. *Metall Mater Trans B* **2001,** *32* (3), 395-399.
5. Jeffrey, M. I.; Choo, W. L.; Breuer, P. L., The effect of additives and impurities on the cobalt electrowinning process. *Minerals Engineering* **2000,** *13* (12), 1231-1241.
6. Veglio, F.; Passariello, B.; Barbaro, M.; Plescia, P.; Marabini, A. M., Drum leaching tests in iron removal from quartz using oxalic and sulphuric acids. *International Journal of Mineral Processing* **1998,** *54* (3-4), 183-200.
7. Atkins, P.; De Paula, J.; Keeler, J., *Atkins' physical chemistry*. Oxford university press: 2018.
8. Lundquist, R.; Lewis, R., Conductivity of Sodium Sulfate Solutions Containing Sodium Hydroxide or Sulfuric Acid. *Industrial & Engineering Chemistry Chemical & Engineering Data Series* **1957,** *2* (1), 69-72.
9. Mostad, E.; Rolseth, S.; Thonstad, J., Electrowinning of iron from sulphate solutions. *Hydrometallurgy* **2008,** *90* (2-4), 213-220.
10. Chen, D.; Hickner, M. A.; Agar, E.; Kumbur, E. C., Optimized anion exchange membranes for vanadium redox flow batteries. *ACS Appl Mater Interfaces* **2013,** *5* (15), 7559-66.
11. Kerres, J. A.; Krieg, H. M., Poly(vinylbenzylchloride) Based Anion-Exchange Blend Membranes (AEBMs): Influence of PEG Additive on Conductivity and Stability. *Membranes (Basel)* **2017,** *7* (2), 32.
12. Varcoe, J. R.; Atanassov, P.; Dekel, D. R.; Herring, A. M.; Hickner, M. A.; Kohl, P. A.; Kucernak, A. R.; Mustain, W. E.; Nijmeijer, K.; Scott, K.; Xu, T. W.; Zhuang, L., Anion-exchange membranes in electrochemical energy systems. *Energy & Environmental Science* **2014,** *7* (10), 3135-3191.
13. Mirza, A.; Burr, M.; Ellis, T.; Evans, D.; Kakengela, D.; Webb, L.; Gagnon, J.; Leclercq, F.; Johnston, A., Corrosion of lead anodes in base metals electrowinning. *Journal of the Southern African Institute of Mining and Metallurgy* **2016,** *116* (6), 533-538.
14. Badenhorst, W. D.; Rossouw, C.; Cho, H.; Kerres, J.; Bruinsma, D.; Krieg, H., Electrowinning of Iron from Spent Leaching Solutions Using Novel Anion Exchange Membranes. *Membranes* **2019,** *9* (11), 137.

15. Darling, H. E., Conductivity of Sulfuric Acid Solutions. *Journal of Chemical & Engineering Data* **1964,** *9* (3), 421-426.

16. Ren, X.; Wei, Q.; Hu, S.; Wei, S., The recovery of zinc from hot galvanizing slag in an anion-exchange membrane electrolysis reactor. *J Hazard Mater* **2010,** *181* (1-3), 908-15.

17. Sopian, K.; Daud, W. R. W., Challenges and future developments in proton exchange membrane fuel cells. *Renewable Energy* **2006,** *31* (5), 719-727.

18. Merle, G.; Wessling, M.; Nijmeijer, K., Anion exchange membranes for alkaline fuel cells: A review. *Journal of Membrane Science* **2011,** *377* (1-2), 1-35.

19. Luo, J. Y.; Wu, C. M.; Xu, T. W.; Wu, Y. H., Diffusion dialysis-concept, principle and applications. *Journal of Membrane Science* **2011,** *366* (1-2), 1-16.

20. Mauritz, K. A.; Gray, C., Proton tunneling within the hydration structure of hydroxyl-containing perfluorosulfonate ionomer membranes. *Macromolecules* **1983,** *16* (8), 1279-1286.

21. Tsampas, M.; Pikos, A.; Brosda, S.; Katsaounis, A.; Vayenas, C., The effect of membrane thickness on the conductivity of Nafion. *Electrochimica Acta* **2006,** *51* (13), 2743-2755.

22. Cho, H.; Krieg, H. M.; Kerres, J. A., Application of Novel Anion-Exchange Blend Membranes (AEBMs) to Vanadium Redox Flow Batteries. *Membranes (Basel)* **2018,** *8* (2), 33.

23. Sivasubramanian, P.; Ramasamy, R. P.; Freire, F. J.; Holland, C. E.; Weidner, J. W., Electrochemical hydrogen production from thermochemical cycles using a proton exchange membrane electrolyzer. *International Journal of Hydrogen Energy* **2007,** *32* (4), 463-468.

24. Sukkar, T.; Skyllas-Kazacos, M., Membrane stability studies for vanadium redox cell applications. *Journal of Applied Electrochemistry* **2004,** *34* (2), 137-145.

25. Shan, J.; Vaivars, G.; Luo, H. Z.; Mohamed, R.; Linkov, V., Sulfonated polyether ether ketone (PEEK-WC)/phosphotungstic acid composite: Preparation and characterization of the fuel cell membranes. *Pure and Applied Chemistry* **2006,** *78* (9), 1781-1791.

26. Akretche, D.-E.; Kerdjoudj, H., Donnan dialysis of copper, gold and silver cyanides with various anion exchange membranes. *Talanta* **2000,** *51* (2), 281-289.

27. Arden, T., 78. The hydrolysis of ferric iron in sulphate solution. *Journal of the Chemical Society (Resumed)* **1951**, 350-363.

28. Fibbioli, M.; Morf, W. E.; Badertscher, M.; de Rooij, N. F.; Pretsch, E., Potential drifts of solid-contacted ion-selective electrodes due to zero-current ion fluxes through the sensor membrane. *Electroanalysis: An International Journal Devoted to Fundamental and Practical Aspects of Electroanalysis* **2000,** *12* (16), 1286-1292.

29. Beukes, N. T.; Badenhorst, J., Copper electrowinning: theoretical and practical design. *J S Afr I Min Metall* **2009,** *109* (6), 343-356.

30. Mott, N. In *The electrical resistance of dilute solid solutions*, Mathematical Proceedings of the Cambridge Philosophical Society, Cambridge University Press: 1936; pp 281-290.

CHAPTER 4

NOVEL AEM PREPARATION AND STABILITY TESTING

Table of Contents

4.1 Introduction

In the previous chapter, the effect of various variables, the operational limits of the AEM-EW unit and a provisional stability determination of the commercial AEMs were presented. The durability test results (Section 3.3.6.3) showed that the FAB-PK-130 experienced slight degradation over time. It is, however, clear that the stability of an AEM used in an AEM-EW unit is critical, influencing both the operational cost and possible downtime of the process. Therefore, this chapter presents a more in-depth durability study of i) the FAB-PK-130 membrane, ii) a novel, not yet commercialised membrane from Fumatech (VM-FAPQ-8130-PK) and iii) AEMs synthesized in conjunction with the group of Dr Kerres (University of Stuttgart).

The novel AEMs from the group of Dr Kerres are newly developed blended AEMs, which are typically produced by blending an anion-exchange polymer or its halo-methylated precursor with a chemically and mechanically stabilizing matrix polymer.[1-3] By combining, for example, polymers such as polybenzimidazole and a sulphonated cation-exchange polymer, ionic cross-links are formed which further chemically stabilize the blended AEMs.[1-3] In a recent study, a 3-component blended membrane consisting of (i) poly(2,6-dimethyl-1,4-phenylene oxide) (PPO) quaternized with tetra-methylimidazole, (ii) a polybenzimidazole (PBI) as the matrix polymer, and (iii) a sulphonated polymer as ionic cross-linker showed excellent stability and performance in VRFB applications.[4] In recent work published by our group, Badenhorst *et al*.[5] obtained excellent performance during the EW of iron using such 3-component blended AEMs.[5] However, the use of these AEMs has not been exhaustively investigated specifically for the notoriously difficult electrowinning (EW) of iron from an acidic environment,[6] which requires high chemical and oxidative stability, a low cation transfer rate, and low electrical resistance.[7] These challenges have been highlighted already in Section 3.3.6.3. It is therefore of significant interest to further study the suitability of these blended membranes for EW applications.

The environment present in the catholyte solution of the AEM-EW unit is highly oxidizing and highly acidic (anolyte), where the oxidative environment results from the oxidation of Fe(II) to Fe(III), which, depending on the accepted mechanism, can either form oxyradicals or peroxides.[8-10] To test the possible oxidative contribution to the degradation of the membranes, the same three-component blended membranes, used previously,[5] were impregnated with Ce_2O_3 (ceria), which is known to act as a radical and oxidant scavenger.[11] Ce_2O_3 is currently incorporated in proton exchange membranes (PEMs) used in fuel cells.[12] Accordingly, it has been shown that the addition of 1 % wt Ce_2O_3 led to a sevenfold lifetime increase during open-circuit voltage testing in a fuel cell compared to the membrane lifetime without Ce_2O_3. Since

the effect of Ce_2O_3 as a radical scavenger has not yet been tested for the membranes used in this study, Fenton tests were done with these membranes with and without Ce_2O_3 alongside the AEMs provided by Fumatech.

In view of the required stability of AEMs for the AEM-EW process, this chapter will focus on i) the preparation of stable novel AEMs (with and without Ce_2O_3), ii) membrane stability characterisation using Fenton testing, and iii) membrane stability testing through prolonged operation in the AEM-EW unit using selected membranes. This allowed the determination of the performance of both membranes on a weekly basis and provided insight into the degradation which may occur during industrial usage of these membranes.

4.2 Method

For this study, two membranes from Fumatech (FAB-PK-130 and VM-FAPQ-8130-PK) were used. The composition of the VM-FAPQ-8130-PK membrane was not provided by Fumatech as it was a non-commercial R&D sample at the time of testing. All the other membranes made in conjunction with the Institute for Chemical Process Engineering (ICVT) of the University of Stuttgart were prepared and characterized as described in Section 4.2.1. Subsequently, the oxidative stability of the membranes was determined using the Fenton test (Section 4.2.2). After establishing the suitability of the membranes in the AEM-EW cell for five hours (Section 4.2.3), 20-hour (Section 4.2.4) and 3-week (Section 4.2.5) experiments were conducted on selected AEMs.

4.2.1 Preparation and Characterization of Novel AEMs

4.2.1.1 AEM Preparation

In view of their previous excellent performance in VRFBs[4] and the EW of iron,[5] two types of blend membranes were synthesized, namely BM-5 and 2408-2. These membranes were prepared from a mixture of a halogenated polymer, a polybenzimidazole (PBI) polymer, a sulphonated polymer and 1,2,4,5-tetramethyl-imidazole (TMIm). The compositions of the membranes are given in **Table 4.1**, while **Table 4.2** provides the structures of the various components used.

For preparation, the halogenated polymer, PBI and sulphonated polymer components (**Table 4.1**) were dissolved in dimethyl sulphoxide (DMSO – Sigma Aldrich) as described previously.[5] Subsequently, the TMIm (Sigma Aldrich) was added to the blend solution. The mixture was then poured onto a level glass plate and spread evenly over the surface, followed by the

evaporation of the DMSO in a Thermo Scientific™ Heratherm™ advanced protocol oven for two hours at a temperature of 150 °C. During solvent evaporation, the TMIm reacted with the halomethyl groups (quaternization of the imidazole to a tetramethylimidazolium anion-exchange group). The membranes were then removed from the glass plate by immersion in water. Subsequently, they were placed in a 10 % sodium chloride (NaCl - Sigma Aldrich) solution for 24 hours at 90 °C, after which they were placed in deionised water for a further 24 hours at 60 °C before being stored in deionised water. Before use, the membranes were pre-treated by immersing them in a 0.5 M NaCl solution at 25 °C for 24 hours. Where required, the Ce_2O_3 powder (Sigma Aldrich) was added before the addition of the TMIm to the polymer blend.

Table 4.1: The different polymers and compositions used for the synthesis of the novel AEMs

Name	Halogenated polymer (g)	Tertiary amine (g)	PBI (g)	Sulphonated polymer (g)	Ce_2O_3 (wt %)
BM-5 (0 %)	PPOBr (0.80)	TMIm (0.65)	PBIOO (1.2)	SAC 096 (0.2)	0
BM-5 (1 %)	PPOBr (0.80)	TMIm (0.65)	PBIOO (1.2)	SAC 096 (0.2)	1
BM-5 (5 %)	PPOBr (0.80)	TMIm (0.65)	PBIOO (1.2)	SAC 096 (0.2)	5
2408-2 (0 %)	PVBCl (1.50)	TMIm (1.3)	F6PBI (2.35)	-	0
2408-2 (1 %)	PVBCl (1.50)	TMIm (1.3)	F6PBI (2.35)	-	1
2408-2 (5 %)	PVBCl (1.50)	TMIm (1.3)	F6PBI (2.35)	-	5

Table 4.2: Polymer components of the PBI-blended membranes.

Halogenated polymers		Tertiary amine
PVBCl	PPOBr	TMIm
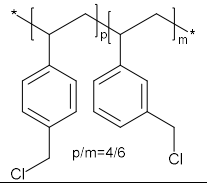	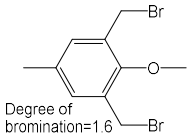	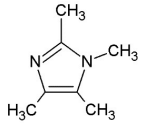
PBI polymers		
F_6PBI	PBIOO	
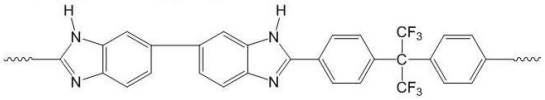	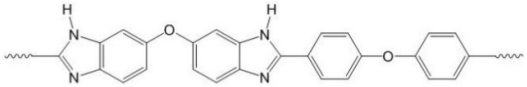	
Sulphonated polymers		
SAC		
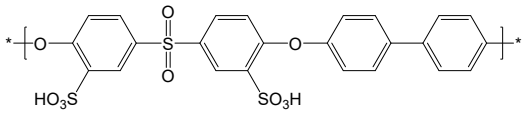		

PVBCl = poly(vinylbenzyl chloride); PPOBr = Poly(p-phenylene oxide) (PPO) brominated; TMIm = 1,2,4,5-tetramethyl-imidazole; F_6PBI = fluorinated polybenzimidazole; PBIOO = polybenzimidazole; SAC = sulphonated poly(phenylethersulphone)

4.2.1.2 AEM Characterization

After synthesis, the membranes were characterized by determining their ion exchange capacity (IEC), conductivity (σ) and water uptake (WU %).

Ion Exchange Capacity (IEC)

To determine the IEC, the membranes were immersed in a 1 M KOH (Sigma Aldrich) solution for 24 hours at 90 °C, converting the AEM from the chloride form to the hydroxide form. Subsequently, the membranes were washed with deionised water to remove excess hydroxide from the membrane before being immersed for 24 h in 60 ml of a saturated sodium chloride solution to exchange the anion-exchange groups with the chlorides. Three ml of a standard 0.1 N hydrochloric acid (Sigma Aldrich) solution was added to the saturated sodium chloride solution containing the membranes and kept overnight. The membranes were then washed with 25 ml deionized water and this water was added to the 60 ml saturated sodium chloride solution. Titration was performed with a 0.1 N sodium hydroxide (Sigma Aldrich) solution. Finally, the membranes were washed several times using deionized water and placed

in an oven where they were dried for 24 h at 130 °C. The total IEC was calculated using **Eq. 4.1**,

$$IEC = (C_{HCl}\, V_{HCl} - C_{NaOH}\, V_{NaOH})/m_{dry} \quad (4.1)$$

where IEC = ion exchange capacity (meq/g), C_{HCl} = concentration of a hydrochloric acid solution (M), V_{HCl} = used volume of the hydrochloric acid solution (ml), C_{NaOH} = concentration of the sodium hydroxide solution (M), V_{NaOH} = added volume of the sodium hydroxide solution (mL) and m_{dry} = dry weight of the membrane (g).

Conductivity of Cl^-

The conductivity of Cl^- (σ_{Cl^-}) through the AEMs was determined using a Zahner-elektrik IM6 impedance spectrometer. The impedance was recorded at room temperature in a 1M NaCl solution with a frequency range of 200 kHz to 8 MHz in the potentiostatic mode (amplitude 10mV). Membrane resistance was calculated from the intercept in the real axis. From this, the conductivity was determined using **Eq. 4.2**, with σ = conductivity (mS/cm), R_{sp} = resistivity (Ω cm), d = thickness of membrane (cm), R = ohmic resistance (Ω) and A = electrode surface (cm^2).

$$\sigma = 1/R_{sp} = d/RA \quad (4.2)$$

Water uptake (WU)

The water uptake (WU) was determined by weighing the dry membrane samples, followed by soaking the membranes in deionised water at 25 °C and 90 °C for 24 hours. Before determining the wet weight, the surface of the membrane was blotted with tissue paper to remove excess water from the surface. Water uptake was calculated using **Eq. 4.3**.

$$WU\ (\%) = (\text{Wet weight} - \text{Dry weight}) / \text{Dry weight} \times 100\% \quad (4.3)$$

4.2.2 Fenton Testing

For the Fenton testing of both the novel AEMs and the membranes obtained from Fumatech GmbH, the membranes were dried for 24 hours at 90 °C. After drying, the dry weight of the membranes was determined. For all membranes, the Fenton solution used consisted of 3 wt % H_2O_2 (Sigma Aldrich) with 4 ppm Fe(II) as $(NH_4)_2Fe(SO_4)_2.6H_2O$ (Sigma Aldrich). The dry membranes were immersed in the prepared Fenton solution for 24, 48, 72 and 96 hours, exposing the membranes to the radical-forming reaction shown in **Eq. 4.4**.[11]. After immersion, the membranes were first rinsed repeatedly using de-ionised water before being immersed in

de-ionised water for two days at 68 °C, thereby terminating the Fenton degradation reaction. After two days, the membranes were again rinsed repeatedly and then dried at 90 °C for one day, before again determining the dry weight. The recorded loss in mass is indicative of the severity of the degradation that the membrane experienced. Finally, SEM images were obtained before and after the Fenton testing of the various membranes (Ce_2O_3, membranes were not imaged using SEM analysis).

$$Fe^{2+} + H_2O_2 \rightarrow Fe^{3+} + OH^- + \dot{O} \quad (4.4)$$

4.2.3 AEM-EW (5 h)

The same experimental procedure as described in Section 3.2.1 was used to characterize the performance of all the AEMs discussed above using the EW flow cell. All membranes were characterized using catholyte solutions containing 80 g/L Fe as $FeSO_4$, 60 g/L Na_2SO_4, and 10 g/L EDTA, while the anolyte solutions consisted of 60 g/L Na_2SO_4. The electrolyte temperatures were held constant at 70 °C, while a current density of 300 A/m^2 and a superficial flow velocity of 1 cm/s were used. Sampling and analysis were done in 1-hour intervals by taking a 10 ml sample each from the catholyte and anolyte in order to determine the pH.

4.2.4 AEM-EW (20 h)

Before testing the two selected AEMs for the extended 3-week period, the FAB-PK-130 membrane was tested for 20 hours in the AEM-EW cell (see Section 3.2.1) to observe the possible degradation in a smaller timeframe. This was again done using the standard electrolyte condition of 80 g/L Fe as $FeSO_4$, 10 g/L EDTA, and 60 g/L Na_2SO_4 for the catholyte and 60 g/L Na_2SO_4 for the anolyte. After every 5 hours, the amount of plated Fe was weighed and the pH of both the catholyte and anolyte was measured.

4.2.5 AEM-EW (3 weeks)

As the AEM should be able to perform for extended periods without maintenance or replacement, the performance of both the FAB-PK-130 and VM-FAPQ-8130-PK membranes was tested over a period of three weeks using 2 L of a solution composed of 80 g/L Fe as

$FeSO_4$, 10 g/L EDTA, and 60 g/L Na_2SO_4 for the catholyte and 60 g/L Na_2SO_4 for the anolyte. Both the catholyte and anolyte were replaced in 1-week intervals, in addition to determining the amount of Fe plated, the Fe flux, and measuring the catholyte and anolyte pH. After three weeks of testing, both AEMs were also analysed using SEM imaging.

4.3 Results and Discussion

4.3.1 Preparation and Characterization of Novel AEMs

After manufacture, the novel AEMs were characterized. The results thereof are presented in **Table 4.3**. For both BM-5 and 2408-2, the data of only the membranes without added Ce_2O_3 are presented as the results did not differ significantly when adding Ce_2O_3. Both membranes showed IEC values that were 2.00 meg/g lower than those obtained for the previously used AEMs for iron EW.[5] The lower IEC values can be attributed to the differing chemical composition compared to previously tested membranes,[5] which led to an increase in covalent bond formation in the polymer blend.[5] While a decline in IEC could indicate higher operational resistances, added crosslinking would lead to an increase in the stability of the membranes. This was confirmed by the lower water uptake values, which were below 11 % compared to the water uptake values of > 30 % obtained previously.[5] This decrease in water uptake should substantially increase the stability of the AEMs during operation in the EW unit. Both the impedance and conductivity values should be adequate for use in an EW unit yielding low enough electrical resistance during operation.

Table 4.3: Characterization data obtained for the novel BM-5 and 2408-2 membrane.

Name	IEC (meq/g)	Impedance (Ohm/cm)	Conductivity (mS/cm)	Water Uptake at 25 °C/90 °C (%)
BM-5 (0 %)	0.45	3204	0.31	10.8/4.1
2408-2 (0 %)	0.28	11052	0.09	7.1/5.9

4.3.2 Fenton Testing

Due to the observed instability of the FAB-PK-130 membrane (Section 3.3.6.) in the acidic and oxidative environment of the AEM-EW cell, the degradation of the two Fumatech membranes as well as the novel AEMs was studied using the Fenton test. For clarity, the two Fumatech membranes will be discussed first, followed by the 3x2 novel AEMs.

The mass loss observed over the four days of Fenton testing for the FAB-PK-130 and VM-FAPQ-8130-PK membranes is shown in **Figure 4.1**. After the first day, the FAB-PK-130 membrane had already lost 18 % of its weight, increasing to a total mass loss of 66 % after four days. In contrast, the VM-FAPQ-8130-PK membrane lost only 8.24 % of its initial mass after one day and 10 % after the third day. The difference in the stability of these two membranes is probably due to the fact that the FAB-PK-130 membrane is a hydrocarbon-based AEM, which are known for their instability in oxidative environments.[13] In contrast, according to personal communications from the suppliers, the VM-FAPQ-8130-PK membrane contains partially fluorinated polymers that are more resilient to radical-facilitated oxidation.[14]

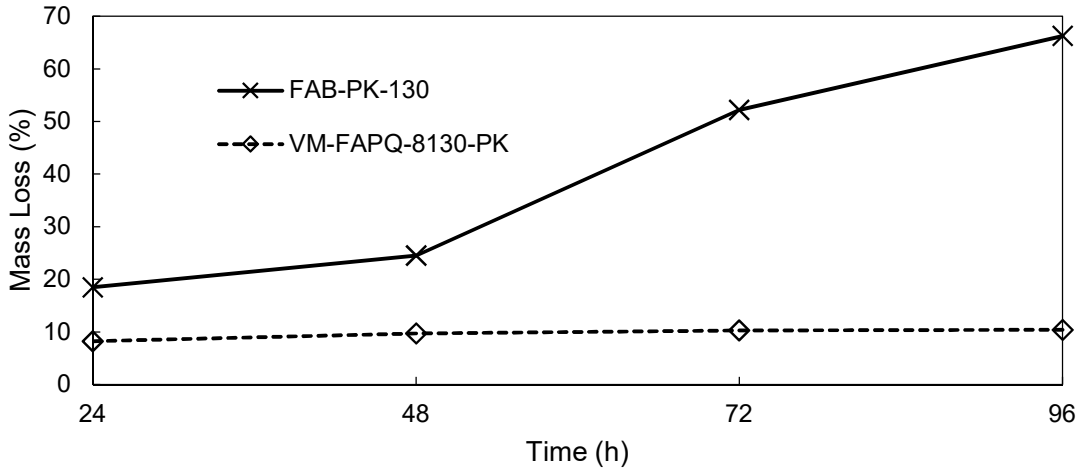

Figure 4.1: Mass loss of the FAB-PK-130 and VM-FAPQ-8130-PK membranes during Fenton testing.

The same Fenton test was performed on the novel 2408-2 and BM-5 membranes containing either 0, 1 or 5 % Ce_2O_3 to determine the radical capturing ability in these environments.[11-12] The mass loss data of the three 2408-2 membrane samples over four days (**Figure 4.2**) indicate that the mass loss was reduced by up to 5 % after 48 hours with 1 and 5 wt.% added Ce_2O_3. However, after 48 hours, the effect of the Ce_2O_3 seemed to decrease, since the mass loss of the 0 wt % and 5 % Ce_2O_3 were nearly identical after 96 hours. For the BM-5 membrane, the inclusion of Ce_2O_3 was only effective during the first 24 hours of Fenton testing. Thereafter, the mass loss was similar, regardless of Ce_2O_3 inclusion.

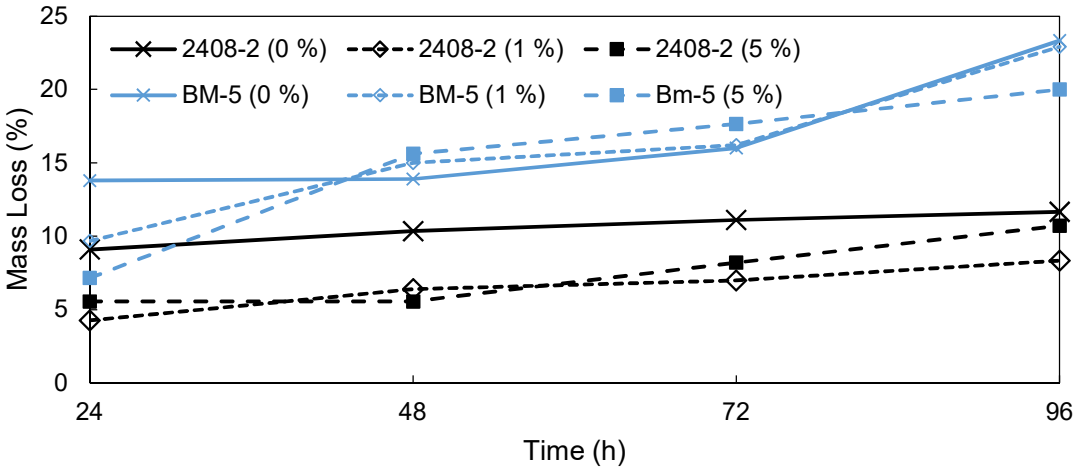

Figure 4.2: The mass loss of both the 2408-2 and BM-5 membranes during Fenton testing with various amounts of Ce_2O_3 integrated into the membranes.

The decreasing functionality of the Ce_2O_3 could be ascribed to the consumption of the Ce_2O_3. In theory, Ce_2O_3 is capable of cyclic radical capture only if adequate amounts of free protons are available for the regeneration step as illustrated in **Figure 4.310**.[11] However, during the EW process, the Ce_2O_3 should be continuously regenerated through proton tunnelling from the anolyte to the catholyte. A possible additional benefit of the inclusion of Ce_2O_3 into the membrane could, therefore, be the consumption of any free protons tunnelling into the catholyte through the membrane.

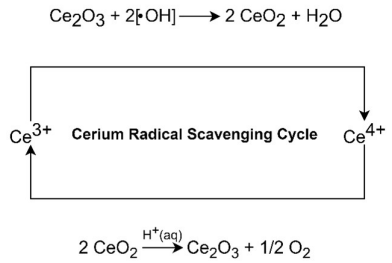

Figure 4.310: Radical scavenging cycle of Cerium.[11]

A summary of all the Fenton test results is given in **Table 4.4**, with the 2408-2 (1 %) membrane showing the highest resistance to oxidation/radical attacks. In contrast, the FAB-PK-130 membrane used thus far showed the least resistance to attack. When comparing the two Fumatech membranes, the VM-FAPQ-8130-PK (partially fluorinated AEM, 10.4 % mass loss) exhibited a mass loss that was nearly 7-fold lower compared to that of the FAB-PK-130 membrane (hydrocarbon-based AEM, 66.3 % mass loss). Partially fluorinated membranes, therefore, perform significantly better in the oxidative/radical Fenton test environment, which

is similar to the conditions present in the EW unit. This is echoed by the difference in performance between the two novel membranes 2408-2 and BM-5 in terms of their mass losses. Membrane BM-5, which contains a non-fluorinated PBI polymer for its backbone, exhibited 20 % mass loss after 96 hours, while the 2408-2 membrane that is composed of a fluorinated PBI backbone exhibited only 10.7 % mass loss over 96 hours. However, regardless of being fluorinated or not, both these novel AEMs exhibited higher oxidative stability than the FAB-PK-130 membrane. Furthermore, the performance of the 2408-2 (5 %) membrane was comparable to the commercial VM-FAPQ-8130-PK membrane.

Table 4.4: A summary of the mass loss of each novel and commercial membrane over four days of Fenton testing.

Membrane	24 Hours	48 Hours	72 Hours	96 Hours
	Mass loss (%)	Mass loss (%)	Mass loss (%)	Mass loss (%)
2408-2 (0 %)	9.09	10.34	11.11	11.67
2408-2 (1 %)	4.26	6.38	6.98	8.33
2408-2 (5 %)	5.56	5.56	8.20	10.71
BM-5 (0 %)	13.8	13.89	16.00	23.33
BM-5 (1 %)	9.68	15.00	16.22	22.92
BM-5 (5 %)	7.14	15.63	17.65	20.00
FAB-PK-130	18.5	24.49	52.22	66.27
VM-FAPQ-8130-PK	8.24	9.72	10.29	10.42

After determination of the mass loss of each membrane, SEM images were obtained of 2408-2, BM-5, FAB-PK-130, and VM-FAPQ-8130-PK. These images are displayed in **Figure 4.4**. All images were captured at a magnification of 400x, except the FAB-PK-130 membrane after Fenton testing, which was captured at a magnification of 87x. Membranes 2408-2 and VM-FAPQ-8130-PK showed slight damage after the Fenton testing. However, no deep cracks or extensive damage can be noted on these membranes. This observation is in line with the mass loss values presented in **Table 4.4**, and confirms the stability of these two membranes in an oxidative environment. In contrast to the high stability observed for the previous two membranes, the BM-5 membrane showed slight damage and cracking of the surface. The FAB-PK-130 membrane showed significant damage and loss of polymeric material, echoed by its previously observed high mass loss. It can be seen in the SEM imaging that only the polyether ether ketone (PEEK) and some parts of the membrane remained after Fenton testing.

Before Fenton Testing		After Fenton Testing	
2408-2			
a)	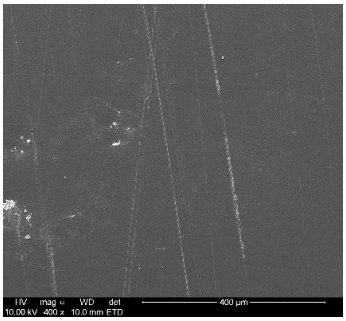	b)	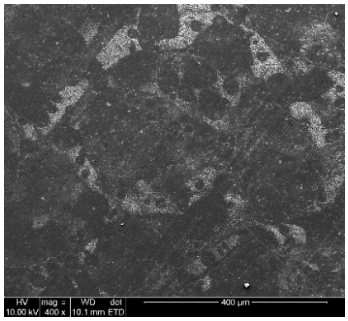
BM-5			
c)	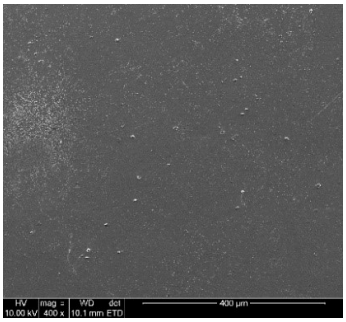	d)	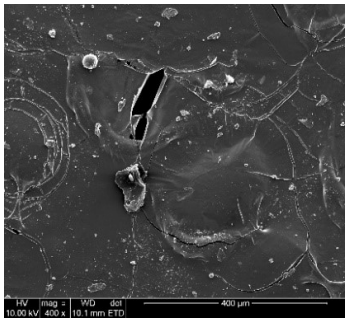
FAB-PK-130			
e)	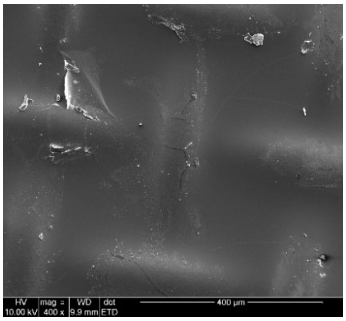	f)	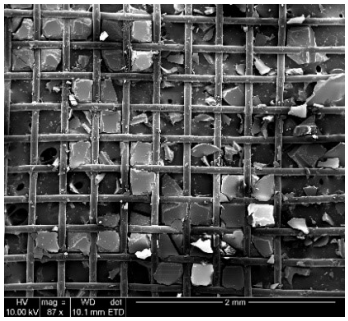
VM-FAPQ-8130-PK			
g)	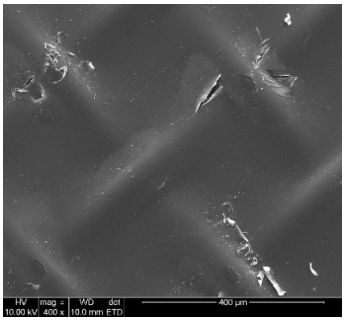	h)	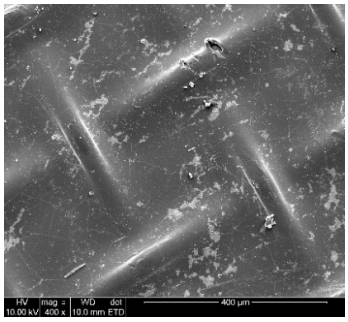

Figure 4.4: SEM Imaging of the ICVT and Fumatech membranes before and after Fenton testing

4.3.3 AEM-EW (5 h)

In view of the slight effect attained when adding Ce_2O_3 during Fenton testing, the AEM-EW studies using the in-house membranes were done without any added Ce_2O_3. In this first AEM-EW experiment, the aim was to use the same conditions and duration (5 h) that had been used in Chapter 3 to facilitate the comparison of the data. The voltage over time of the two Fumatech AEMs and the two ICVT AEMs is depicted in **Figure 4.5**. The FAB-PK-130 AEM used previously (Chapter 3) showed an increase in voltage over the duration of the EW experiment, starting at a voltage of 3.57 V and ending at 4.12 V with an average voltage of 3.87 V. This correlates with **Figure 3.2**, where a similar trend was observed earlier. The other three membranes showed either a stable voltage over the duration of the EW experiment, or even a slight decrease in the voltage applied to the EW unit. The VM-FAPQ-8130-PK membrane operated with the lowest average voltage of 3.60 V, compared to the 3.64 V and 3.81 V of the BM-5 and 2408-2 membranes, respectively. This reflects what has been noted in Chapter 3 regarding the high electrical resistance of the FAB-PK-130 membrane, with the three other membranes offering substantially lower and more stable electrical resistances.

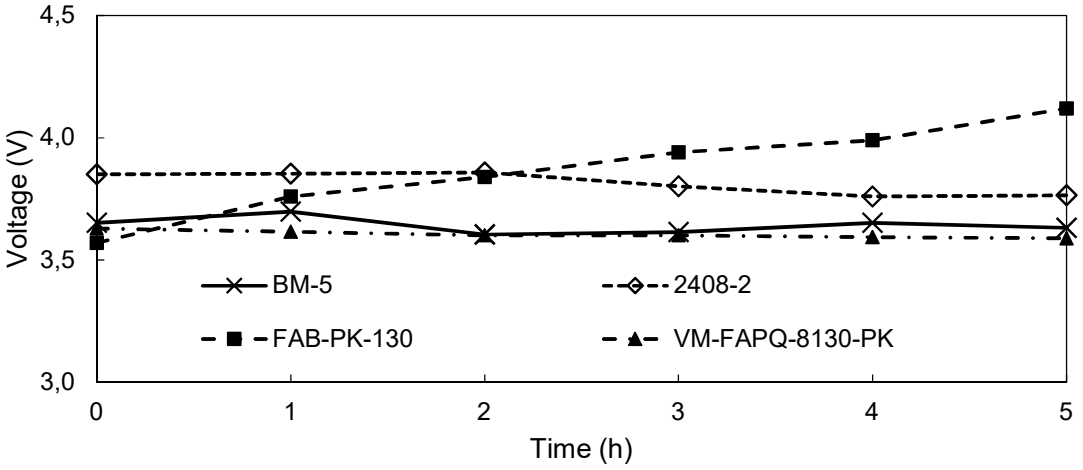

Figure 4.5: Influence of Fumatech and ICVT AEMs on the voltage behaviour in the AEM-EW unit.

Another critical parameter to consider during the EW process is the effect of the membrane on the catholyte pH, which is shown in **Figure 4.6**. Both the FAB-PK-130 and the VM-FAPQ-8130-PK showed a positive upward trend in the catholyte pH, reaching pH values of 3.17 and 3.34, respectively, which correlate with current efficiencies of 91 % and 99 %, respectively. Despite the similar performance of the two Fumatech AEMs, the lower voltage and higher current efficiency attained with the VM-FAPQ-8130-PK membrane in the AEM-EW unit

resulted in a significantly lower SEC of 3.49 kWh/kg Fe compared to the 4.08 kWh/kg obtained with the FAB-PK-130 membrane.

Despite their low-end catholyte pH values of 2.39 and 1.90 for the BM-5 and 2408-2 membranes, respectively, both the novel AEMs performed well in the AEM-EW unit. The BM-5 membrane operated at a current efficiency of 95 % and the 2408-2 membrane at 88 %. The high performance of these two membranes despite the low catholyte pH values obtained in both cases is attributed to the low applied voltages that were required, implying a decrease in the overpotential, thus reducing the H_2 production at the cathode. During EW, the BM-5 membrane yielded an SEC of 3.66 kWh/kg Fe, while the 2408-2 membrane yielded an SEC of 4.15 kWh/kg Fe.

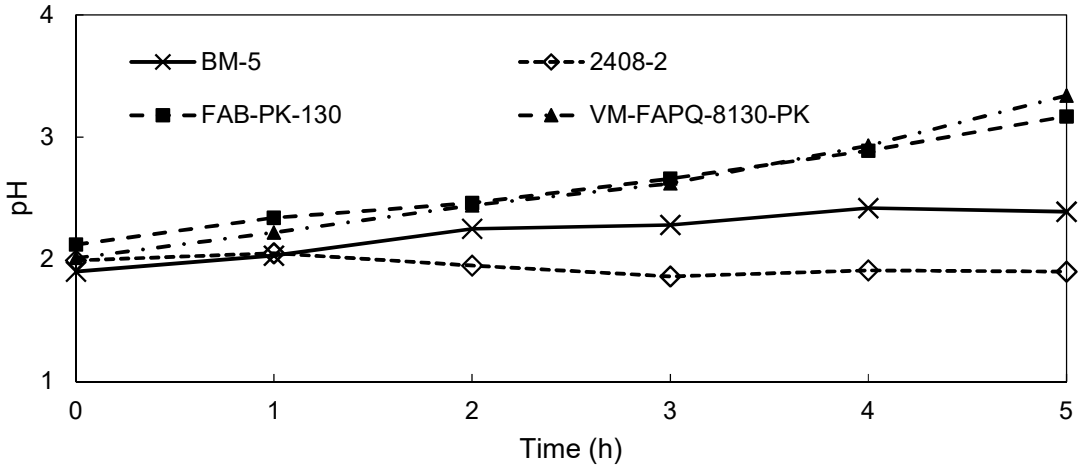

Figure 4.6: Influence of various AEMs on the catholyte pH behaviour in the AEM-EW unit.

The anolyte pH data obtained when using the two Fumatech AEMs and the two ICVT AEMs are shown in **Figure 4.7**. Accordingly, all four of the membranes exhibited similar performances over the length of the 5-hour experiment. The FAB-PK-130 reached a slightly lower anolyte pH of 1.35 compared to the pH values of 1.46, 1.47 and 1.64 obtained for the BM-5, 2408-2 and VM-FAPQ-8130-Pk membranes, respectively.

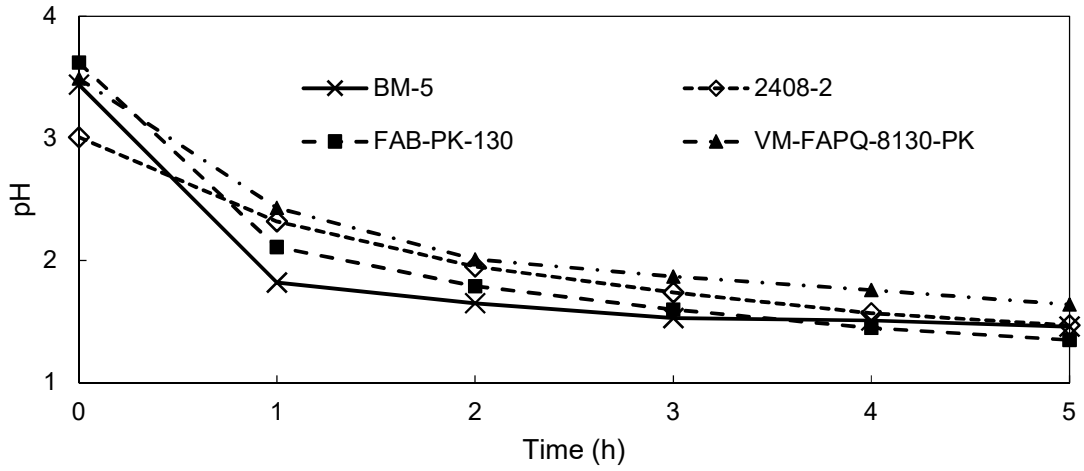

Figure 4.7: Influence of various AEMs on the anolyte pH behaviour in the AEM-EW unit.

According to the summary of the performance of the four AEMs (**Table 4.5)**, it is clear that the new VM-FAPQ-8130-PK membrane outperformed the FAB-PK-130 membrane in terms of most of the crucial performance parameters, excluding the anolyte pH. It operated at an efficiency of 99 % and an SEC of 3.49 kWh/kg Fe, representing an increase of 8 % in terms of current efficiency and a decrease of 0.59 kWh/kg Fe in the SEC compared to that obtained with the FAB-PK-130 membrane. The ICVT AEM, BM-5, performed similarly to the VM-FAPQ-8130-PK membrane, yielding an SEC of 3.66 kWh/kg Fe, only 0.17 kWh/kg Fe higher than the SEC obtained with the VM-FAPQ-8130-PK membrane. It is thus concluded that either one of these three membranes would be more suitable than the FAB-PK-130 membrane for the EW of Fe.

Table 4.5: Summary of key variables obtained from the AEM-EW unit employing Fumatech and ICVT membranes.

Membrane	Current Efficiency (%)	SEC (kWh/kg)	Catholyte pH (End)	Anolyte pH (End)
FAB-PK-130	91	4.08	3.17	1.35
VM-FAPQ-9130-PK	99	3.49	3.34	1.64
BM-5	95	3.66	2.39	1.46
2408-2	88	4.15	1.90	1.47

4.3.4 AEM-EW (20 h)

As the FAB-PK-130 membrane underwent the most degradation in the stability tests discussed in Section 4.3.4, it was tested for a continuous 20-hour EW experiment .[15-16] The voltage and current efficiency obtained during this experiment are depicted in **Figure 4.8**. Unlike the results obtained with the 5 h AEM-EW experiment, no signs of reduced performance were noted even after 20 hours of operation of the EW unit with the FAB-PK-130 membrane. After the first ten hours, the EW unit achieved a plateau at 99 % current efficiency, which was maintained up to the end of the experiment at 20 hours. Also, the voltage stabilized after ten hours at a voltage of 3.90 V, indicating stable performance of the FAB-PK-130 membrane over a 20-hour period.[16] The initial increase in voltage to 4.09 V after one hour correlates to the increase noted in Figure 4.1, where the voltage increased to 4.12 after 5 h. These results do, however, show that the voltage actually stabilizes and even declines somewhat after ten hours of operation. This implies that the membrane seemed to take ten hours for complete conditioning before operating at optimal performance.

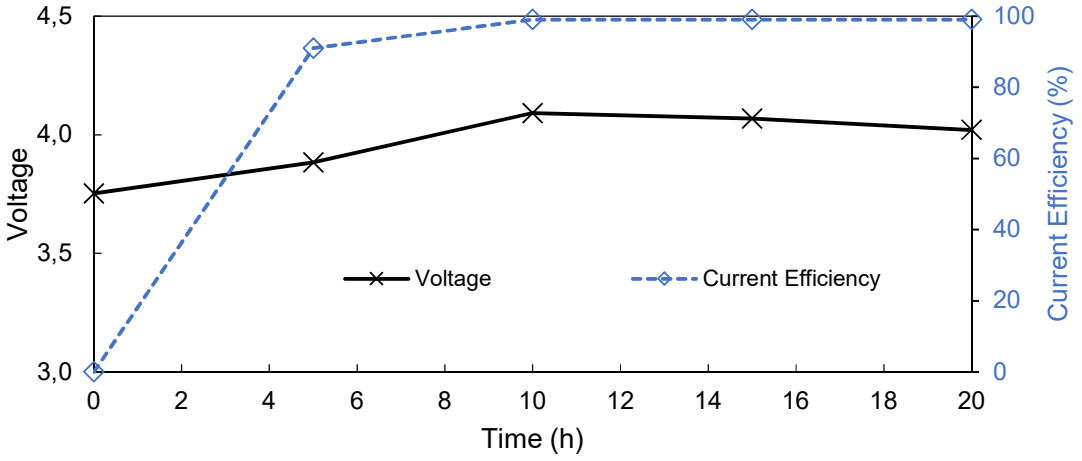

Figure 4.8: Influence of extended AEM-EW unit operation on both the voltage and current efficiency obtained during operation of the EW unit for 20 hours, with the voltage on the primary x-axis and the current efficiency on the secondary x-axis. Catholyte: 80 g/L Fe as $FeSO_4$, 10 g/L EDTA, 60 g/L Na_2SO_4. Anolyte: 60 g/L Na_2SO_4.

In agreement with the results shown above (**Figure 4.8)**, the anolyte and catholyte pH of the EW unit over 20 hours, as depicted in **Figure 4.9**, were promising. The catholyte pH stabilized at around a pH of 4 after ten hours, with minor fluctuations thereafter. This indicates that the AEM was sufficiently selective and rejected the H^+ ions from entering the catholyte,[15] which confirms the high current efficiency (99 %) that was observed. The anolyte pH, on the other hand, decreased as expected from 3.11 to a minimum value of 0.43. The graph also shows the repeatability attained in this study when comparing it to Figure 4.6, where the pH reached

1.35 after 5 h when using the FAP-PK-130 compared to the 1.35 attained after five hours in this study. According to the stable pH values and high current efficiencies, the SEC of the EW unit was stable at approximately 3.90 kWh/kg Fe, varying less than 0.2 kWh/kg Fe over the duration of the experiment.

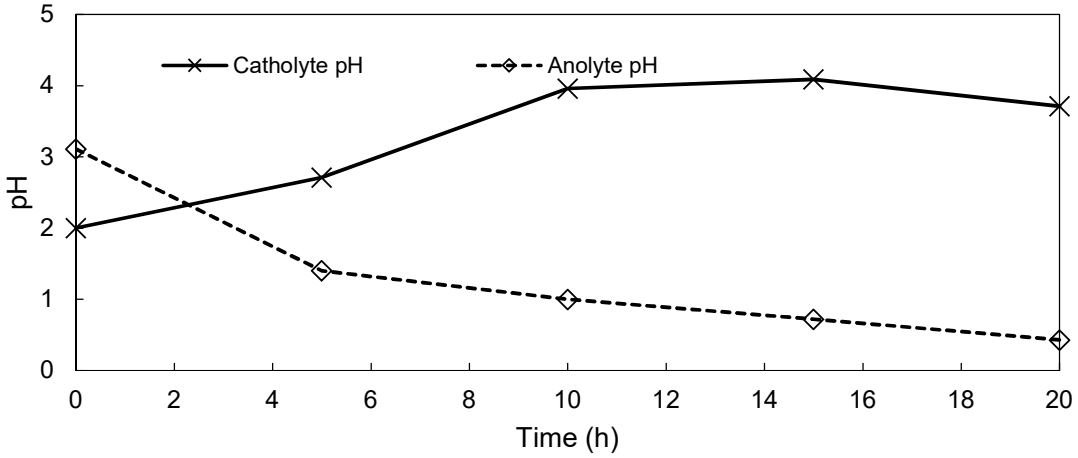

Figure 4.9: The anolyte and catholyte pH obtained during operation of the EW unit for 20 hours.

4.3.5 AEM-EW (3 weeks)

While the AEM showed sufficient stability during extended operation of up to 20 hours, the Fenton test results (Section 4.3.2) indicated that the FAB-PK-130 membrane might not be sufficiently stable for even longer operating periods. Since the FAB-PK-130 membrane also exhibited a decrease in performance in terms of current efficiency and SEC during membrane durability testing (Section 3.3.6.4), it was decided to study the performance of the membrane over a period of three weeks (Section 4.3.5.1). Similarly, the VM-FAPQ-8130 membrane, which was the most promising membrane according to Section 4.3.3, was also tested for three weeks. The results thereof are discussed in Section 4.3.5.2.

4.3.5.1 FAB-PK-130

The data obtained after three weeks of operation using the FAB-PK-130 membrane are summarised in **Table 4.6**. It can be noted that the current efficiency of the EW unit decreased rapidly. Initially, an efficiency of 94 % was recorded during Week 1, which declined to 69 and 43 % in Weeks 2 and 3, respectively. In addition to the decrease in current efficiency, a substantial increase in the Fe flux of the membrane was observed, while the catholyte end-pH of 4.92 for Week 1 decreased to 2.4 after Week 3. This indicates that, while the membrane remained stable for the first week, its performance declined substantially during Weeks 2 and 3.

Table 4.6: Summary of key variables obtained from the continual operation of the EW unit for three weeks with the FAB-PK-130 membrane.

Parameter	Week 1	Week 2	Week 3
Average Voltage (V)	3.57	3.76	3.85
Current Efficiency (%)	94	69	43
SEC (kWh/kg Fe)	3.65	5.23	8.60
Catholyte pH (End)	4.92	4.4	2.4
Anolyte pH (End)	0.89	0.88	0.67
Flux (g/h/m2 Fe)	0.013	3.55	13.78

It is interesting to note that the FAB-PK-130 membrane did not show the same degree of degradation during the prolonged exposure to H_2SO_4 as discussed in Section 3.3.6.3. This implies that the performance degradation observed here was not solely attributable to the long-term operation in an acidic environment. Rather, this confirms that the degradation of the membrane is largely caused by the formation of in situ radicals through the oxidation of the Fe(II) to Fe(III) by oxygen entering the test system. This was also confirmed by the slight discolouration of the catholyte solution, indicating the increased presence of Fe(III) in the system. It is well known that the formation of either oxyradicals or peroxides (see Eq 4.4 & 4.5)[8-10] during the oxidation of Fe(II) to Fe(III) is accelerated in the presence of impurities.[10] It is clear that such radical formation is detrimental to membrane stability, which is the reason for using the Fenton test as an accelerated stability test for membranes.

$$2Fe^{2+} + O_2 \rightarrow 2Fe^{3+} + H_2O_2 \qquad (4.5)$$

SEM imaging of the FAB-PK-130 was done after operation in the EW unit for three weeks. The images obtained using various magnifications (a-d) are shown in **Figure 4.10**, where severe degradation of the membrane can be noted between the supporting PEEK mesh material. It is clear that the AEM became brittle and cracked after the continued operation. This damage to the AEM explains both the decreased efficiency of the AEM and the high flux of Fe through the AEM. A large crack (approximately 100 μm in length) can be noted in **Figure 4.10d**. Compared to the overall thickness of the AEM (130 μm), the possibility of this crack continuing through the breadth of the membrane is likely. This shows the unsuitability of the FAB-PK-130 for long-term use in the EW of iron, as was indicated earlier by the Fenton testing.

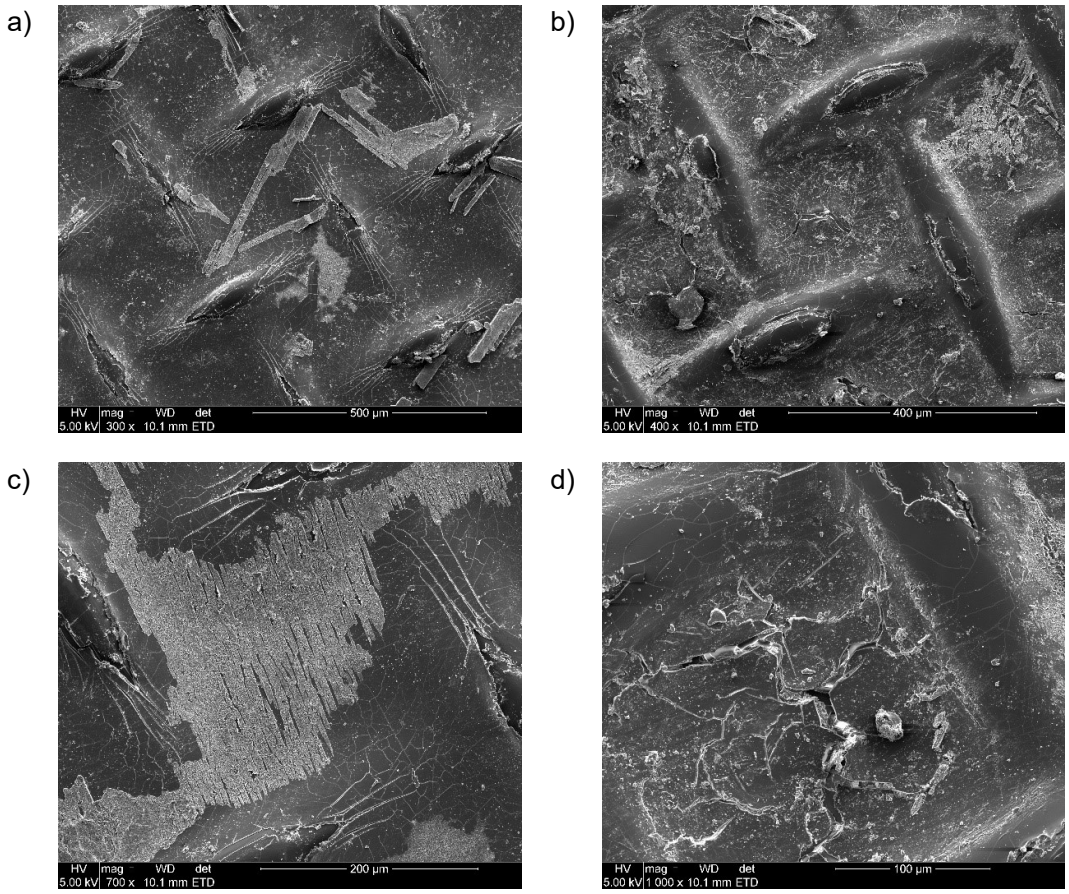

Figure 4.10: SEM imaging of the FAB-PK-130 membrane at varying magnifications (a; 300x, b; 400x, c; 700x, d; 1000x) after being used in the EW unit for three weeks.

4.3.5.2 VM-FAPQ-8130-PK

Finally, the durability of the VM-FAPQ-8130-PK membrane was determined in the same AEM-EW unit under the exact same conditions applied to the FAB-PK-130 membrane, as discussed above. According to the excellent Fenton test results described in Section 4.3.2 (only 10.4 % mass loss after four days), it would have been expected that the VM-FAPQ-8130-PK might outperform the FAB-PK-130 membrane in the durability study as well. A summary of the performance of the VM-FAPQ-8130-PK membrane is given in **Table 4.73**, from which it is clear that the VM-FAPQ-8130-PK membrane indeed outperformed the FAB-PK-130 membrane significantly. In contrast to the FAB-PK-130 membrane, which only attained a current efficiency of 43 % after three weeks, the VM-FAPQ-8130-PK membrane was still able to operate at a current efficiency of 82 % after three weeks, nearly double the performance of the PAB-PK-130. In addition, the VM-FAPQ-8130-PK membrane yielded a catholyte pH end value that was approximately 0.5 lower than that obtained with the FAB-PK-130 membrane.

This coincided, as was expected, with a decreased iron flux which remained stable after Week 2.

Table 4.73: Summary of key variables obtained from the continual operation of the EW unit for three weeks with the VM-FAPQ-8130-PK membrane.

Parameter	Week 1	Week 2	Week 3
Average Voltage (V)	4.30	5.23	4.98
Current Efficiency (%)	90	86	82
SEC (kWh/kg Fe)	4.59	5.84	5.83
Catholyte pH (End)	3.42	2.21	2.18
Anolyte pH (End)	0.22	0.16	0.24
Flux (g/h/m2 Fe)	0.90	2.98	2.96

SEM Imaging obtained of the VM-FAPQ-8130-PK membrane after use in the EW unit for three weeks is shown in **Figure 4.11**, confirming that this membrane is much more suitable for the EW of iron compared to the FAB-PK-130 membrane. Slight superficial cracks can be noted over the surface of the membrane and are attributed to the SEM imaging beam damaging the AEM despite the gold/palladium coating. Only minimal pitting of the AEM can be observed on the largest magnification of 1000x (**Figure 4.11d**). Therefore, SEM indicates that the AEM underwent nearly no degradation due to operation in the EW unit for three weeks.

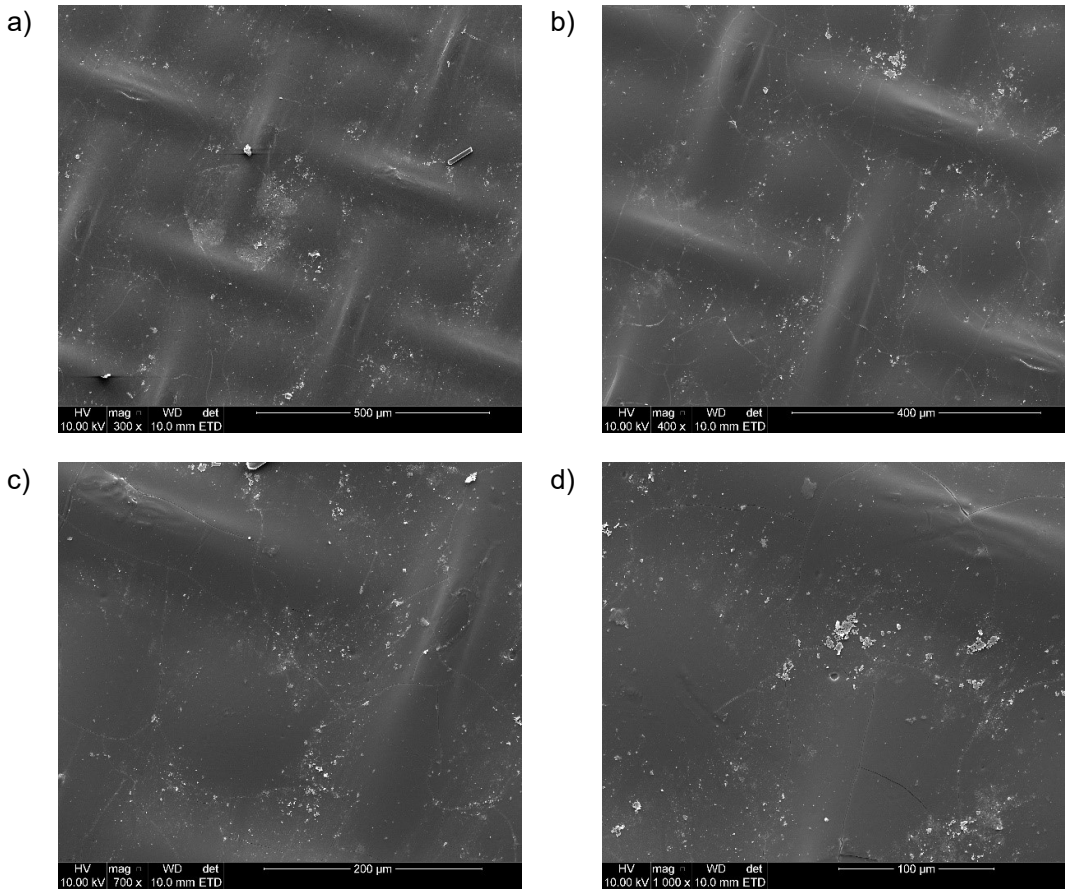

Figure 4.11: SEM imaging of the VM-FAPQ-8130 membrane at varying magnifications (a; 300x, b; 400x, c; 700x, d; 1000x) after being used in the EW unit for three weeks.

4.4 Conclusion

Two ICVT AEMs were successfully prepared with and without the inclusion of Ce_2O_3. It was shown during the Fenton testing and 5 h operation in an AEM-EW that these membranes were comparable to the two membranes that had been provided by Fumatech. The FAB-PK-130 membrane was the most unstable in terms of the Fenton test results, exhibiting a mass loss of 66.3 % after four days. In contrast, the AEM 2408-2 and VM-FAPQ-8130-PK membranes showed superior stability in the oxidative environment, undergoing approximately only 10 % mass loss after four days. Under the given conditions, it became apparent that the slight increase in stability provided by the Ce_2O_3 would not warrant the cost and additional processing steps required for its inclusion in the membranes.

The 5 h AEM-EW operation showed comparable performances for three of the membranes tested, with declining performance observed for the FAB-PK-130. However, when testing the same FAB-PK-130 for 20 hours, it became clear that the membrane did stabilize slightly after

ten hours of operation. Using the least stable and most stable membranes according to the Fenton test (FAB-PK-130 and VM-FAPQ-8130-PK), 3-week operations of the EW unit were conducted. This confirmed that the VM-FAPQ-8130-PK membrane outperforms the FAB-PK-130 membrane considerably. The FAB-PK-130 membrane showed rapid degradation during operation in the AEM-EW unit, which was ascribed to its non-fluorinated backbone which is more prone to degradation in an oxidative/radical environment. The VM-FAPQ-8130-PK membrane was still able to operate at a current efficiency of 82 % after three weeks, compared to the current efficiency of 42 % attained by the FAB-PK-130 membrane after three weeks. This increased stability is also echoed by the SEM imaging, where the FAB-PK-130 had significant cracking and damage after three weeks, compared to the VM-FAPQ-8130-PK which showed minimal damage. This chapter has clearly demonstrated that the VM-FAPQ-8130-PK membrane is most suitable for use in a commercial AEM-EW process.

4.5 Bibliography

1. Morandi, C. G.; Peach, R.; Krieg, H. M.; Kerres, J., Novel morpholinium-functionalized anion-exchange PBI–polymer blends. *Journal of Materials Chemistry A* **2015,** *3* (3), 1110-1120.
2. Morandi, C. G.; Peach, R.; Krieg, H. M.; Kerres, J., Novel imidazolium-functionalized anion-exchange polymer PBI blend membranes. *Journal of Membrane Science* **2015,** *476*, 256-263.
3. Kerres, J. A.; Krieg, H. M., Poly(vinylbenzylchloride) Based Anion-Exchange Blend Membranes (AEBMs): Influence of PEG Additive on Conductivity and Stability. *Membranes (Basel)* **2017,** *7* (2), 32.
4. Cho, H.; Krieg, H. M.; Kerres, J. A., Application of Novel Anion-Exchange Blend Membranes (AEBMs) to Vanadium Redox Flow Batteries. *Membranes (Basel)* **2018,** *8* (2), 33.
5. Badenhorst, W. D.; Rossouw, C.; Cho, H.; Kerres, J.; Bruinsma, D.; Krieg, H., Electrowinning of Iron from Spent Leaching Solutions Using Novel Anion Exchange Membranes. *Membranes (Basel)* **2019,** *9* (11), 137.
6. Tanaka, Y.; Moon, S.-H.; Nikonenko, V. V.; Xu, T., Ion-exchange membranes. *International Journal of Chemical Engineering* **2012,** *2012*.
7. Carrillo-Abad, J.; Garcia-Gabaldon, M.; Ortiz-Gandara, I.; Bringas, E.; Urtiaga, A. M.; Ortiz, I.; Perez-Herranz, V., Selective recovery of zinc from spent pickling, baths by the combination of membrane-based solvent extraction and electrowinning technologies. *Separation and Purification Technology* **2015,** *151*, 232-242.
8. Lamb, A. B.; Elder, L. W., The electromotive activation of oxygen. *Journal of the American Chemical Society* **1931,** *53* (1), 137-163.
9. Cher, M.; Davidson, N., The kinetics of the oxygenation of ferrous iron in phosphoric acid solution. *Journal of the American Chemical Society* **1955,** *77* (3), 793-798.
10. Stumm, W.; Lee, G. F., Oxygenation of ferrous iron. *Industrial & Engineering Chemistry* **1961,** *53* (2), 143-146.
11. Xue, Y.; Luan, Q. F.; Yang, D.; Yao, X.; Zhou, K. B., Direct Evidence for Hydroxyl Radical Scavenging Activity of Cerium Oxide Nanoparticles. *J Phys Chem C* **2011,** *115* (11), 4433-4438.
12. Pearman, B. P.; Mohajeri, N.; Brooker, R. P.; Rodgers, M. P.; Slattery, D. K.; Hampton, M. D.; Cullen, D. A.; Seal, S., The degradation mitigation effect of cerium oxide in polymer electrolyte membranes in extended fuel cell durability tests. *Journal of Power Sources* **2013,** *225*, 75-83.
13. Ghassemzadeh, L.; Kreuer, K.; Maier, J.; Müller, K., Evaluating chemical degradation of proton conducting perfluorosulfonic acid ionomers in a Fenton test by solid-state 19F NMR spectroscopy. *Journal of power sources* **2011,** *196* (5), 2490-2497.

14. Chen, D.; Hickner, M. A., V 5+ degradation of sulfonated Radel membranes for vanadium redox flow batteries. *Physical Chemistry Chemical Physics* **2013,** *15* (27), 11299-11305.

15. Varcoe, J. R.; Atanassov, P.; Dekel, D. R.; Herring, A. M.; Hickner, M. A.; Kohl, P. A.; Kucernak, A. R.; Mustain, W. E.; Nijmeijer, K.; Scott, K.; Xu, T. W.; Zhuang, L., Anion-exchange membranes in electrochemical energy systems. *Energy & Environmental Science* **2014,** *7* (10), 3135-3191.

16. Ohma, A.; Yamamoto, S.; Shinohara, K., Membrane degradation mechanism during open-circuit voltage hold test. *Journal of Power Sources* **2008,** *182* (1), 39-47.

CHAPTER 5

Evaluation and Recommendations

Table of Contents

5.1 Introduction

Three different processes for the recovery of iron from spent leaching solutions (SLS) were initially proposed in this study. According to the results obtained, the most effective EW method for the recovery of iron from SLSs was the anion exchange membrane-based electrowinning process (AEM-EW). Subsequently, numerous variables affecting the AEM-EW process were evaluated in Chapter 3 to determine the optimal process conditions in terms of current efficiencies and specific energy consumption (SEC) values. This was followed (Chapter 4) by determining the stability of different commercial and novel AEMs to estimate the lifetime of each in the aggressive environment found in the AEM-EW of iron. A summary of the results from Chapter 3 and 4 are presented in Section 5.2. Based on these results, a process configuration and an introductory economic evaluation of the AEM-EW process are presented in Section 5.3. Subsequently, the chapter is concluded (Section 5.4) with an evaluation of all aspects pertaining to, and the recommendations from, this study.

5.2 Summary of Results

5.2.1 Process Variables

Testing of the three EW methods introduced in **Figure 1.1**, namely (i) non-divided EW, (ii) porous membrane EW, and (iii) the AEM-EW showed that the AEM-EW process significantly outperformed the other two processes, confirming what has been found in literature.[1-3] Under optimal conditions, the AEM-EW unit yielded a current efficiency of up to 99 %, compared to the non-divided and porous membrane EW unit that operated at efficiencies of 21 and 77 %, respectively. In addition, the AEM-EW process produced significantly lower anolyte pH values compared to the other two processes, indicating that the process is capable of generating more concentrated sulphuric acid (H_2SO_4) solutions. Additionally, it was also found that the addition of EDTA was needed to prevent the precipitation of iron oxyhydroxides. In the presence of EDTA (**Appendix C.2**), precipitation of iron oxyhydroxides only occurred on the walls of the container and surface of the catholyte solution, with no precipitation in the catholyte itself, thus preventing damage to both the AEM and equipment.[4]

The effect of (i) boric acid concentration, (ii) catholyte pH, (iii) anolyte pH, (iv) temperature, (v) sodium sulphate concentration, (vi) different membranes, and (vii) the catholyte iron concentration on the AEM-EW process was subsequently determined. The boric acid concentration showed a negligible effect on the AEM-EW process and was therefore not further used. Conversely, the addition of H_2SO_4 to the catholyte, simulating unspent acid in

the SLS (12.5 g/L H_2SO_4), led to a significant decrease in the current efficiency (declining to 9 %). Similarly, the addition of H_2SO_4 to the anolyte led to a decrease in current efficiency due to proton tunnelling followed by the parasitic formation of H_2 on the cathode. According to these results, 100 g/L H_2SO_4 was the maximum concentration where operation at relatively high current efficiencies with the FAB-PK-130 membrane was still possible. It was then shown that both an increase in temperature (up to 70 °C) and the addition of Na_2SO_4 to both electrolytes (up to 100 g/L Na_2SO_4) led to a significant decrease in the SEC and hence to an improvement of the AEM-EW process. Additionally, operation of the AEM-EW unit at a reduced iron concentration of 10 g/L resulted in a sharp increase in the SEC and a decrease in the current efficiency.[5-6] This could, however, be compensated for by the addition of, for example, 100 g/L Na_2SO_4.[5] Finally, in the iron depletion experiment using the enlarged AEM-EW unit, a current efficiency of 99 % was attained over the complete duration (5 hours), during which the iron concentration was reduced from 40 g/L to 2.70 g/L before the occurrence of side reactions.[1] The information obtained from the operation of the enlarged AEM-EW unit will be used in Section 5.3 to determine the process configuration and for the economic evaluation.

5.2.2 Novel AEMs and Stability Testing

Following the characterization and optimization of the various AEM-EW process variables using the Fumatech FAB-PK-130 membrane, the durability of various AEMs were investigated in Chapter 4. Although the FAB-PK-130 initially showed excellent performance, all the membranes tested in Chapter 3 showed some degradation during the 4-week exposure to elevated anolyte acid concentrations (Chapter 3). Hence, to gain further insight into AEM durability, the FAB-PK-130, two three-component novel AEMs (2408-2 and BM-5), and a novel non-commercial membrane from Fumatech (VM-FAPQ-8130-PK) were subjected to Fenton tests. The test results showed that the FAB-PK-130 membrane (66.3 % mass loss) underwent rapid degradation in an oxidative/radical environment, whereas the novel 2408-2 membrane (10.7 % mass loss), BM-5 membrane (20.0 % mass loss), as well as the VM-FAPQ-8130-PK membrane (10.4 % mass loss) showed significantly higher stability after four days.[7-8] This was also confirmed by the extended durability tests that lasted three weeks, in which current efficiencies of 94 %, 69 %, and 43 % after each of the three weeks were obtained with the worst performing FAB-PK-130 membrane. In contrast, current efficiencies of 90 %, 86 %, and 82 % were obtained over the three-week period with the best-performing VM-FAPQ-8130-PK membrane.[7]

5.3 Process Design and Economic Evaluation

As mentioned in Chapter 1, an objective of the study was to propose and evaluate a process based on the results obtained from this study. In this section, a possible process configuration is proposed, followed by some initial economic considerations. Both of these are necessary before evaluating the proposed process, which will be discussed in Section 5.4. For the process design, a feed flow rate of 0.56 m^3/h SLS containing 80 g/L Fe was used based on a plant that should be able to process 45 kg/h Fe. The target composition of the leaving SLS was taken as 5 g/L Fe.

5.3.1 Process Configuration

To estimate the membrane area required to treat a 0.56 m^3/h SLS containing 80 g/L Fe, the process configuration as illustrated in the block flow diagram (BFD) in **Figure 5.1** seems most feasible. To accommodate the decreasing catholyte Fe concentration, a two-stage process consisting of AEM-EW 1 & 2, where AEM-EW Unit 1 is operated at higher iron concentrations and higher current densities and AEM-EW Unit 2 at lower iron concentrations and current densities is proposed. The purpose of the two units is to reduce the SEC, which would decrease the OPEX. However, this would obviously be at the expense of the CAPEX. Nonetheless, it can be assumed that the CAPEX would be lower compared to the operation of a single-stage process, which would have to be operated at a lower current density to maintain high current efficiencies when reducing the iron content to the target of 5 g/L.

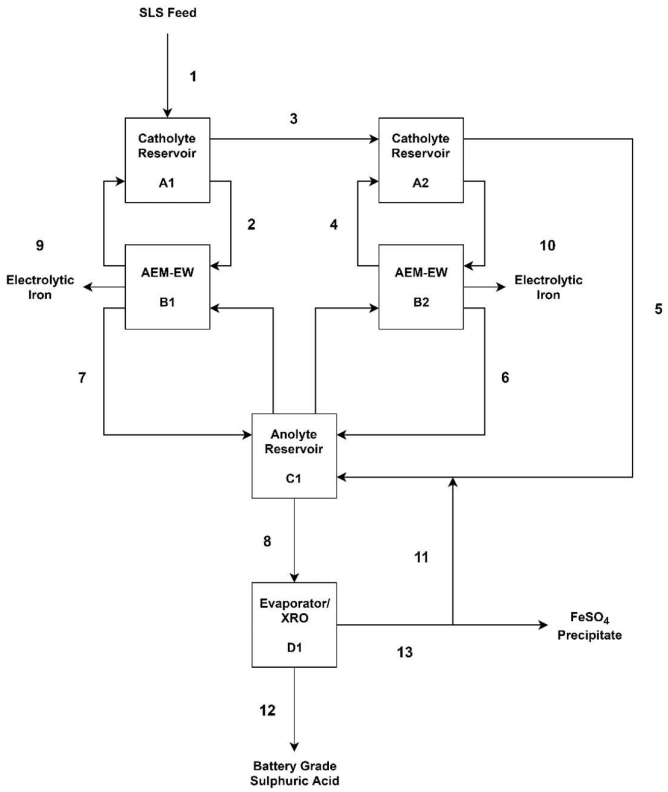

Figure 5.1: Proposed two stage AEM-EW process configuration for the treatment of an Fe-containing SLS.

The proposed process configuration shown in **Figure 5.1** can be summarized as follows:

- The SLS (80 g/L Fe) enters the feed and bleed tank (catholyte reservoir A1), which is maintained at 20 g/L Fe.
- The catholyte from reservoir A1 is circulated over AEM-EW B1, where the iron is plated, while the sulphates are transferred through the AEM to the acid stream (7) before entering the anolyte reservoir C1.
- Simultaneously, the catholyte from reservoir A1 is sent via (3) to the catholyte reservoir B2, which is maintained at 10 g/L Fe via a bleed stream.
- The catholyte from B2 is circulated over AEM-EW B2, where iron is plated, while the sulphates are transferred through the AEM to the acid stream (6), before entering the anolyte reservoir C1.
- Simultaneously, the bleed stream from B2 is also sent to the anolyte reservoir C1 via (5).
- The anolyte reservoir C1 contains concentrated H_2SO_4 and is fed to either an evaporator or an Xtreme Reverse Osmosis (XRO) setup D1 to further concentrate the produced acid.

- On a weekly basis, electrolytic iron is harvested from the electrodes of AEM-EW B1 and AEM-EW B2.
- The evaporator or XRO produces battery-grade acid (12) of 380 g/L H_2SO_4. The condensate produced from the evaporator/XRO (13) is fed back to the anolyte reservoir C1 tank through stream 11.
- The battery-grade acid (12) is sent to the leaching process.

Using the information obtained from the 20 x30 cm AEM-EW unit described in Chapter 3, the compositions and flow rates of all the streams presented in **Figure 5.1** were calculated (**Table 5.1**). A current efficiency of 95 % was assumed for this discussion, which is slightly below the 99 % actually attained. It was shown in this study that a current density of 300 A/m^2 was suitable for high Fe concentrations (> 10 g/L). Since AEM-EW B1 operates at Fe concentrations of approximately 20 g/L, 300 A/m^2 was used for the design of AEM-EW B1. In AEM-EW B2, the iron content is maintained at 10 g/L. At these lower Fe concentrations, it is expected that the diffusion of iron to the cathode also decreases. Hence, if the same 300 A/m^2 is used in AEM-EW 2 at such slower diffusion rates, more side reactions will occur, resulting in a decreased efficiency. It is for this reason that a lower current density of 75 A/m^2 is proposed for AEM-EW B2. The minimization of side reactions was also the reason for the equilibrium Fe concentrations chosen as 20 g/L and 10 g/L in AEM-EW B1 and B2, respectively. Using these assumptions and current densities, the total membrane area required was calculated as 114 m^2 and 109 m^2 for AEM-EW B1 and AEM-EW B2, respectively.

According to the obtained mass balance (**Table 5.1**), AEM-EW B1 would remove approximately 33.75 kg/h of iron from the catholyte solution, while AEM-EW B2 would remove 8.44 kg/h of iron. This totals to 42.19 kg/h of iron being removed, compared to the 45 kg/h iron fed to the AEM-EW process. The remaining 2.81 kg/h of iron is contained in the produced anolyte (containing approximately 50 g/L H_2SO_4), which is fed to an evaporator or XRO (Stream 8) to concentrate the acid to 380 g/L (Stream 12). After concentration, the condensate formed in the evaporator (0.36 m^3/h) is fed back to the anolyte reservoir (Stream 11). This stream would dilute the anolyte stream to maintain the H_2SO_4 concentration below 50 g/L, which is required to keep proton tunnelling and subsequent H_2 evolution to a minimum.

Table 5.1: Calculated composition and flow rate of each stream in the proposed process configuration.

	1	2	3	4	5	6	7	8	9	10	11	12	13
Stream	**SLS Feed**	**AEM-EW 1 Catholyte Recirculation**	**AEM-1 Bleed**	**AEM-EW 2 Catholyte Recirculation**	**Process water**	**AEM-EW 1 Anolyte Recycle**	**AEM-EW 2 Anolyte Recycle**	**AEM-EW Acid Product**	**AEM-EW 1**	**AEM-EW 2**	**Return Condensate**	**Battery Grade H_2SO_4**	**Condensate**
Flow (m^3/h)	**0.56**	**102**	**0.56**	**102**	**0.56**	**20**	**20**	**0.89**			**0.35**	**0.21**	**0.35**
Fe (g/L)	**80**	**20**	**20**	**5**	**5**	**5**	**5**	**5**			**0**	**13.53**	**0**
SO_4 (g/L)	**138**	**34**	**34**	**9**	**9**	**49**	**49**	**49**			**0**	**372.25**	**0**
H_2SO_4 (g/L)	**0**	**0**	**0**	**0**	**0**	**50**	**50**	**50**			**0**	**380.00**	**0**
Fe (kg/h)	**45**	**2046**	**11**	**511**	**2.81**	**2.81**	**2.81**	**2.81**	**33.75**	**8.44**	**0**	**2.81**	**0**
SO_4 (kg/h)	**77**	**3519**	**19**	**880**	**5**	**1002**	**1002**	**77**			**0**	**77.41**	**0**

5.3.2 Economic Evaluation

As stated in the introductory chapter, the cost of the AEM-EW process is critical for it to become an industrially feasible process. The results of a preliminary estimation of the capital expense (CAPEX) and operating expense (OPEX) of the central and probably most expensive part of the proposed AEM-EW process are given in **Table 5.2**. Note that neither the construction and labour costs, nor the piping, storage vessels, pumps or any additional required equipment were considered when calculating the CAPEX. The cost of the AEMs were based on personal communications with Fumatech GmbH, while the cost of a single 1 m^2 AEM-EW unit was derived by upscaling the construction cost of the 20 x 30 cm AEM-EW unit used in this study. Additional information that was required for the cost estimation was based on personal communication with Tharisa PLC, who funded this study.

Table 5.2: CAPEX and OPEX calculations for the construction and operation of an industrial-scale 45 kg/h Fe AEM-EW plant.

CAPEX		
AEM Area Required	228	m^2
Units Required	228	1/m^2 unit
Power Supply Unit	R160,000.00	R
AEM Price	R3,120.00	R/m^2
AEM-EW Unit	R2,000.00	R/unit
CAPEX	R1,327,360	

OPEX		
AC/DC Conversion Efficiency	0.81	
SEC	5.83	kWh/kg Fe
AC Power	324	kW
DC Power	262	kW
AC Price	R1.60	R/kWh
OPEX	R4,145,777	R/Year

The above OPEX estimate does not include the full cost of operation as it does not include the membrane and power supply lifetimes. From Fenton testing and the membrane durability tests conducted on the VM-FAPQ-8130-PK membrane, it was assumed that the AEM would have an operational lifetime of 6 months, while a lifetime of approximately 5 years was assumed for the power supply units. Considering the AEM and power supply unit (PSU) lifetime, maintenance cost, and

depreciation, a levelized OPEX for the cost per kg Fe treated was calculated, with the assumptions and results given in **Table 5.3**. From the levelized OPEX it is clear that the cost per kg Fe recovered is approximately 17 R/kg Fe.

Table 5.3: Levelized OPEX calculations for the operation of an industrial-scale 45 kg/h Fe AEM-EW plant.

Levelized OPEX		
AEM Lifetime	0.5	Years
Power Supply Unit Lifetime	5	Years
Maintenance	10	% of CAPEX
Depreciation	5	% of CAPEX
Power Consumption	5.83	kWh/kg Fe
OPEX	R6,222,364	R/Year
OPEX	R17	R/kg Fe

From the levelized OPEX, the cost breakdown for the operation of the AEM-EW process (**Table 5.4**) could be determined. As expected, and noted in Chapter 1, the majority of the cost (72 %) is related to the power required for the operation of the AEM-EW process. The second-highest cost element was found to be related to membrane replacements, which accounted for 25 % of the OPEX. Lastly, both the PSU replacement and maintenance cost account for the final 3 % of the OPEX.

Table 5.4: Breakdown of the OPEX cost for the industrial AEM-EW process.

OPEX Breakup		
Component	Yearly Cost	% of OPEX
Power	R4,145,777	72
Membrane Replacement	R1,422,720	25
Maintenance	R132,736	2
Power Supply Unit	R32,000	1
Total	R5,733,233	

5.4 Evaluation and Recommendations

5.4.1 Process Variables

In this study, almost all the parameters that could affect the performance of an AEM-EW process for the recovery of iron from SLSs were studied and the optimal values were identified. The importance of the optimization of the AEM-EW process is illustrated in the OPEX breakup results (**Table 5.**) where it was shown that the power consumption accounts for 72 % of the OPEX. The optimization of the membrane, temperature and Na_2SO_4 addition aided in reducing the projected power consumption (SEC) of the process, and thus also reduced the total OPEX. Recommendations for further work include the few parameters not investigated for their influence on the AEM-EW process in this study. These include the effect of (i) current density, (ii) anode material, and (iii) impurities on process performance. Optimization of the current density used for AEM-EW 1 and AEM-EW 2 (**Figure 5.1**), carries the possibility of reducing both the plant size and the required AEM area. Reduction in the required AEM area can significantly reduce the membrane replacement costs,[9] which could result in reduced OPEX. In line with these optimizations, current density could also be increased by using alternative anode materials (materials other than lead as mentioned in Section 2.3.2.1) such as dimensionally stable anodes (DSAs).[6] However, implementation of alternative types of anodes should be weighed against the increase in cost. Finally, investigations regarding the purity of the electrolytic iron produced when treating real SLSs using AEM-EW could prove profitability since the purity of the electrolytic iron can influence the OPEX.

5.4.2 Novel AEMs and Stability Testing

In this study, the stability of the novel AEMs and of the commercial membranes was tested. As is the case with the optimization, the stability improvement had a significant effect on the possible OPEX of the AEM-EW process, considering that the AEMs are estimated to account for 25 % of the OPEX. The Fenton testing confirmed that the prepared novel AEMs and the VM-FAPQ-8130-PK membrane showed substantially higher stability compared to the previously used FAB-PK-130 membrane.[10] The increased stability was confirmed through durability testing of the FAP-PK-130 membrane, from which it was determined that the VM-FAPQ-8130-PK was significantly more stable in the AEM-EW unit, providing nearly twice the performance compared to that of the FAP-PK-130 after three weeks of operation . Further work regarding the AEMs could include also testing the stability of the two novel AEMs 2408-2 and BM-5 in the AEM-EW unit. Furthermore, while the use of Ce_2O_3 showed increased stability in Fenton testing, this would have to be confirmed with durability testing in the AEM-EW unit.[11-12] Should the AEMs tested exhibit superior stability to the currently used AEMs, the OPEX of the AEM-EW process would be reduced even further due to the longer

membrane replacement intervals. This should, however, be weighed against the cost of these membranes.

5.4.3 Process Configuration

Using the proposed block flow diagram together with AEM-EW operation data from Chapter 3, the flow and composition of the AEM-EW process could be determined. The flow was calculated for an AEM-EW process capable of processing 0.56 m^3/h of 80 g/L SLS in a two-stage AEM-EW process. This two-stage process should significantly decrease the OPEX cost of the process as described earlier, despite leading to an initial increase in the CAPEX. The membrane area requirement for AEM-EW Units 1 and 2 was determined as 114 m^2 and 109 m^2, respectively, and therefore a total of 223 x 1 m^2 EW units are required to meet the processing requirements. Future studies could compare different multi-stage AEM-EW process configurations (two and more stages) in order to further reduce both the OPEX and CAPEX. This could also include testing the proposed two-stage AEM-EW process on either lab or pilot scale for verification.

5.4.4 Economic Evaluation

While both the CAPEX and OPEX calculated in this chapter only represent a preliminary cost estimate, they serve to illustrate the major cost elements of the proposed AEM-EW process. From the levelized OPEX (**Table 5.3**) it is evident that the majority of the cost is related to the power required to drive the AEM-EW process (72 %), followed by the cost of the AEM replacement every 6 months (25 %). As stated in Section 5.3.1 and Section 5.3.2, the levelized OPEX results confirm that investigation into process variables such as current density, anode material and more stable AEMs can significantly reduce the cost of the AEM-EW process.

5.5 Bibliography

1. Badenhorst, W. D.; Rossouw, C.; Cho, H.; Kerres, J.; Bruinsma, D.; Krieg, H., Electrowinning of Iron from Spent Leaching Solutions Using Novel Anion Exchange Membranes. *Membranes (Basel)* **2019,** *9* (11), 137.
2. Ren, X.; Wei, Q.; Hu, S.; Wei, S., The recovery of zinc from hot galvanizing slag in an anion-exchange membrane electrolysis reactor. *J Hazard Mater* **2010,** *181* (1-3), 908-15.
3. Csicsovszki, G.; Kekesi, T.; Torok, T. I., Selective recovery of Zn and Fe from spent pickling solutions by the combination of anion exchange and membrane electrowinning techniques. *Hydrometallurgy* **2005,** *77* (1-2), 19-28.
4. Pachla, S. K.; Taylor, R. S.; Delorey, J. R., Method of preventing precipitation of iron compounds during acid treatment of wells. Google Patents: 1991.
5. Mostad, E.; Rolseth, S.; Thonstad, J., Electrowinning of iron from sulphate solutions. *Hydrometallurgy* **2008,** *90* (2-4), 213-220.
6. Cardarelli, F., Electrochemical process for the recovery of metallic iron and sulfuric acid values from iron-rich sulfate wastes, mining residues and pickling liquors. Google Patents: 2011.
7. Ohma, A.; Yamamoto, S.; Shinohara, K., Membrane degradation mechanism during open-circuit voltage hold test. *Journal of Power Sources* **2008,** *182* (1), 39-47.
8. Stumm, W.; Lee, G. F., Oxygenation of ferrous iron. *Industrial & Engineering Chemistry* **1961,** *53* (2), 143-146.
9. Lloyd, D.; Sanz, L., Aqueous all-copper redox flow battery. Google Patents: 2018.
10. Ghassemzadeh, L.; Kreuer, K.; Maier, J.; Müller, K., Evaluating chemical degradation of proton conducting perfluorosulfonic acid ionomers in a Fenton test by solid-state 19F NMR spectroscopy. *Journal of power sources* **2011,** *196* (5), 2490-2497.
11. Trogadas, P.; Parrondo, J.; Ramani, V., Degradation mitigation in polymer electrolyte membranes using cerium oxide as a regenerative free-radical scavenger. *Electrochem Solid St* **2008,** *11* (7), B113-B116.
12. Xue, Y.; Luan, Q. F.; Yang, D.; Yao, X.; Zhou, K. B., Direct Evidence for Hydroxyl Radical Scavenging Activity of Cerium Oxide Nanoparticles. *J Phys Chem C* **2011,** *115* (11), 4433-4438.

APPENDIX A

STANDARD DEVIATION

During testing some experiments were repeated in order to obtain error margins and standard deviations. This was not done for all experiments due to time constraints, and the deviations experienced were assumed to hold true for all other experiments. The first experiment repeated for error calculations used a catholyte concentration of 80 g/L Fe as $FeSO_4$, 60 g/L Na_2SO_4 and 10 g/L EDTA, with the anolyte consisting of 60 g/L Na_2SO_4. All other variables were as indicated in the main text. The experiment was repeated a total of 5 times, the information for the voltage, catholyte pH, anolyte pH and current efficiency/SEC is given in **Tables 1-4**. From the standard deviations it can be noted that a catholyte pH difference of more than 5.71 % is significant, anolyte pH change of more than 5.37 % is significant, current efficiency (CE) change of more than 1.01 % is significant, and a specific energy consumption change of more than 2.05 % is significant.

Table 1: Standard deviation of the voltage applied to the AEM-EW Unit over 5 experiments.

Time (h)	Run 1 (V)	Run2 (V)	Run 3 (V)	Run 4 (V)	Run 5 (V)	Standard Deviation	Relative Standard Deviation (%)
0	4.02	3.81	3.93	3.84	3.57	0.15	3.94
1	3.86	3.79	3.56	3.66	3.76	0.10	2.82
2	3.88	4.10	3.66	3.70	3.85	0.16	4.06
3	3.94	4.18	3.59	3.73	3.94	0.20	5.21
4	3.98	4.21	3.71	3.80	3.99	0.17	4.39
5	4.05	4.40	3.73	3.86	4.12	0.23	5.71

Table 2: Standard deviation of the catholyte pH values in the AEM-EW Unit over 5 experiments.

Time (h)	Run 1 (pH)	Run 2 (pH)	Run 3 (pH)	Run 4 (pH)	Run 5 (pH)	Standard Deviation	Relative Standard Deviation (%)
0	2.03	2.10	2.07	2.02	2.12	0.04	1.87
1	2.19	2.22	2.23	2.05	2.33	0.09	4.10
2	2.37	2.30	2.41	2.17	2.47	0.10	4.40
3	2.58	2.40	2.58	2.35	2.65	0.12	4.62
4	2.83	2.60	2.83	2.58	2.91	0.13	4.88
5	3.15	2.97	3.37	2.88	3.19	0.17	5.54

Table 3: Standard deviation of the anolyte pH values in the AEM-EW unit over 5 experiments.

Time (h)	Run 1 (pH)	Run 2 (pH)	Run 3 (pH)	Run 4 (pH)	Run 5 (pH)	Standard Deviation	Relative Standard Deviation (%)
0	3.50	3.42	3.87	4.05	3.62	0.23	6.38
1	2.11	2.13	2.12	2.13	2.13	0.01	0.38
2	1.68	1.70	1.71	1.73	1.76	0.03	1.59
3	1.52	1.51	1.59	1.63	1.64	0.05	3.44
4	1.34	1.27	1.37	1.38	1.44	0.06	4.08
5	1.25	1.15	1.23	1.30	1.35	0.07	5.37

Table 4: Standard deviation on both the current efficiency and specific energy consumption of the AEM-EW unit over 5 experiments.

Parameter	Run 1 (pH)	Run 2 (pH)	Run 3 (pH)	Run 4 (pH)	Run 5 (pH)	Standard Deviation	Relative Standard Deviation (%)
CE (%)	90.40	90.60	88.40	88.70	89.00	0.90	1.01
SEC (kWh/kg Fe)	4.64	4.67	4.44	4.55	4.70	0.09	2.05

APPENDIX B

CONTROL SOFTWARE

Python 3 code for controlling of the TDK-LAMBDA 400 W power supply unit (PSU) and logging the signal output. Where the length of the experiment can be set and the current output that the PSU should supply. Both the voltage and current is logged as a function of time.

```
import matplotlib.pyplot
import datetime
import pandas
import serial
import numpy
import time
import glob
import sys


# Power supply physical settings
# BAUD rate = 9600
# Connection type
# Interface USB
# Language GEN
# Address 06


def serial_ports():                                                    #
Searches for available COM ports

    if sys.platform.startswith('win'):
        ports = ['COM%s' % (i + 1) for i in range(256)]
    elif sys.platform.startswith('linux') or sys.platform.startswith('cygwin'):
        ports = glob.glob('/dev/tty[A-Za-z]*')
    elif sys.platform.startswith('darwin'):
        ports = glob.glob('/dev/tty.*')
    else:
        raise EnvironmentError('Unsupported platform')

    result = []

    for port in ports:

        try:
            s = serial.Serial(port)
            s.close()
            result.append(port)
        except (OSError, serial.SerialException):
            pass
    return result


print('Available serial ports: ', serial_ports())                      #
Prints all available ports

with serial.Serial(port='COM3', baudrate=9600, bytesize=8, parity='N', stopbits=1,  #
Initiates communication with PSU
                   xonxoff=False, rtscts=True, dsrdtr=False, timeout=1) as ser:

    ser.set_buffer_size(rx_size=12800, tx_size=12800)                  #
Sets buffer sizes, arbitrary?

    ser.write_timeout = None                                           #
Some PySerial functions require
```

```
    ser.read_timeout = None                                                    #
this to properly work

    if str(ser.is_open) == 'False':                                            #
Opens the port if closed
        print('\nOpening port', ser.name)
        ser.open()

    print('\nIs the port open: ', ser.is_open)                  # Checks if the port is
open
    print('Is port writable: ', ser.writable())                # Checks if the port is
writable
    print('Is port readable: ', ser.readable())                # Checks if the port is
readable

    print('\nConnected device information: ', ser)              # Prints device
information

    try:

        ser.write(b'ADR 06\r')                                 # Instantiates the power
supply, for commands

        time.sleep(0.1)                                        # Delays the read of the
data, to allow for response

        if ser.inWaiting() > 0:                                # Validates whether input
was delivered
            print('\nCommand message found in input buffer....')
        else:
            print('\nCommand message not found in input buffer')

        response = ser.read(2).decode()                        # Reads 2 bits and
decodes into ASCII characters

        if response == 'OK':                                   # Checks if correct
response is returned from the
            print('Instrument response:', response)            # PSU, 'OK' in this case
            print('\nInstrument ready for further commands')

        else:
            print('Instrument did not accept instantiation')   # Prints error if
instantiation failed
            exit()

    except serial.SerialException as ex:
        print('Unable to write command to instrument on port', ser.name)
        exit()

    start_time = time.time()                                   # Records the initial
time for drift correction
    end_time = start_time + 1 * 18000                          # Sets the end time of
the experiment (+ seconds)

    # Initiates all the arrays used to capture data as empty arrays, numpy.append will be
used to increase their
    # length after each new data input

    date_time_list = numpy.array([])                           # Initiates the date time
measurement list
    ampere_reading_list = numpy.array([])                      # Initiates the ampere
measurement list
    voltage_reading_list = numpy.array([])                     # Initiates the vol
measurement list
    date_time_list_seconds = numpy.array([])                   # Initiates the sec
measurement list

    ser.write(b'GPC 18.00\r')
    time.sleep(0.1)

    while time.time() < end_time:
```

```
        # The instrument does seem to flush the input and output buffer after a
successful read
        # as such these two lines might be arbitrary additions, nonetheless they remain

        ser.flushInput()                                        # Flushes the input, for
next command
        ser.flushOutput()                                       # Flushes the output, for
next reading

        ser.write(b'MV?\r')                                     # Send the measure
voltage command
        time.sleep(0.1)                                         # Allows for response
from the instrument
        voltage_measurement = ser.read(10).decode()             # Reads the voltage
reading from the instrument

        ser.flushInput()                                        # Flushes the input, for
next command
        ser.flushOutput()                                       # Flushes the output, for
next reading

        ser.write(b'MC?\r')                                     # Send the measure
current command
        time.sleep(0.1)                                         # Allows for response
from the instrument
        ampere_measurement = ser.read(10).decode()              # Reads the measured
current reading from instrument

        # Captures all the relevant data points and appends them to the appropriate
arrays
        # This might not be the optimal method for this as numpy.append creates a
entirely
        # new array and copies the old data into the new one with the extra value
        # Switched over to classical python lists, occurs 10 times faster, however, still
        # using numpy for its append function

        date_time_list_seconds = numpy.append(date_time_list_seconds, (time.time()-
start_time))
        date_time_list = numpy.append(date_time_list, time.asctime(time.localtime()))
        voltage_reading_list = numpy.append(voltage_reading_list, voltage_measurement)
        ampere_reading_list = numpy.append(ampere_reading_list, ampere_measurement)

        # Removal of carriage return added to values when reading from instrument
(expected)
        # Increases readability and eases future use of data

        voltage_reading_list = [i.strip() for i in voltage_reading_list]
        ampere_reading_list = [i.strip() for i in ampere_reading_list]

        # As the carriage return was part of the data stored in the numpy array the
values are now of the type str
        # for the values to be used and exported they should be converted back into a
float (preserving decimals)

        for i in range(len(voltage_reading_list)):
            ampere_reading_list[i] = float(ampere_reading_list[i])
            voltage_reading_list[i] = float(voltage_reading_list[i])

        # Captures the real time data, this is used to determine if something has gone
wrong in the internal system
        # through plotting of the data. As physically detecting problems with the run
will be near impossible.

        matplotlib.pyplot.plot(date_time_list_seconds, voltage_reading_list)
        matplotlib.pyplot.ylabel('Voltage (V)')
        matplotlib.pyplot.xlabel('Time (s)')
        matplotlib.pyplot.pause(0.1)

        time.sleep(5 - ((time.time() - start_time) % 5.0))      # Corrects for time drift
due to code execution
```

```
    # Exporting of the data using the Pandas library, works more effortless than the csv
module commonly used.
    # The index can be set to False, I however, will use it for time calculations and
checking for drift of the
    #  timer used in the program.

    data = pandas.DataFrame({'Time': date_time_list, 'Seconds': date_time_list_seconds,
                             'Current': ampere_reading_list, 'Volt':
voltage_reading_list})
    data.to_csv(datetime.datetime.today().strftime("%d%m%Y")+'.csv', index=True)

# Indicates that the program has successfully finished and shows the name of the csv file
generated containing
# all the data obtained during the run, which includes the time, amperes and the voltage
applied.

ser.open()
ser.write(b'GPC 0.0\r')
ser.close()

print('\nRun has successfully been completed')
print('Output stored in:', datetime.datetime.today().strftime("%d%m%Y")+'.csv')
```

APPENDIX C

1) Enlarged EW unit

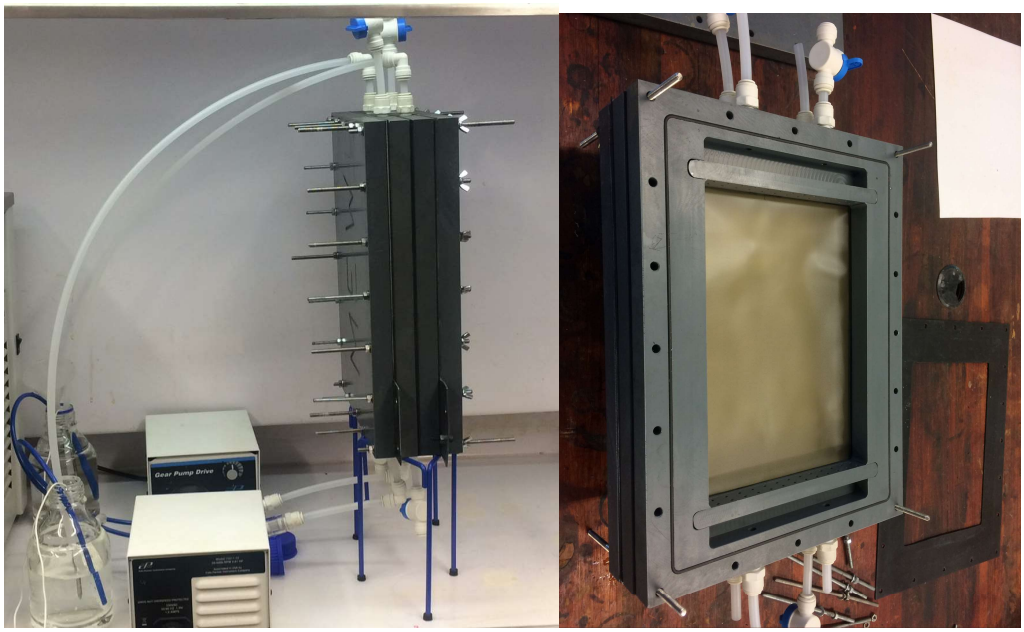

Figure 1: Images of the enlarged 20 x 30 cm active area EW unit.

2) Ferric Oxyhydroxide Formation

During testing the formation of ferric oxyhydroxides were formed, however, the addition of EDTA prevented its precipitation in the main catholyte solution. Precipitation only occurring on the surface of the solution and the container walls.

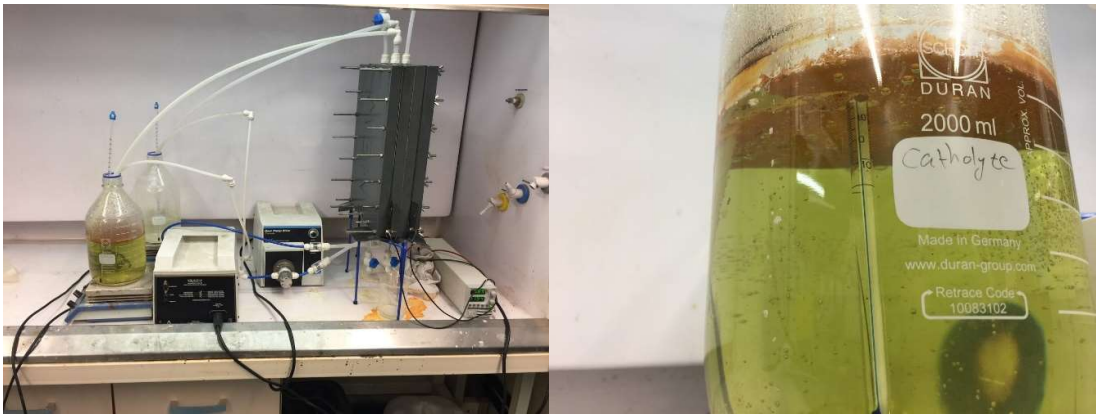

Figure 2: Formation of ferric oxyhydroxide during operation

APPENDIX D

membranes

MDPI

Article

Electrowinning of Iron from Spent Leaching Solutions Using Novel Anion Exchange Membranes

Wouter Dirk Badenhorst [1], Cloete Rossouw [1], Hyeongrae Cho [2], Jochen Kerres [1,2], Dolf Bruinsma [3] and Henning Krieg [1,*]

1 Focus Area: Chemical Resource Beneficiation, Faculty of Natural Sciences, North-West University, Potchefstroom 2520, South Africa; 24250643@nwu.ac.za (W.D.B.); 22114688@nwu.ac.za (C.R.); J.Kerres@gmx.de (J.K.)

2 Institute of Chemical Process Engineering, University of Stuttgart, D-70199 Stuttgart, Germany; hyeongrae.cho@icvt.uni-stuttgart.de

3 Bruinsma Solutions, 10 Mclagen Str., Potchefstroom 2531, South Africa; dolf.bruinsma@gmail.com

* Correspondence: Henning.Krieg@nwu.ac.za

Received: 30 September 2019; Accepted: 18 October 2019; Published: 24 October 2019

check for updates

Abstract: In the Pyror process, electrowinning (EW) is used to recover acid and iron from spent leaching solutions (SLS), where a porous Terylene membrane acts as a separator between the cathode and anode. In this study, a novel anion exchange membrane (AEM)-based EW process is benchmarked against a process without and with a porous Terylene membrane by comparing the current efficiency, specific energy consumption (SEC), and sulfuric acid generation using an in-house constructed EW flow cell. Using an FAP-PK-130 commercial AEM, it was shown that the AEM-based process was more efficient than the traditional processes. Subsequently, 11 novel polybenzimidazole (PBI)-based blend AEMs were compared with the commercial AEM. The best performing novel AEM (BM-5), yielded a current efficiency of 95% at an SEC of 3.53 kWh/kg Fe, which is a 10% increase in current efficiency and a 0.72 kWh/kg Fe decrease in SEC when compared to the existing Pyror process. Furthermore, the use of the novel BM-5 AEM resulted in a 0.22 kWh/kg Fe lower SEC than that obtained with the commercial AEM, also showing mechanical stability in the EW flow cell. Finally, it was shown that below 5 g/L Fe, side reactions at the cathode resulted in a decrease in process efficiency, while 40 g/L yielded the highest efficiency and lowest SECs.

Keywords: electrowinning; anion exchange membranes; waste treatment; iron sulphate disposal; acid regeneration

1. Introduction

A South African mining group is investigating the use of electrowinning (EW) to recover iron and H_2SO_4 from an iron sulphate waste solution produced during metal beneficiation. For the purpose of this paper, the term electrowinning, as is commonly applied for this process, is used throughout the paper. The spent leaching solution (SLS) consists mainly of iron sulphate, unspent sulfuric acid, and some minor metal impurities such as cobalt (Co), nickel (Ni), and chromium (Cr). Traditionally, such SLSs have been treated using either active or passive methods such as oxidative, bacterial, or limestone precipitation [1,2]. These methods, however, rarely yield marketable products when used to treat the SLSs [1].

The most prevalent method for treatment involves the use of chemical neutralization agents [2]. The addition of a base (NaOH, CaO, or $FeCO_3$) raises the pH of the solution, lowering the solubility of many metal species, thereby facilitating the precipitation of metal hydroxides [2]. In the case of iron, oxidizing chemicals such as H_2O_2, or non-chemical methods such as active aeration can be used to